personal buildup for

Force Motors Ltd.

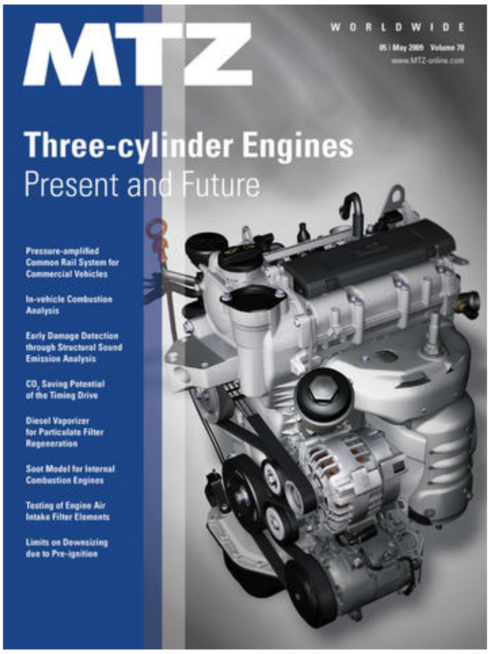

MTZ worldwide 5/2009, as epaper released on 16.04.2009
http://www.mtz-worldwide.com

content:

MTZ

WORLDWIDE

05 | May 2009 Volume 70

www.MTZ-online.com

Three-cylinder Engines
Present and Future

Pressure-amplified Common Rail System for Commercial Vehicles

In-vehicle Combustion Analysis

Early Damage Detection through Structural Sound Emission Analysis

CO_2 Saving Potential of the Timing Drive

Diesel Vaporizer for Particulate Filter Regeneration

Soot Model for Internal Combustion Engines

Testing of Engine Air Intake Filter Elements

Limits on Downsizing due to Pre-ignition

For more information visit:
www.MTZ-online.com

COVER STORY

Three-cylinder Engines
Present and Future

4
A turbocharged **Three-cylinder Engine** saves about 3 % of fuel compared to a four-cylinder engine of the same power. Volkswagen is a pioneer in this powertrain concept and, at the request of MTZ, presents this overview of current developments.

COVER STORY

DEVELOPMENT

RESEARCH

RUBRICS

Neither Hot nor Cold

Dear Reader,

"Heat is life" was the slogan used by a certain energy provider a few years ago. This applies not only to human beings but also to technical systems, a fact that was demonstrated here at the 9th International Stuttgart Symposium. Taking energy from a lithium-ion battery at a much higher temperature than its optimum temperature window of 25 to 35 degrees Celsius has the effect of shortening the battery's lifetime. At very low temperatures, on the other hand, the charging capacity is severely limited or charging is even impossible. As a result, the subject of battery cooling will become extremely important over the next few years. As is often the case in engineering, the optimum concept does not exist. The company Behr has developed a fast, pragmatic solution for the hybrid version of the S-Class – by converting the existing coolant circuit for the air conditioning system.

In future, we will need to address the issue of how electric vehicles are to be heated. In his paper, Dr. Steffen Korfmann from Audi questioned the idea of an electric heating system. During average operation, a CO_2 emission of 50 grams per minute would be produced on the basis of the efficiency chain, whereas a conventional, petrol-powered auxiliary heating system produces only 27 grams per minute.

The fact that the internal combustion engine itself still has considerable fuel-consumption potentials is shown by Porsche with its concept for the Panamera. Differentiated control of the engine cooling system – even deactivating it completely after a cold start – achieves a 2 percent reduction in fuel consumption in the NEDC.

While still in Stuttgart, I'm already looking forward to seeing you at the Vienna Motor Symposium, where we can discuss this and other topics.

Johannes Winterhagen
Stuttgart, 25 March 2009

Johannes Winterhagen
Editor-in-Chief

MTZ WORLDWIDE
05I2009

Founded 1939 by
Prof. Dr.-Ing. E. h. Heinrich Buschmann and
Dr.-Ing. E. h. Prosper L'Orange

Organ of the Fachverband Motoren und Systeme im VDMA, Verband Deutscher Maschinen- und Anlagenbau e. V., Frankfurt/Main, for the areas combustion engines and gas turbines

Organ of the Forschungsvereinigung Verbrennungskraftmaschinen e. V. (FVV)

Organ of the Wissenschaftliche Gesellschaft für Kraftfahrzeug- und Motorentechnik e. V. (WKM)

Organ of the Österreichischer Verein für Kraftfahrzeugtechnik (ÖVK)

Cooperation with the STG, Schiffbautechnische Gesellschaft e. V., Hamburg, in the area of ship drives by combustion engines

Three-cylinder Engines from Volkswagen

Present and Future

The trend towards vehicle powertrains that are ever more frugal is increasingly leading to the use of three-cylinder engines. This is because the concept makes it possible to save fuel with a turbocharged three-cylinder engine compared to a four-cylinder engine of the same power. Volkswagen is a pioneer in this powertrain concept and, at the request of MTZ, presents this overview of current developments.

1 Three-cylinder Engines at Volkswagen

There is a long tradition of developing modern and low-consumption three-cylinder engines at Volkswagen. In 1998, Volkswagen started series production of the first three-cylinder diesel engine with 1.4 l cubic capacity and 55 kW rated power. This unit was still based on a grey cast-iron cylinder block. One year later, in 1999, this was followed by a second and completely new developed TDI engine with an aluminium construction. The 1.2 l engine with 45 kW rated power was used as the engine for the Lupo 3L (means a consumption of about 3 l/100 km) and the Audi A2. Today too, ten years later, this engine concept is still regarded as innovative and also sets a new standard that has never been achieved before in a series production vehicle.

One year later, the first three-cylinder gasoline engine (1.2 l cubic capacity, four-valve technology, 47 kW rated power) also celebrated its premiere in the Polo. The three-cylinder concepts, both gasoline and diesel, currently achieve an installation quota of about 50 % in the Polo, while the quota in the Fox is significantly higher still.

During the last decade, engine development was preliminary concerned with achieving goals such as increased power and cost reductions. Now, in view of the major reductions in fleet consumption values, topics such as downsizing and lightweight construction are becoming ever more important whilst downwards pressure on costs is just as high. As a result, attention is increasingly focussing on three-cylinder engines as a means for developing especially frugal vehicles.

Nowadays, the three-cylinder engine can be found in the vehicle segment of the Polo class and smaller. However, the fuel savings that can be achieved mean that it could theoretically be expanded into larger vehicle segments.

2 Development Targets

Whether it is a matter of performance, emissions, comfort, service life, purchase price, running or servicing costs: the internal combustion engine always represents a compromise between a whole host of requirements. It is the local market that decides which of these requirements is particularly relevant, **Figure 1**.

For European customers, it is emissions and consumption that are of primary importance in the purchase decision. The North American market, however, regards emissions and, in particular, performance as especially important. In developing countries, the choice of engine is principally based on purchase price, in order to make individual mobility affordable. However, local expectations for comfort must not be disregarded.

It is not just the requirements of international markets that differ, they also change within a market over the course of time. Whilst the various EU emissions requirements were being introduced during the 1990s, meeting these directives was a primary factor in introducing new developments. Today, the automo-

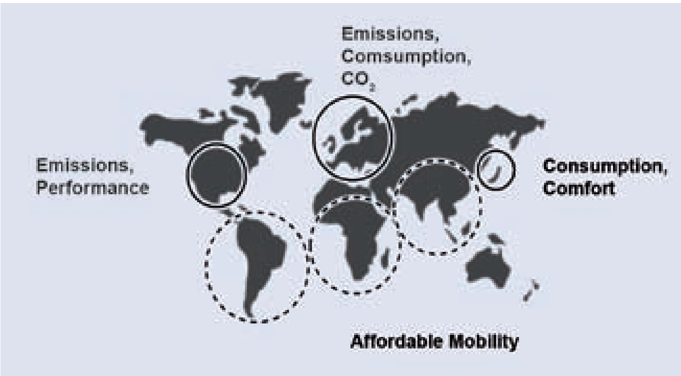

Figure 1: Different requirements on mobility

The Author

Dr.-Ing. Jens Hadler is Director of Powertrain Development at Volkswagen AG in Wolfsburg (Germany).

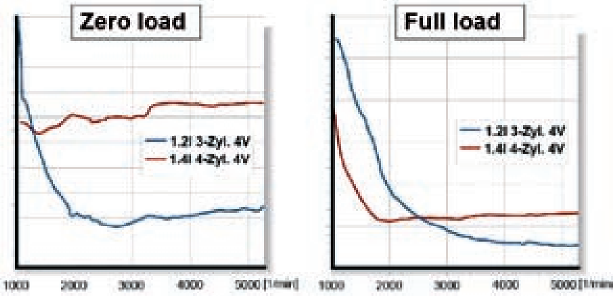

Figure 2: Comparison between vibration pathways in the engine mountings

tive industry is having to meet new regulations for fleet consumption not only with regard to further tightening of exhaust limit values in Europe, America and Japan but also because of the increasing scarcity of fossil fuels and global warming. Engine downsizing can help to achieve these targets.

The first step towards downsizing is to reduce the number of cylinders whilst keeping the same cubic capacity per cylinder. This offers the advantage of being able to adopt large parts of the combustion process from the four-cylinder engine. As a second step, reducing the number of cylinders is combined with reducing the cubic capacity of each cylinder so as to achieve additional consumption savings.

3 Three or Four Cylinders?

The following section presents a comparison between inline engines with three and four cylinders. The criteria used are fuel consumption and comfort, both of which have a decisive influence on the automobile customer‘s purchasing behaviour.
The three-cylinder engine offers the following advantages in terms of consumption:
– low friction within the engine
– greater suitability for turbocharging because of the larger ignition interval
– with a larger individual cylinder volume: Greater thermal efficiency because of lower wall heat losses compared to a four-cylinder engine with the same cubic capacity
– lower weight.
This is offset by a slightly increased idling speed because of the larger ignition interval, although this disadvantage can be ruled out as soon as a start/stop device is installed. Overall, even without a start/stop system, the NEDC consumption benefit for three-cylinder engines is in a single-digit percentage range, whereas it is a little bit higher for the turbocharched compared to the naturally aspirated engine.

As far as comfort is concerned, the three-cylinder engine does suffer from disadvantages at lower engine speeds and high loads due to the gas force excitation (attributable to the ignition interval). At relatively higher engine speeds, it is the influences of free mass forces and moments that predominate. However, at this point it is necessary to draw the following distinction: Compensating the free first order mass moments by means of a balancer shaft results in a reduction in the vibration excitations in the assembly mounting of the three-cylinder engine compared to the four-cylinder one. This is because the four-cylinder‘s free second order mass forces are higher than the still free second mass moments of the three-cylinder. As a result, the comfort of a three-cylinder engine with a balancer shaft as perceived by the customer is approximately that of a four-cylinder engine without balancer shafts. The typical three-cylinder acoustics can be configured so that a new and interesting sound is created, **Figure 2**.

Another advantage of the three-cylinder engine is that it needs less space, and the shorter length of the engine in particular offers advantages for hybrid applications. On the cost side too, the three-cylinder engine offers advantages over the four-cylinder engine. However, some of this benefit is eroded by the possible need to use a balancer shaft.

One disadvantage of the three-cylinder engine is its low level of market acceptance in some regions, particular in North America. However, changing conditions can be expected to prevail in the future. This is because low fuel consumption can be expected to become an ever more important purchase criterion in the USA and Canada as well.

4 Currently in Series Production

The most important technical properties of the current inline three-cylinder diesel and gasoline engines are presented below.

4.1 The 1.4 l TDI Engine in the Polo BlueMotion

The 1.4 l TDI engine with 59 kW rated power achieves an average consumption of 3.8 l/100 km (99 g CO_2/km) in the Polo and currently represents the most advanced stage of diesel three-cylinder development, **Figure 3** and **Table 1**. The performance figures of the Polo BlueMotion

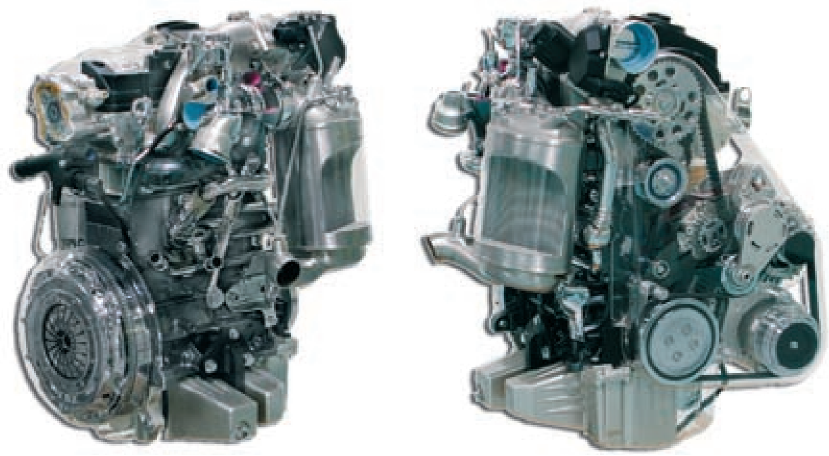

Figure 3: Cutaway model of the three-cylinder TDI engine with 1.4 l cubic capacity and 59 kW rated power

Table 1: Technical data of the three-cylinder TDI engine for the Polo BlueMotion

Design, working method	–	3-cylinder, 4-stroke turbo diesel inline
Number valves / cylinder	–	2/3
Displacement	**cm³**	1422
Bore	**mm**	79.5
Stroke	**mm**	95.5
Cylinder distance	**mm**	88
Power	**kW**	59
at rpm	**1/min**	4000
Torque	**Nm**	195
at rpm	**1/min**	1800 to 2200
Compression ratio	–	18.5:1
Exhaust aftertreatment	–	Particulate filter, catalytic layer
Emission standard	–	EU4 with EOBD

provide impressive proof that it has been possible to combine fuel efficiency with enjoyable driving.

As well as optimising the aerodynamics of the vehicle and setting up the gearbox with an emphasis on comfort, it is above all the measures taken on the engine that have contributed to bringing this ambitious consumption objective within reach. Friction losses have been reduced by minimising the cylinder distortions as well as by taking a range of other measures. At the same time, the charge change has been optimised by using a turbocharger with variable turbine geometry and by reducing throttle losses.

The maximum torque of 195 Nm is available from only 1800 rpm onwards to provide powerful in-gear acceleration. The grey cast-iron crankcase has a stroke-to-bore ratio of 1.2. A compensating drive completely eliminates the first order mass moments.

The injection pressure has been increased to more than 2200 bar, thereby improving mixture formation and reducing soot production. This means the diesel particulate filter does not have to be regenerated so often, which in turn delivers a consumption benefit.

These diverse engine measures have allowed reductions of between 5 and 10 % to be achieved across broad areas of the performance diagram compared to the basic engine. Above all, it is in important medium part-load operation up to 3500 rpm that a significant fuel saving has been achieved.

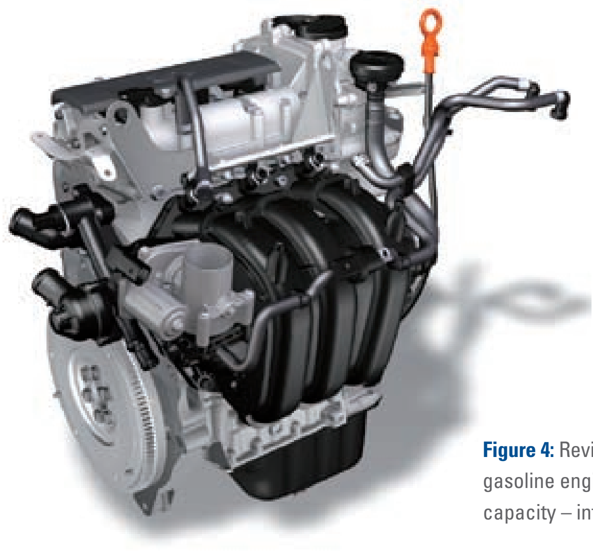

Figure 4: Revised three-cylinder gasoline engine with 1.2 l cubic capacity – intake side

4.2 The New 1.2 l Gasoline Engine in the Polo

The entry-level engines for the new VW Polo are the three-cylinder units with 1.2 l cubic capacity and power levels of 44 and 51 kW resulting from customer and market demands as well as the competitive situation. These engines are characterised by the familiar advantages of modern three-cylinder engines. Consequently, a relatively high level of torque is available even at low rpm values, thereby permitting a frugal driving style.

For use in the new Polo, the engines have been extensively revised with regard to consumption and CO_2 emissions, weight, engine acoustics and compliance with the EU5 exhaust standard, **Cover Figure** and **Figure 4**. For example, a toothed chain with optimised acoustic and friction properties is used for the timing gear and oil pump drive. A new, weight-optimised crankshaft in the basic engine of the three-cylinder units provides further acoustic and consumption advantages.

Additional measures taken on the injection system such as constricting the tolerances of the injection valves as well as fine-tuning and adapting the injection volumes deliver more consumption and emissions benefits for the VW entry-level models in the A0 class.

This extensive package of optimisations, combined with a new gearbox set-up and further measures taken in the vehicle, has resulted in a reduction in fuel consumption of 0.4 l/100 km (10 g CO_2/km) for both performance versions compared to the previous model, **Table 2**.

5 Outlook

In the future, fuel consumption will be one of the main sales arguments for a vehicle, in all regions, for reasons relating to taxation and fuel costs. Furthermore, there is a trend towards smaller and cheaper cars in the competitive environment. This means there is a need to develop engines that are smaller, lighter, more efficient and less expensive, as far as possible. The three-cylinder engine, whether as a diesel or gasoline unit, offers significant potential for unifying these conflicting objectives.

This is why Volkswagen is pushing further ahead with three-cylinder technology.

Table 2: Technical data of the three-cylinder gasoline engine with 1.2 l cubic capacity

	1.2 l MPI	1.2 l MPI
Engine layout	Inline 3 Otto	Inline 3 Otto
Mixture formation	Port fuel injection	Port fuel injection
Engine management	Simos 9	Simos 9
Displacement	1198 cm^3	1198 cm^3
Bore / stroke	76.5 mm	76.5 mm
Compression ratio	10.3:1	10.5:1
Max. power	44 kW at 5200 /min	51 kW at 5400/min
Max. torque	108 Nm at 3000/min	112 Nm at 3000/min
Fuel	ROZ 95 / 91	ROZ 95 / 91
Emission standard	EU5	EU5
Consumption, in the city	7.2 l	7.2 l
Consumption, over land	4.5 l	4.5 l
Consumption, combined	5.5 l	5.5 l
CO_2-Emission	128 g / km	128 g / km
Transmission	Manual, 5-gear	Manual, 5-gear

Figure 5: The new 1.2 l 4V common rail diesel engine

The main objectives in this development effort are to reduce fuel consumption whilst maintaining good performance levels and offering high levels of acoustic and vibration comfort. It goes without saying that all these efforts need to be accompanied by measures to meet emissions limits. This will then lead us to completely new applications and vehicle concepts which would not be imaginable without these new three-cylinder engines.

For diesel engines, this means not only using the latest common rail technology and reducing friction but also achieving significantly smoother running and an improved acoustic impression from these engines in order to increase customer acceptance, **Figure 5**. Only then will the three-cylinder engine become attractive in vehicle segments that are still dominated by four-cylinder engines at present. Combined with a totally new combustion process as well as more advanced mixture preparation, turbocharging and exhaust treatment technology, it will be possible to achieve significant optimisations in fuel consumption, emissions, acoustic presence and driving comfort. Similar goals apply to the three-cylinder gasoline engines. Here too, the specifications issued to the development teams have focussed on reducing friction, optimising the combustion process and exhaust treatment, lightweight construction, compactness and low specific consumption, as well as giving particular consideration to the cost aspect.

Depending on whether they are configured as MPI or TSI, the future three-cylinder engines will be able to cover a performance range from 40 to well in excess of 60 kW. As a result, VW is continuing its successful strategy of downsizing towards cubic capacities even below 1.2 l whilst upholding driving pleasure.

Reference

[1] Winterkorn, M.; Bohne, P.: Das Drei-Liter-Auto von Volkswagen – der Lupo 3L TDI: Teil 1. In: ATZ 101 (1999), Nr. 6, S. 390ff

Pressure-amplified Common Rail System for Commercial Vehicles

The key to a successful layout of a combustion system for commercial vehicles is in the management of peak torque operation points. For this purpose, Bosch has enhanced its Common Rail System with increasing degrees of freedom – i.e. with flexible rate shaping. A second solenoid valve activates a pressure-amplifier inside the injector, an optimized offset of nozzle needle timing reduces the injection rate by half right at the start of injection, and the formation of nitrogen oxide is reduced considerably. This enables the engine manufacturer to adhere to the emission limits while further reducing fuel consumption and the engine-related effort for the air sytem.

1 Introduction

With the introduction of the future emission levels US10/Euro6 for heavy duty engines, the Unit Pump/Unit Injector Systems today still used in many applications will increasingly be replaced by Common Rail Systems.

The main driver for this is the use of exhaust gas recirculation with all relevant combustion systems. Engines using this system have to be able to handle injection pressure peaks at part load, and this can only be implemented in a hydraulically efficient way by using a rail as pressure accumulator.

The product portfolio of Bosch offers two variants of Common Rail Systems to facilitate combustion at operating points with high load. The system „CRSN3.3“ offers the freedom of fully flexible multiple injections.

It is used for combustion systems with high boost in combination with high exhaust gas recirculation rates. At present, for adaptation to the specific engine requirements, the injection pressure can be configured at a range of 2200 to 2500 bar, **Figure 1**.

The pressure-amplified system „CRSN4.2“ offers the possibility to select the injection rate in a flexible way at start of injection, thereby reducing the formation of nitrogen oxide in the area of the NO_x-sensitive engine map. **Figure 2** below shows an example for this application. At the same peak pressure of a conventional CRS, the pressure-amplified system utilizes the advantage of a lower NO_x emission for a reduction of the fuel consumption during pressure peaks. Additionally, the effort for the air system and for the cooling system can be limited.

While optimizing an engine with the pressure-amplified system, fuel consumption is reduced up to 3.5 % under real load conditions. Projected onto an operating life of four years in European long haul traffic, up to 200 t of CO_2 or 10.000 € of fuel costs, respectively, can be saved [1].

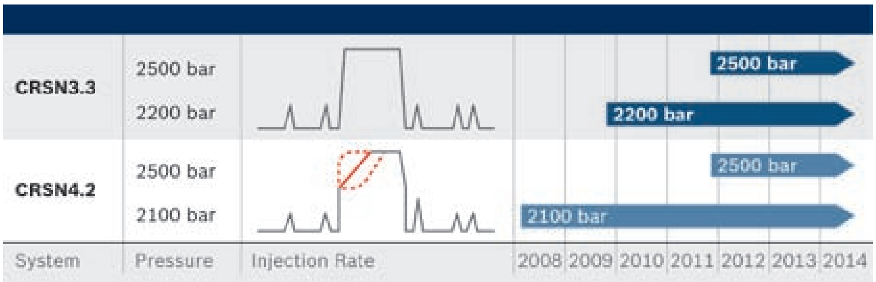

Figure 1: Roadmap Common Rail Systems for commercial vehicles

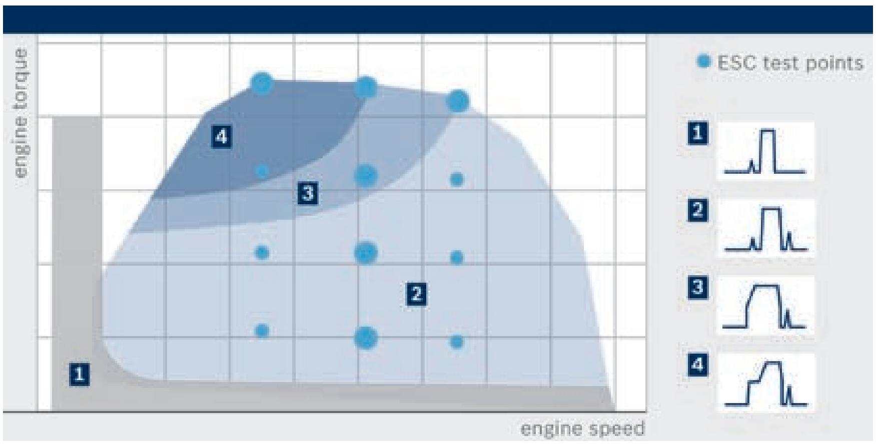

Figure 2: Optimum rate shaping in engine map

The Authors

Dr. Rolf Leonhard
is Executive Vice President Engineering, Bosch Diesel Systems in Stuttgart (Germany).

Dr.-Ing.
Marcus Parche
is Senior Vice President Diesel Systems for Commercial Vehicles at Robert Bosch Diesel Systems in Stuttgart (Germany).

Dipl.-Ing. Carlos Alvarez-Avila
is Director Platform Projects for Commercial Vehicles at Robert Bosch Diesel Systems in Stuttgart (Germany).

Dipl.-Ing. Jost Krauß
is Director System Development Common Rail Platform at Robert Bosch Diesel Systems in Stuttgart (Germany).

Dipl.-Ing. (FH)
Bernd Rosenau
is Director Productmanagement Common Rail System for Passenger Cars at Robert Bosch Diesel Systems in Stuttgart (Germany).

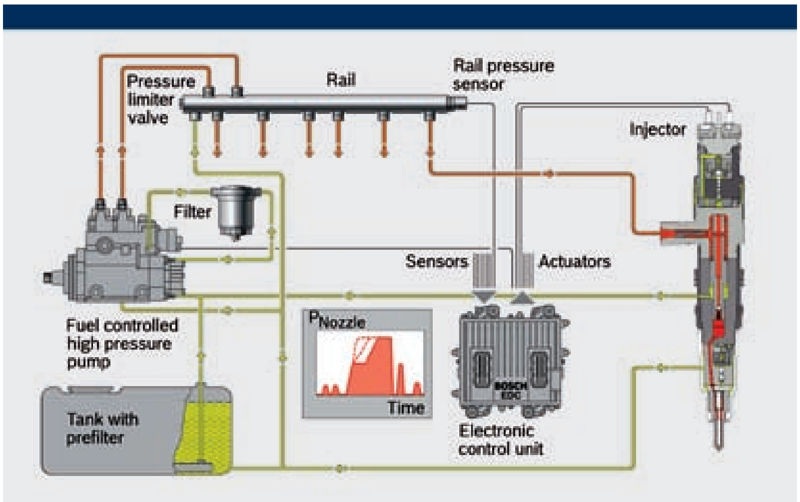

Figure 3: Injection system „CRSN4.2“ with pressure-amplified injector

2 System Design

The basic design of a pressure-amplified system, **Figure 3**, consists of the known components/functions of a CRS, like:
- fuel delivery by high pressure pump
- pressure accumulation and dispersion onto cylinders in rail
- fuel injection in injectors.

When compared with conventional CRS, a major distinguishing feature is the way the function “pressure generation“ is divided into two stages in the system. During the first stage of pressure generation, the high-pressure pump compresses fuel to 250 to 900 bar. In the second stage, fuel is compressed up to 2100 bar by a pressure-amplyfier integrated in the injector. The pressure amplification is controlled by a separate solenoid valve.

When a system configuration with pressure amplifier ist chosen, it offers the following advantages for the development of modern engine concepts:
- flexible and hydraulically efficient rate shaping for optimized fuel consumption during pressure peaks
- pre-injection/post-injection with a rail pressure of ≤ 900 bar reduces the spray momentum, the wetting of the cylinder liner walls with fuel and the subsequent dilution of engine oil with fuel
- reduction of number of injector parts affected by peak pressure; Pump and rail as well as high-pressure lines only have to be designed for a pressure of up to 900 bar.

An important driver for the maximization of lifetime of an exhaust gas recirculation system is that any contact between engine oil and fuel is avoided. For the pressure-amplified system, the drivetrain of the pump, usually lubricated with engine oil for commercial vehicle appications, is lubricated with fuel instead.

A rail in the length of a heavy-duty engine is designed with the following advantages:
- reduction of variants of high-pressure lines to one third
- compact packaging of lines
- reduction of pressure oscilliations in the rail injector lines
- reduction of vibrations in rail and lines through a ridgid connection.

3 The Injector of the Pressure-amplified System

As a result of the tasks and requirements they have to cope with, 4th generation injectors for commercial vehicles are substantially different from their predecessors regarding functionality and design. The concept of a pressure-amplified injector was implemented by a reduction of the original injector to a fraction of the size know for heavy duty CRS. More precisely, that part of the injector was minimized, which is responsible for the injection function and for the control thereof by means of an electronic actuator. This was necessary in order to make room for an extended range of functions.

The miniaturization was accomplished with a newly developed pressure-balanced 2/2-way solenoid valve, which is directly connected hydraulically to the nozzle needle. In combination with the nozzle module (already used in Bosch 3rd generation passenger car injectors), one gets a compact and highly dynamic “injection module” with the complete functionality of a classical injector, **Figure 4**.

The concept of a modular structure with numerous advantages resulting from it has altogether shaped the design of the 4th generation, **Figure 5**. The now increased functionality of the separately selectable pressure amplification has also been depicted in modules: one “pressure amplifier” and one related „control module“.

The pressure-amplifier module is used for the actual generation of high pressure inside the injector. The principle of

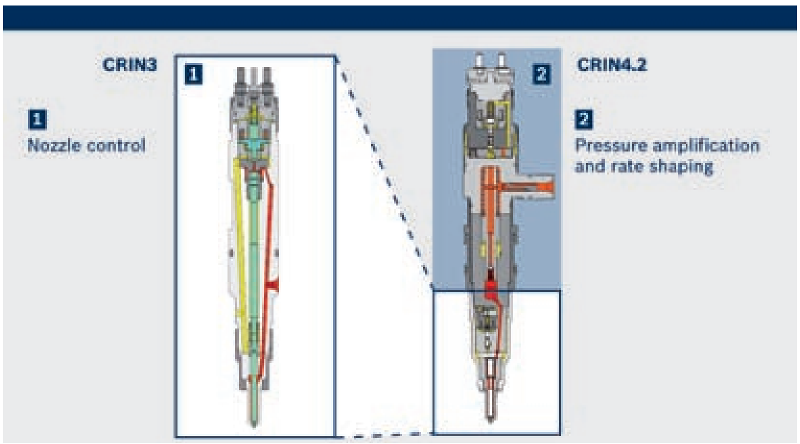

Figure 4: Transformation of the conventional nozzle management in the injection module of CRIN4.2

function is that of a hydraulic piston: Via a surface ratio a lower fluid pressure, in this case the system pressure in of rail, is amplified to a higher pressure beneath a smaller surface. This means the ratio of these two surfaces to each other determines the factor of pressure amplification. This static (i.e. geometrically defined) pressure-amplification rate in connection with a system pressure that can theoretically be scaled freely within a CRS, makes it possible that all ranges from minimum to maximum pressure within the engine map can be realized.

This means, depending on the relevant goal, the ratio of the pressure-amplifier can be adjusted to achieve the optimum result between injection pressure and hydraulic efficiency. The functionality "pressure amplification" is designed as a separately selectable option so that the injector can be used both in the pressure-amplified and in the unamplified mode. This distinctly sets itself apart from alternative solutions, which directly connect the activation of the injector with the pressure-amplification. This freedom (of using the injector in both modes) was achieved with the development and integration of another module for the 4th generation injector: the so-called "control module".

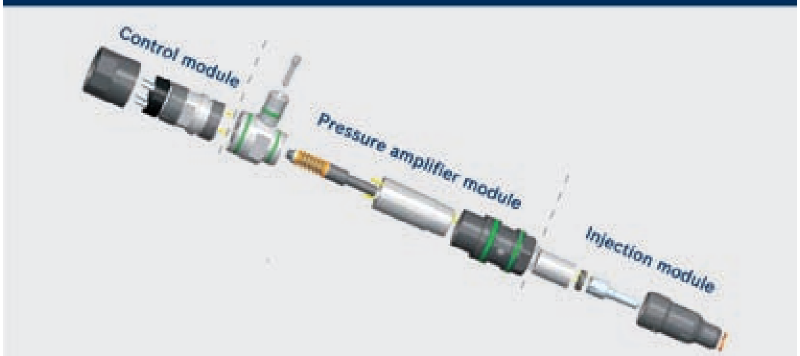

Figure 5: Modular structure of the pressure-amplified injector

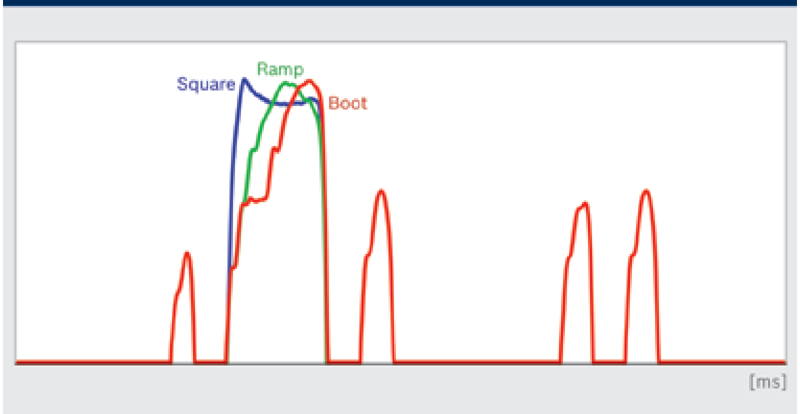

Figure 6: Variants of multiple injection and rate shaping

The movement of the pressure-amplifying piston is prevented or activated, respectively, depending on whether the relevant point in the engine map requires "only" rail pressure or pressure-amplified fuel injection instead.

The control function is implemented by means of a specifically for this application newly developed directly controlled 3/2-way solenoid valve. If the valve is triggered, the control chamber of the pressure-amplifier is decoupled from the rail pressure and is short-circuited to the fuel return line. Once the hydraulic pressure on the control chamber has been released, this leads to excess force on the surface affected by the rail pressure.

The pressure-amplifier piston now starts moving, and the "high-pressure chamber", now exclusively feeding the injection, is closed via a check valve integrated into the piston. This way, the "locked up" fluid is compressed to a higher pressure level. If the fuel is injected without pressure-amplification, due to a balance of forces and supported by spring force, the pressure-amplifying piston remains in its position at the upper end. This means, the spring is not only responsible for supporting the reset but also for ensuring that the piston is always in the same initial position when the system is started. The fuel then flows with unamplified injection pressure through the pressure-amplifier piston and through the open check valve to the nozzle. The real strength of the 4th generation injectors can be explained when combining the aforementioned function options, supported by the modular design: the decoupling of the function blocks "injection control" and "pressure-amplification control". This facilitates flexible rate shaping. Not only can the customer select between unamplified and pressure-amplified injection – also the point in time when the pressure-amplification is to start can be selected independently of the beginning of the injection. The rate shapes named "Boot", "Ramp" and "Square", **Figure 6**, in connection with the feature "multiple injections" offer engine developers further possibilities from the optimization of combustion to a reduced fuel consumption, improved emission rates and an increased specific efficiency. At the same time, the adaptation of different applications e.g. to regional legislation based on different emission laws can be accomplished more easily due to this system freedom.

There are further advantages that have not been described before: By integrating the pressure-amplification into the injector, only those components in the "bottom" half of the injector are affected by the amplified pressuer. The pump, the lines, the rail as well as the major part of the injector are only affected by the standard rail pressure. Since the requirements on the system components are determined by the pressure they have to handle, those parts not affected by higher pressure have to fit for rail pressure only. The implementation of subsequent pressure increases are simplified considerably. Production and series maintenance profit from the modular structure of the injectors, since function tests and debugging can be carried out on each module individually.

4 The High-pressure Pump Family

In the first stage of the two-stage high-pressure generation process, the „CPN5-9/2" (5. generation – 900 bar and two pistons) – a pump of the „CPN5" pump family – is used. By the evolutionary development of the basic design, this pump concept is capable to cover the increasing system requirements of future Common Rail Systems. With identical or even reduced pump weight, the hydraulic power can be increased distinctly, Figure 7.

The „CPN5" pump family is based on an inline pump concept. Compared to other pumps in this power segment, this type is lubricated with fuel instead of engine oil. The drivers behind this fundamental switch were the increasing demands of emission legislation, in particular regarding soot.

While oil-lubricated types require a considerable effort to minimize leakages along the pump piston, the fuel-lubrication facilitates a perfect separation between oil circuit and fuel circuit. With the implementation of constructive manufacturing measures, an impact on robustness caused by lower fuel lubricity is avoided. The buildup of the lubricating film between those parts moving relatively against each other is specifically supported by design features of those components and their environment. For the cam drive e.g. a roller shoe concept is used which has been derived from the „CP4" – the pump that has already proven itself successful in newer common rail pumps of passenger cars, light duty and heavy duty systems. Furthermore, friction-minimizing coatings as well as special bearing material are also used to meet the requirements of variing fuel qualities.

The „CPN5" pump family is characterized through its modular design. Using adequate combinations of cam numbers, piston diameter and piston lift as well as a transmission ratio suitable for the engine speed, volume and pressure ranges from 250 l/h at 2500 bar up to 520 l/h at 900 bar can be covered.

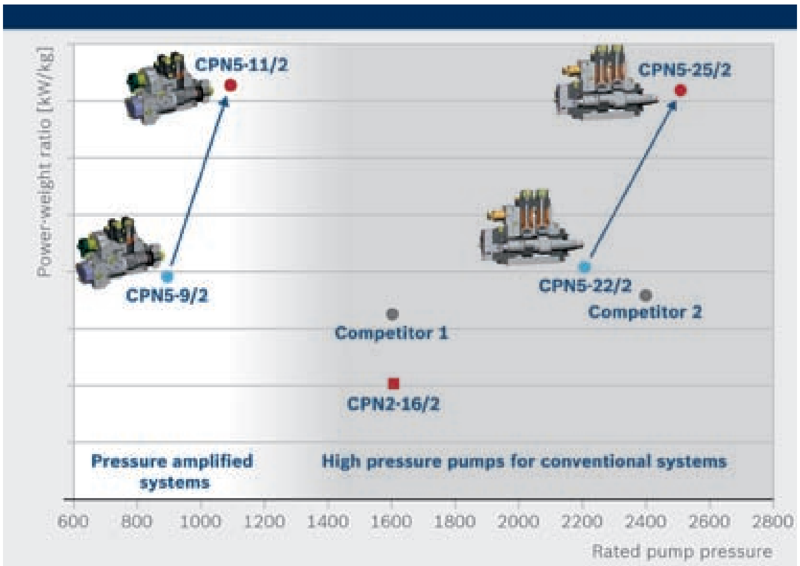

Figure 7: The „CPN5" pump family

In particular the selection of a suitable combination of speed ratio to the number of cams can support the adherence to narrow injection tolerance limits. By using adequate combinations, the delivery stroke of the pump elements is either synchronized to the fuel injections or each individual injector is always assigned to the same pump element. This so-called injection-synchronous or element-synchronous delivery ensures that the influence of a strewing rate shape on the injection quantity tolerance is minimized from injection to injection. The described modular structure of the „CPN5-9/2" pump generation can best be depicted by the example of Figure 8.

The fuel is pre-delivered by a gear pump, which is integrated into the pump housing. The fuel delivery is controlled by the solenoid valve of the measuring unit. Depending on the combination chosen and the drivetrain ratio, two or three loads per pump element are located on the camshaft. The barrels with its pistons consist of steel and are mounted as one unit into the aluminum pump housing.

Also in the commercial vehicle sector the demands on noise emissions are gaining importance. Corresponding demands on the injection system are derived of this. Apart from measures to optimize the combustion noise, there are growing demands regarding measures to reduce

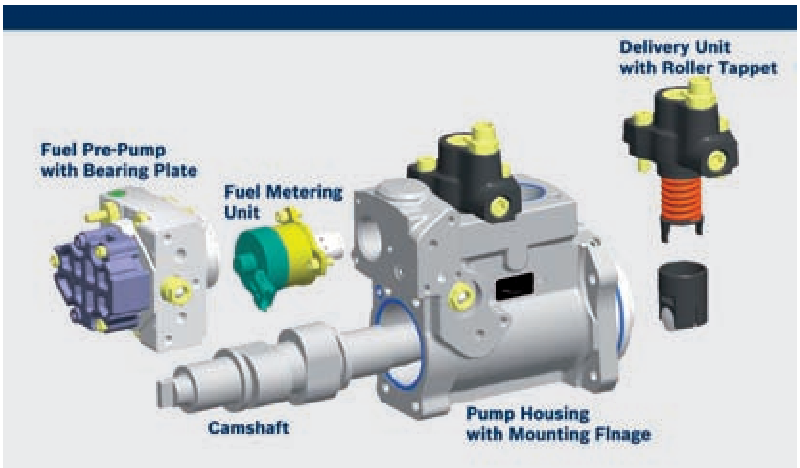

Figure 8: Assembly of a „CPN5-9/2"

noise emission of the components of the fuel injection. One of the dominant noise sources is the pressure generation inside the pump. The growing demands for higher pressure levels and the increasing energy consumption resulting thereof ensure that these newer pump generations are more sophisticated.

The dynamic of the piston movement is a major influence factor on the noise emitted by the pump. One oft he dominant noise sources of the high-pressure pump itself is the moment when during delivery the piston comes into contact with the “locked up” and compressed fuel in the element room. Regarding the noise emission of the entire system, the effective torque in the drivetrain of the pump is a major factor. This torque puts the drivetrain under a pre-tension, and causes the characteristic “ratteling noise” when the tension is released and the metallic drivetrain components hit on each other. The same effect is caused by backing torques.

The transmission of these exitations to the gearbox of the engine and the resulting amplification of this noise due to the “loudspeaker effect” of the engine components elevate this parameter to the central factor of the hydraulic system that has to beoptimized to achieve optimum noise emissions.

The best results can be obtained by a suitable design of the camp loop geometry to reduce torque fluctuations. Combined with damping measures on the coupling elements between the drivetrain and the gearbox, the noise level can be reduced significantly.

5 Validation Strategy

Due to the high lifetime requirements of 1.2 million miles in combination with a very tight project schedule, the demands on the validation efficiency of components and of the entire system have become more and more important. In view of this background, a new and optimized validation strategy has been worked out and implemented.

The previous validation concept, with its runtime-intensive endurance tests, usually only detects the weakest part of each product. This results in a high number of necessary iterations. The new validation is focused on the lifetime-sensitive assemblies and machine elements of the products and their specific testing. The assemblies to be tested are determined making use of experience with similar assemblies or of theoretical considerations i.e. calculations. The so-called HALTs (Highly Accelerated Life Tests) play a major role in it. During these tests, critical factors, for example temperature and pressure, are gradually increased to detect machine elements “reacting” on these parameters.

In the next step, the load collectives are identified under real life conditions in close cooperation with the engine manufacturer. Based on these load collectives, so-called QALTs (Quantitative Accelerated Life Tests) are defined. This way, targeted, component-specific accelerated tests can be performed under critical conditions correlating with lifetimes in the field, **Figure 9**.

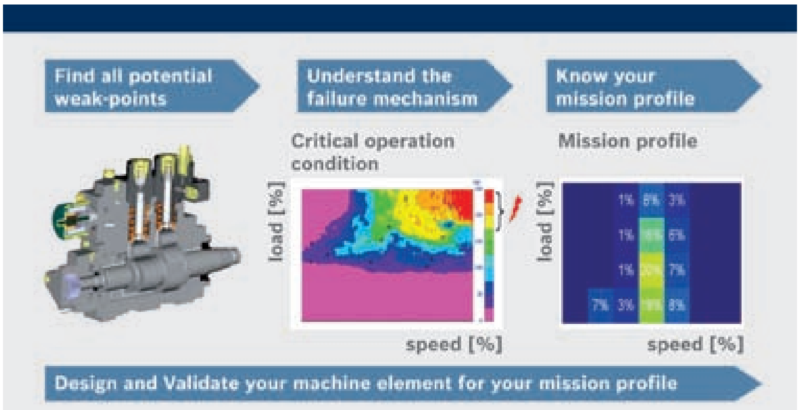

Figure 9: Quantitatively Accelerated Life Testing (QALT)

The modular structure of the products used supports this concept. It facilitates the accelerated optimization and validation of various assemblies and machine elements in parallel. Long lasting endurance tests are only performed with “mature“ products to verify the trouble-free interaction at the different component interfaces. Particular importance is placed on the testing of the products under real life conditions. Therefore, the test benches have been modified in such a way that the use of cylinder heads and of the entire lower pressure circuit became possible.

The high quality standard of the recently started series production confirms impressively the effectiveness of this validation strategy.

6 Prospect

Preliminary investigations demonstrates, that further development of conventional combustion methods for commercial vehicles with the target to improve fuel consumption is possible. A major element of this measures package is a futher increase of the injection pressure.

Based on the features described before, the „CRSN4.2“ with its pressure-amplified injector is ideally suited for another pressure increases. The evolutionary development of this platform for pressure levels up to 2500 bar as well as of for the platform for conventional fuel injection systems, with one-stage pressure generation, has already been started. This means all application-specific customer requirements can be fulfilled. In order to be able to respond to future requirements for even higher pressure levels, Bosch already conducts research for target pressure levels of up to 3000 bar.

References

[1] Schmid, W.; Heil, B.; Harr, T.; Maderthaner, K.: Combustion Process for the New Generation of DaimlerChrysler Heavy Duty Diesel Engines and Requirements to Fuel Injection Systems. 28. Internationales Wiener Motorensymposium

[2] Albrecht, W.; Dohle, U.; Gombert, R.; Krauss, J.; Leonhard, R.; Wannenwetsch, P.: Das innovative Bosch Common Rail System CRSN4.2 für die neue Generation von schweren DaimlerChrysler Nutzfahrzeug – Dieselmotoren. 28. Internationales Wiener Motorensymposium

[3] Dohle, U.; Dürnholz, M.; Kampmann, S.; Hammer, J.; Hinrichsen, C.: 4th Generation Diesel Common Rail System for Future Emissions Legislations. FISITA World Automotive Congress, Barcelona, 2004

A New Data Acquisition and Processing System for In-vehicle Combustion Analysis

With "KiBox", Kistler Instrumente AG has developed a new data acquisition and processing system specially designed for in-vehicle combustion analysis. Apart from its innovative data acquisition concept and easy integration into the INCA calibration system, KiBox comes with a number of features representing the leading edge of technology and beyond. This enables combustion analysis values to be displayed in real-time and to be analyzed simultaneously with other control variables of the engine management system.

1 Introduction

The measurement and thermodynamic analysis of in-cylinder pressure (referred to in this article as „combustion analysis“) continues to be the essential tool for determining the quality of energy conversion in internal combustion engines. The evaluation of combustion pressure and the related change in combustion chamber volume provides data which permit a characterization of the combustion and a quantification of the thermodynamic process. Combustion pressure can be measured directly with piezoelectric pressure sensors. The volume change in the combustion chamber can be measured only indirectly from the acquisition of the crank angle position, the crank drive kinematics and the geometrical data of the cylinder.

Today, combustion analysis is typically carried out on engine test stands for both steady state and transient engine speed and load. In addition, combustion analysis is extremely useful in on-road testing for validating the calibration of the engine management system and for trouble-shooting purposes. Only combustion analysis makes it possible to observe and quantify precisely the effects that the highly complex control processes of the complete engine system have on the actual combustion under all real operating conditions. Thus, combustion analysis helps to improve our mastery of complex modern engine control units (ECU), to carry on system optimization under everyday driving conditions and to shorten the overall development process. In-vehicle combustion analysis is becoming even more important in view of the greatly increased engine performance levels of down-sizing concepts.

2 Basic Layout of Combustion Analysis Systems

A conventional combustion analysis system consists of a pressure sensor, connecting cable, amplifier and crank angle encoder, together with data acquisition and evaluation.

In view of the wide pressure range, the high operating temperatures in the combustion chamber and the ultra-fast combustion processes, piezoelectric pressure sensors are needed to achieve precise pressure measurements. These sensors yield a charge proportional to the pressure. Apart from the physical characteristics of the sensor itself, one of the main factors affecting the achievable precision of measurement is the way in which it is installed in the engine.

The connecting cable serves to transmit the electrical charge from the sensor to the amplifier. As the sensor charge yields are extremely small in absolute terms, the cable and the connector must provide a very high degree of electrical insulation. In addition, the cable needs to be triboelectrically optimized in order to minimize parasitic charge shifts caused by friction on the inner insulation arising from cable movements.

The electrical charge of the pressure sensor is converted, with great precision, into a proportional voltage signal through integration in the amplifier.

The crank shaft angle serves as the basis for the acquisition of the related data and the calculation of the combustion analysis values. For each revolution, the optical incremental encoders that are typically used provide a fixed number (e.g. 360) of crank degree marks (CDM) and a synchronization mark (TRG).

In the systems now in common use, the pressure signals are sampled on the basis of the crank angle and the combustion analysis values are calculated accordingly. The layout shown in **Figure 1** has the disadvantage that the sampling frequency varies with engine speed. This

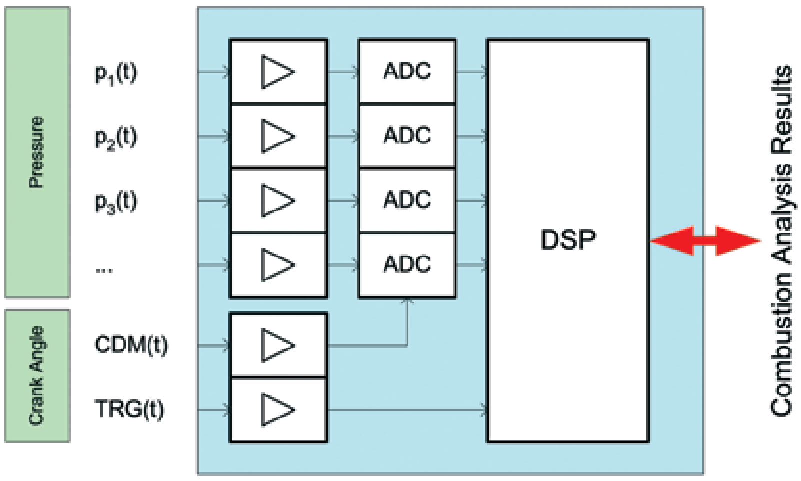

Figure 1: Structure of a combustion analysis system

The Authors

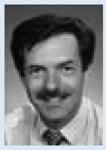

Dipl.-Ing.
Heinz Jenny
is Head of Electronics Development and Project Manager of the KiBox with Kistler Instrumente AG in Winterthur (Switzerland).

Dipl.-Ing.
Wolfgang Sailer
is Product Manager in the Business Unit Engines with Kistler Instrumente AG in Winterthur (Switzerland).

Dipl.-Ing.
Thomas Walter
is Head of the Business Unit Engines with Kistler Instrumente AG in Winterthur (Switzerland).

Figure 2: Measuring spark plug and glow plug adapter with sensor for the measurement of combustion pressure

means that it is more difficult to obtain typically time-related evaluations (e.g. filtering and spectral analysis).

3 In-vehicle Combustion Analysis

The environmental and operating conditions of an in-vehicle combustion analysis system differ significantly from those of an engine test stand. The main requirements of an in-vehicle combustion analysis system may be summarized as follows:

- compact design
- resistant to harsh operating environment conditions
- use of engine-mounted crank angle position device
- operation with vehicle supplied electrical power
- fast and simple installation
- easy parameterization and operation
- reliable acquisition of measured values, even with transient engine operation
- simple integration into the calibration system.

Unlike typical engine test stand operating conditions, transient engine operating states are predominating on the road. With the use of an in-vehicle combustion analysis system, it is important for the calibration engineer to be able to assign the combustion analysis values to the engine control variables with high certainty. Only then it is possible, for example, to identify a direct relationship between interventions of the engine controller (cause) and misfires (effect). This means that the integration of the in-vehicle combustion analysis system with the engine calibration system is an essential precondition for engine calibration and trouble-shooting to take full advantage of in-vehicle combustion analysis.

3.1 Mounting of Cylinder Pressure Sensors

The deployment of in-vehicle combustion analysis technology is generally characterized by poor accessibility and restricted space for the components to be mounted. Mounting must be both time-saving and adapted to the harsh operating conditions in the engine compartment. In addition, it is important that the operation of all components should be simple and should not require any great efforts for parameterization. The use of measuring spark plugs [1] and glow plug adapters, **Figure 2**, permits high precision combustion pressure sensors to be mounted in the existing combustion chamber access points without need for additional preparation work.

3.2 Engine-mounted Crank Angle Position Device

The installation of an optical crank angle encoder for an in-vehicle engine has generally been very time-consuming. However, now that all vehicle engines are supplied with a trigger wheel and a Hall or inductive sensor to acquire the crank angle position for electronic control purposes, it is possible to use this crank angle position device also for the purpose of in-vehicle combustion analysis. **Figure 3** shows a typical 60-2 trigger wheel with a Hall sensor. With a 60-2 trigger wheel, there is a resolution of 6 °CA or 18 °CA at the mark gap. The gap

Figure 3: 60-2 trigger wheel with Hall sensor

is for synchronization. As a rule, engine combustion analysis requires a crank angle resolution of 0.1 °CA. To increase this resolution by a factor of 60 or 180 while ensuring a high degree of reliability, even under transient engine operation, is a demanding task.

3.3 Interfacing with the Engine Calibration System

The objective of calibration is the optimization of control functions of the ECU. The algorithms of the control functions are programmed in the ECU. Only the parameter values (maps, characteristic curves, and characteristic values) can be changed. To interpret and optimize these parameters, countless electric and physical signals are measured at the test stand and in test drives, and then evaluated. Many of the calibration target values depend heavily on combustion. The characteristic combustion analysis values permit a rapid identification of the corresponding setting parameter and the di-

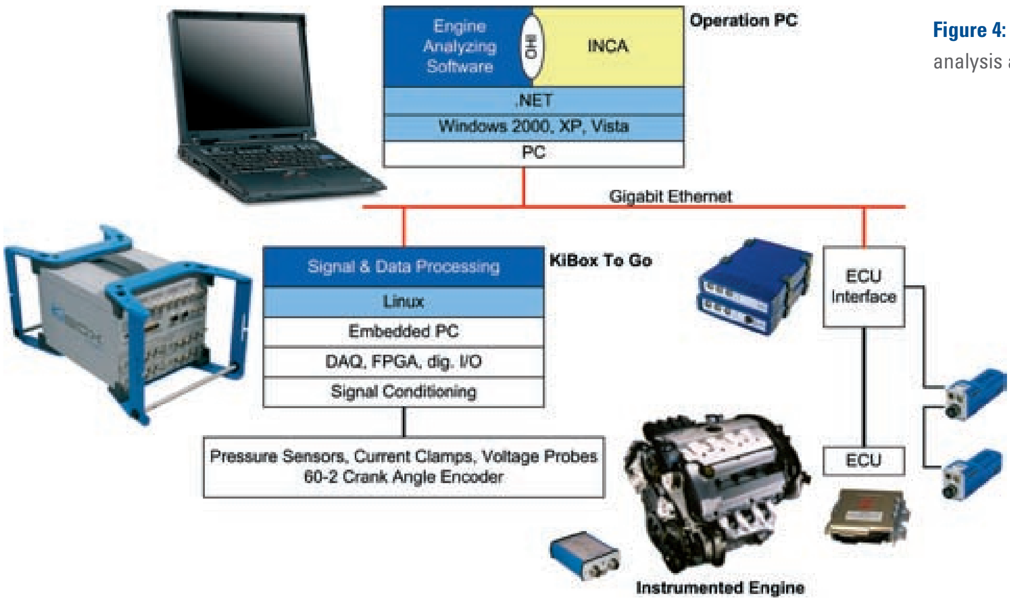

Figure 4: Interfacing of the combustion analysis and engine calibration system

rection and size of the necessary adjustment. **Figure 4** shows the coupling of the analysis system and the INCA calibration system via the INCA open hardware interface (OHI). This arrangement ensures that first class results are obtained much easier and quicker.

4 Data Acquisition and Evaluation

For in-vehicle combustion analysis data acquisition has to fulfill special needs. For example: the engine-mounted crank angle position device has to be continuously monitored. At the same time, the highly transient engine operation must be measured and the naturally present signal interference must be accounted for.

In 1991, Kistler began developing the first control monitor device for integrated process monitoring in manufacturing. The “CoMo II” digital measuring system records two time-discrete measurands. In press-fit processes, for example, this includes press force and displacement. The transformation for the force versus displacement evaluation as well as the display of the measurement data and cycle-related values takes place in real-time. Since the first version, several generations of Kistler‘s devices, some of them with more than two channels, have been brought into the market worldwide. These devices permit universal parameterization and are deployed for the monitoring of processes of all kinds. For this purpose, sampling rates of up to 10 kHz are sufficient. The principle of time-discrete sampling is ideally suited to fulfill the requirements of a modern combustion analysis system. It permits the correction of phase shift of measuring signals, signal filtering in the time domain and the transformation of measuring signals into the angle domain. Due to the high engine speeds and the high precision required, extremely high sampling rates are needed. Commercial availability of very powerful data acquisition and data processing devices now made it possible to build a compact combustion analysis system for in-vehicle operation using this principle.

4.1 Data Acquisition

The central requirement of multi-channel data acquisition systems is that the analog signals – in the present case, the cylinder pressures, the injection signals, the ignition signals and the crank angles – have to be acquired simultaneously and in-phase with the least possible delay. Otherwise, it is impossible to obtain correct comparisons and calculations. Even signal run time differences of two to three microseconds can have a considerable impact on the quality of the results. To avoid aliasing effects, bandwidth limitations are placed on the analog measuring signals prior to the analog to digital conversion. The Shannon theorem is taken into consideration in the digitization of the analog measuring signals. **Figure 5** provides a schematic representation of the data acquisition structure.

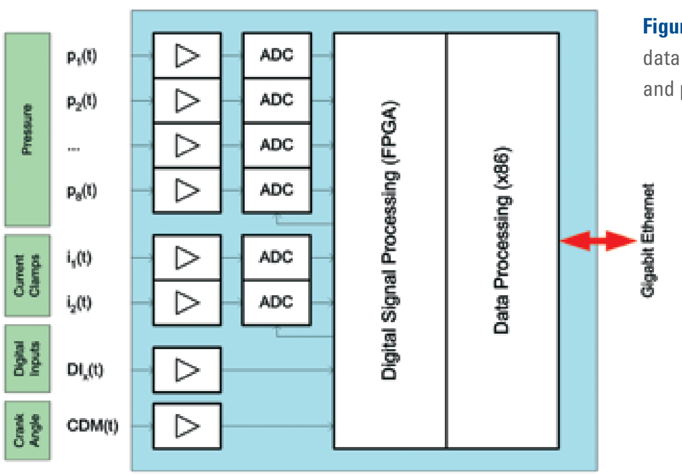

Figure 5: KiBox data acquisition and processing

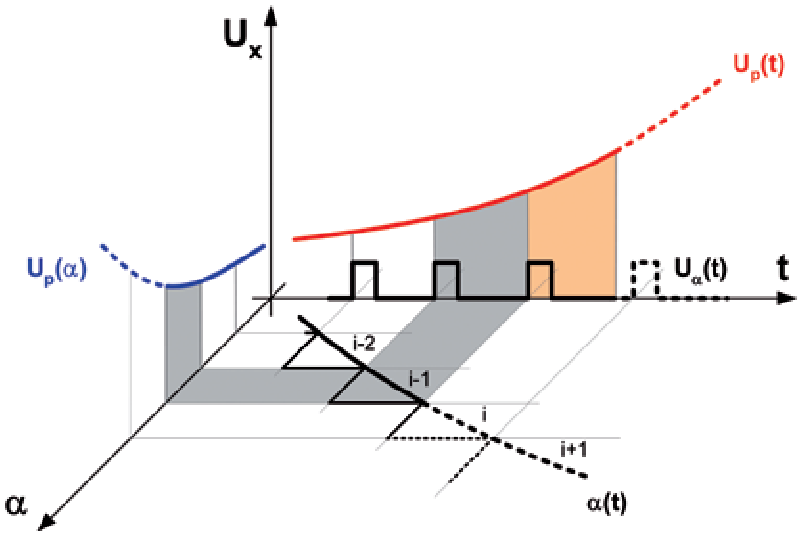

Figure 6: Measurement data transformation of time domain to the angle domain

4.2 Signal and Data Processing

After digitization, the individual delay times of all the measuring signals are corrected. The absolutely synchronous measuring data are then interpolated on a crank angle resolution of 0.1°CA, **Figure 6**. As the interpolation is always executed after the acquisition of a full angle increment (with a 60-2 trigger wheel there is a regular 6°CA or 18°CA at the gap), a correct interpolation is simple. This takes into consideration the irregularity of angular speed of the engines crankshaft. A stream of time and crank angle resolved data is thus available for the calculation of the combustion analysis values. Where necessary, the analog measuring signals can also be filtered on a channel-specific basis using a digital low pass filter before the angle data are generated and, as the time delay of the low-pass filter is known, it can be eliminated easily. As a result, it is possible to have in-phase suppression of interference signals (e.g. from pipe oscillation, or valve impact as shown in **Figure 7**).

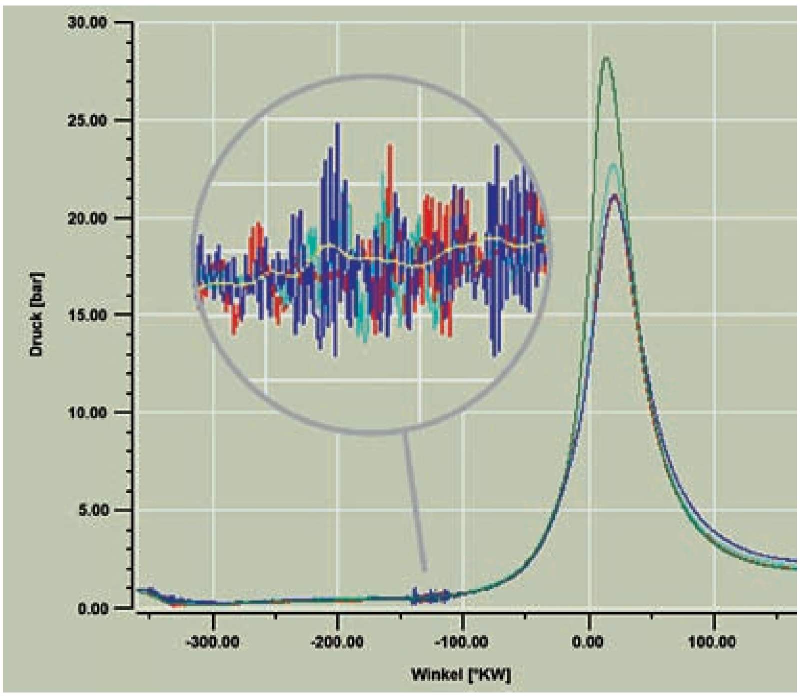

Figure 7: In-phase elimination of valve impact interference with low pass filter (yellow curve)

4.3 Data Evaluation

The evaluation of the measurement data supplies engine developers with the vital combustion analysis values in real-time. The standard characteristic values can be obtained from the cylinder pressure curve p(t) and p(α):

- mean effective pressure IMEP, PMEP and NMEP
- peak pressure pmax and its crank angle position a(pmax)
- energy conversion (heat release), start of combustion, 50 % mass fraction burned (MFB) and duration of combustion
- increase in pressure dp/dα, dp/dt plus maximum increase in pressure and its crank angle position
- combustion noise
- assessment of combustion stability: cycle-to-cycle variation and individual differences between cylinders
- knock analysis.

Through the additional acquisition of injection and ignition timing signals, it is possible to optimize the injection angle InjA(α) and injection duration InjD(Δα) or InjD(Δt) and ignition angle IgnA(α). If intake and exhaust manifold pressures are measured as well, the gas exchange process can also be analyzed.

5 System Parameterization

In view of the need for fast and simple mounting and ease of operation, it is clear that parameterization plays a crucial role. The use of sensors with integrated transducer electronic data sheet (TEDS) permits automatic parameterization of the whole measuring chain. The sensor characteristics stored on an integrated memory are transmitted to the amplifier modules and all of the relevant parameters are set automatically. For example, in the case of cold start testing under very cold conditions, TEDS ensures the avoidance of erroneous results due to incorrect parameterization although the acquisition system has to be installed and removed frequently and correct parameterization of the whole measuring chain is essential from the

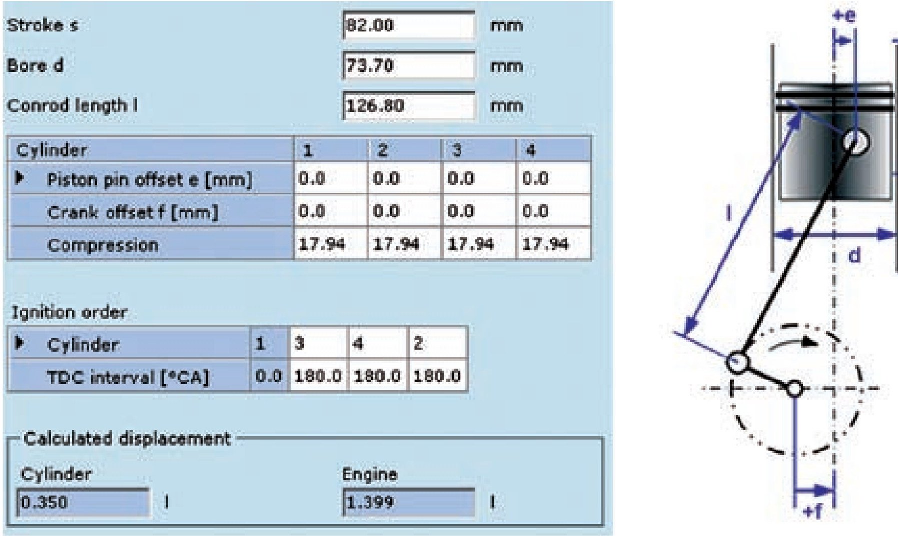

Figure 8: GUI for engine parameters

first attempt. Further functions of the TEDS can also be used, such as the acquisition of the sensor operating hours for purposes of quality assurance and resource management.

The entry of specific engine parameters (bore, stroke, piston rod length, etc.) can be accomplished by reading predefined files or direct entry via the graphical user interface (GUI), **Figure 8**.

As shown in the **Table**, accuracy of most combustion analysis values show a strong dependency on the synchronization between the individual combustion pressure values and the associated crank angle values. The slightest error in the assignment of the correct top dead center (TDC) reference point can cause unacceptable errors. For example, an incorrect angle assignment of 1°CA at an indicated mean effective pressure of 10 bar can generate a NMEP error of 0.3 bar. The approximate percentage error over the NMEP stands at around 3 %.

6 Use of In-vehicle Combustion Analysis in the Engine Calibration

This section presents a number of examples of the use of in-vehicle combustion analysis for engine development and engine control calibration.

6.1 Cold Start

The optimization of the few individual working cycles when starting the engine is important to ensure a high degree of operating reliability and low degree of pollutant emissions. This means that combustion analysis is a vital necessity for the determination of cycle resolved measurement of the starting process [2]. An evaluation based on external sensors is, in principle, inadequate due to the distance from the process, low time resolution and lack of time versus working cycle reference. The evaluation is confined exclusively to visual assessment in the crank angle domain by considering pressure curves in combination with the actual engine speed and the injection or ignition timing.

For the assessment of combustion, it is essential to know the combustion efficiency [3], which relates the quantity of fuel supplied to the quantity of fuel actually burned per working cycle. In addition, the current engine speed and the NMEP trend over the working cycles are used to assess the idle quality of the engine.

6.2 Drivability

The optimization of drivability requires tuning between the driver‘s torque requirement (accelerator pedal position) and the reaction of the engine (NMEP). What is sought is the smallest possible delay in implementing the driver‘s torque requirement. The criterion for the build-up of torque is the increase in NMEP per working cycle taken from the combustion analysis, as exemplified in

Table: TDC reference point accuracy for relevant combustion analysis values

Combustion analysis values	Accuracy TDC reference point
Peak pressure p_{max} (peak-peak)	No need, except cycle identification
Peak pressure $\alpha(p_{max})$	Average accuracy (≤ 0.5° CA)
Ignition angles	Average accuracy (≤ 0.5° CA)
NMEP, and statistics for NMEP (misfire, cycle-to-cycle variation)	High accuracy (≤ 0.1° CA)
Beginning of injection (for DI)	High accuracy (≤ 0.1° CA)
Beginning of combustion, 50 % MFB	High accuracy (≤ 0.1° CA)
Average frictional pressure FMEP	High accuracy (≤ 0.1° CA)
Knocking intensity	Low accuracy because the TDC reference point is necessary only for determination of the evaluation window
Combustion noise level	No need, except cycle identification

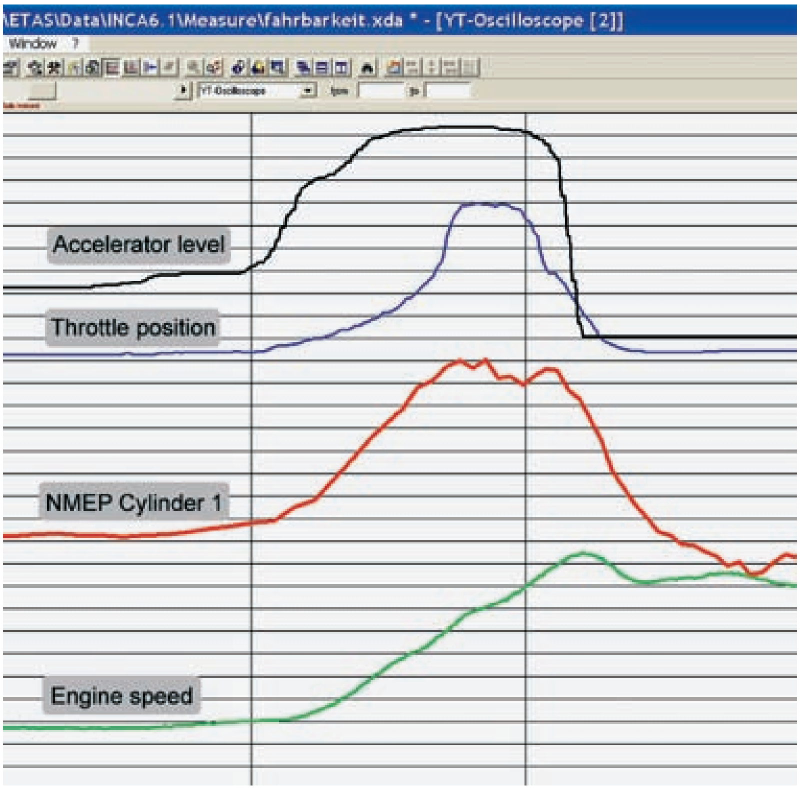

Figure 9: Illustration of acceleration in the INCA system

Figure 9. The accelerator pedal position is shown in black, the throttle position in blue, the engine speed in green and the NMEP curve during an acceleration process in red.

Through overshoots, transient on-road operating conditions harbour the potential to generate critical safety conditions that do not arise under normal test-bed operation. Typical examples of this are peak pressure being exceeded or heavy knocking in individual working cycles. These conditions can be quantified and analyzed only with the help of combustion analysis and reduced or avoided altogether through the proper adjustment of the control parameters.

6.3 Trouble-shooting

Mobile combustion analysis is an extremely valuable tool for rapid combustion analysis and safeguarding of the calibration in trouble-shooting during on-road trials. The transfer of the combustion analysis values into the INCA calibration system and the synchronous display of the working cycle with engine control parameters permit fast and efficient identification of malfunctions and perturbations.

The synchronous display of the pressure and heat curve facilitates trouble-shooting with engine problems (e.g. compression or injector problems). This display is particularly useful for the optimization of combustion parameters during on-road trials. Modifications in the calibration data of the engine and associated effects on combustion stability, are immediately displayed and quantified. In the case of diesel engines, for example, the strategy for the regeneration of a particle filter is quickly optimized (definition of injection timing). It is also possible to quickly detect any inaccuracies in the calibration data set (e.g. consideration of cylinder pressure and exhaust gas temperature before turbo charger) or to check the calibration data set of the engine under dynamic operation and test drives in hot/cold regions, or high/low altitudes, or in operation with a trailer. The ECU values and the combustion analysis results are inherently synchronized within each engine cycle, providing immediate results to the display without the need for manual synchronization.

7 Summary

KiBox, the new combustion analysis system from Kistler Instrumente AG, was developed particularly for in-vehicle operation. Under real driving conditions, the system provides the ability to execute combustion analysis in real-time and provides combustion analysis data with a high degree of accuracy. Due to the use of the engine-mounted crank angle position device and interpolation of the intermediate crank angle values, the crank angle information is presented with high precision and low mounting costs. The integration of KiBox into the INCA calibration system ensures that the combustion analysis values can be displayed and analyzed simultaneously with the engine control actuating values. In short, KiBox represents a mobile combustion analysis tool that ensures an efficient method of working both for engine calibration and for trouble-shooting.

References

[1] Walter, T.; Brechbühl, S.; Gossweiler, C.; Schnepf, M.; Wolfer, P.: Druckindizierung mit Messzündkerzen an einem DI-Ottomotor, Kistler Document 920-333d-09.04
[2] Kufferath, A.; Lejsek, D.; Scherrer, D.; Kulzer, A.: Einsatz der Brennverlaufsanalyse im Motorhochlauf. In: MTZ 67 (2006), no. 6, pp. 434-438
[3] Zülch, C.: Konzepte für einen sicheren Direktstart von Ottomotoren. University of Stuttgart, Dissertation, 2007

The new dimension of information: eMagazines!

One click – all the latest news! Experience our electronic magazines in English. You simply flip through the pages via mouse click. But there is far more to the new electronic magazine:

- **No distribution cost:**
  Every issue delivered directly on to your screen.
- **Keyword search:**
  Find contents by simply entering a keyword.
- **Online-archive:**
  As a subscriber, you will have full access to our online publication database containing all articles from 2000 up to the present.
- **6 issues ATZautotechnology for free:**
  You will also receive 6 issues/year of the FISITA magazine ATZautotechnology in printed form – at no extra cost!

Experience the new dimension of information. Check out your test issue online at: **emagazine.ATZonline.com**

Springer Automotive Media subscription service | Abraham-Lincoln-Str. 46 | D-65189 Wiesbaden | Phone: +49 611.7878-151 | Fax: +49 611.7878-423
SpringerAutomotive@abo-service.info | www.ATZonline.com

Early Damage Detection through Structural Sound Emission Analysis

Durability assessment and prototype testing are absolute prerequisites for automobile products development. In the past, developers were satisfied if a statistical portion out of a large enough group of products would survive field usage. Today engines and gearboxes operate much closer to their physical limits. With the assistance of the Early Damage Detection Technology from Reilhofer KG it is possible to protect engines from otherwise unexpected and severe damage to facilitate the process of analyzing.

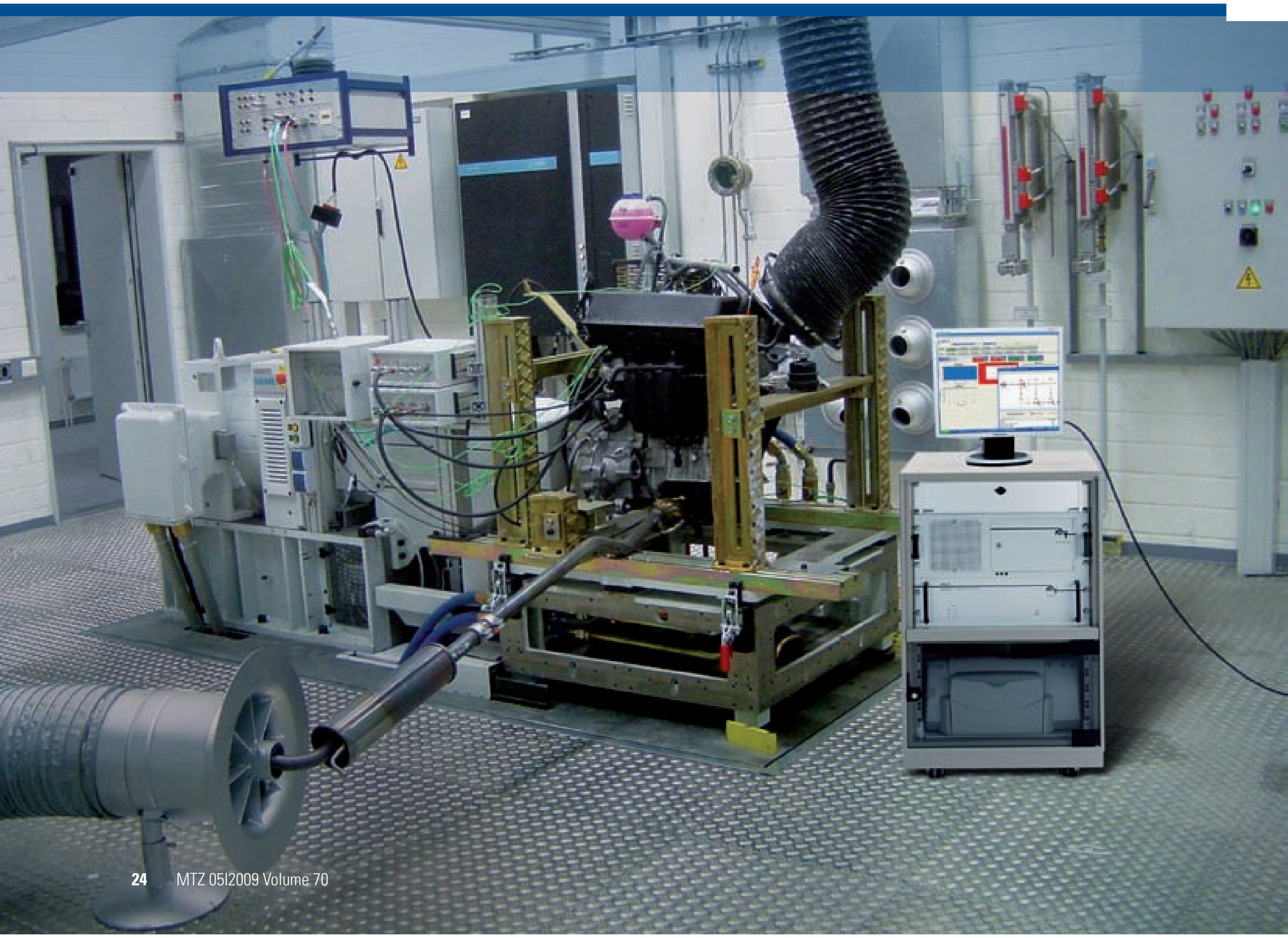

1 Introduction

Today's development focuses on the optimum combination of parameters like material, design and process. Already the first prototype is generally quite well calculated through the use of Simulation programs, but still there is a need for real load testing to reach the final optimisation. This of course costs time – and more costly development time. With the assistance of proper measurement techniques defects can be detected very early, in fact before they develop into permanent damage of the product under test.

Mostly, defects originally appearing as minimal will in time develop into something much more severe, and in extreme cases can small primary defects escalate into secondary defects which will finally destroy a complete engine. Not only is the object under test very expensive but the entire test-rig can also experience considerable consequential damage. When a severe damage has occurred it is almost impossible to identify its origin out of the material pieces. For a completely valid engine test the vibration analysis offers an outstanding technology for a final characterisation of parameter variations, which other methodologies fail to detect. This is the structural sound emission. When the amplitude of the indicated parameter variation becomes large enough, there is a possibility to switch off the test through an alarm relay functionality. It is also possible to relatively simple, and immediately, extract and visualise both the true origin of the damage and the time of its origin, from the collected data. This technology is available through the „delta-ANALYSER" from Reilhofer KG. It has been in usage since 2005 as a supportive technology in the surveillance of engine durability testing at Volkswagen.

2 Methodology

The engine starts to change its vibration pattern at the beginning of a damage scenario. A sensitive diagnostic process recognises the change and causes the test cell to end the ongoing test. A combustion engine can suddenly loose its maximum exhaust pressure from just one cycle to another, and in a totally unpredictable pattern. The mechanical underlying reasons inside the machine are to a large extent embedded in noise. As already explained the engine changes its vibration pattern at the beginning of a defect scenario, but by how much in relationship to the original parameter variation? It would be an all together meaningless task to try and work related to the entire noise picture. The total noise emission always exceeds any parameter variation contribution at the damage starting point by a multiple. It would be equally meaningless to try and use the vibration pattern of an undamaged structure as a reference for comparison. Even two seemingly equal test objects, taken from the same production batch, will show much larger parameter variations between themselves than what would be found as a result of the much smaller variations during the start of a damage process.

To capture the origin of the damage the only possibility is to monitor the change in the individual itself, from its normal vibration pattern and through the parameter variation and on to the beginning damage. The largest conformity is found when the comparison is made to itself. The diagnose system learns the "normal" behaviour of the test object at start up of a test. The test starts with documenting the state of normality and then, later as the test commences, the trend from the initial state is captured.

In doing so it is important to take into account the state of every single spectral line (Order analysis). If a change in the typical amplitude variation of one line is detected, then that is a clear indication for a selective and more in-dept surveillance. Several analysis methods are used in order to correctly understand the true origin of the developing damage process.

2.1 The Order Analysis

The Order analysis produces spectral lines synchronised with the turning speed of a machine. The absolute amplitude of an individual spectral line is of little interest. Of much more interest is the calculation of the build-up of the amplitude distribution of that particular line. A large change in this distribution is a clear indicator of a structural change and a possible start of a defect process.

The Authors

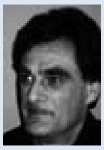

Dipl.-Ing.
Bernd Orend
is Employee in the Aggregate Test Field at Volkswagen AG in Wolfsburg (Germany).

Dipl.-Ing. Ingo Meyer
is responsible for Consulting and Sales at Reilhofer KG in Karlsfeld (Germany).

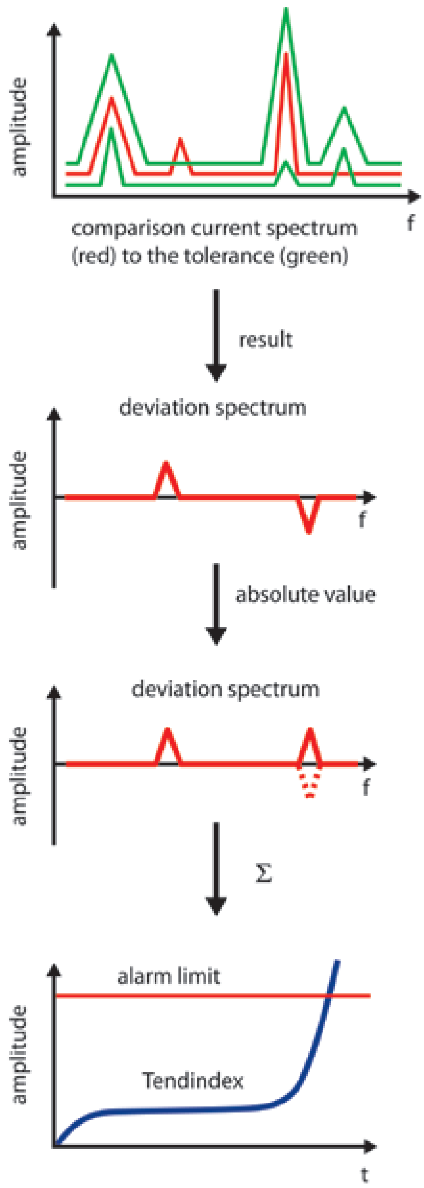

Figure 1: The methodology in four steps

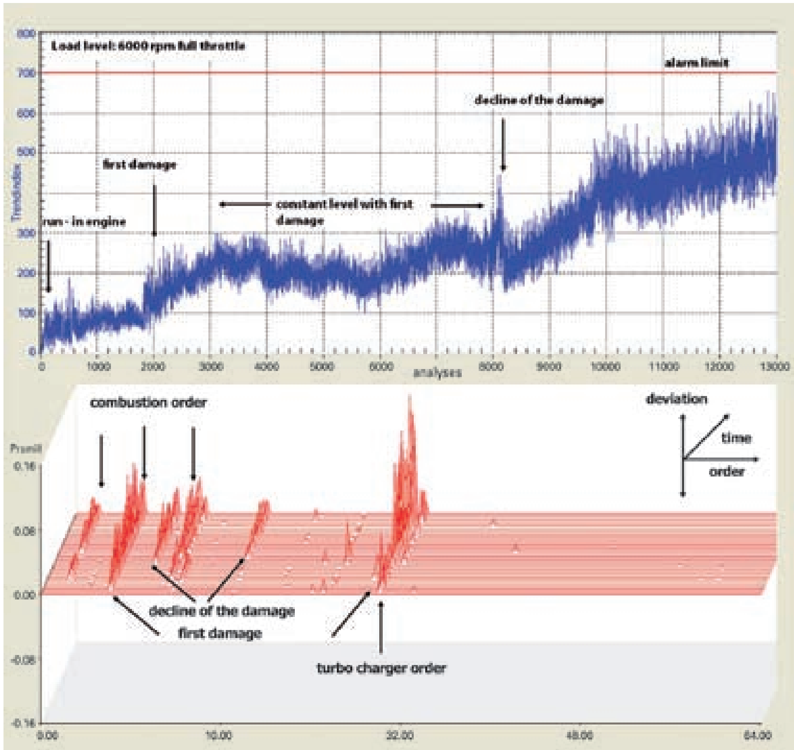

Figure 2: Trendindex and waterfall diagram from a turbo charger damage

2.2 The Frequency Analysis

The frequency analysis shows for example how affected an engine block is regarding its natural frequency. (the build-up of the amplitude distribution).

2.3 The Relative Spectrum

An additional, simultaneous, methodology for frequency and order analysis, which is rather looking at the probability of amplitude distribution changes.

2.4 The Classification

The time series classification provides for every service load point (revolution, torque) a typical pattern for the further statistical analysis.

2.5 "Hunting Wavelets"

The "Hunting Wavelet" recognises irregular phenomena in for example the spring/mass system, which feeds the non linear mechanical excitation. Strokes, grinding and scratching noise, nearly all unwanted effects become visible.

A combustion engine running low revs/loads is quieter than one running high revs. Since a test cycle contains not only one revs step and one load step, but is rather built up of many different combinations betweens revs speed and loads, there is a need for several reference points with quite different tolerances.

In order to correctly characterise all these dynamic revs/load steps and to be able to set fairly small overall tolerances a matrix set of datacards is created, and the varying conditions are all saved in each corresponding datacard.

For each and one of these combinations the natural behaviour is captured (reference value and tolerances) and after this learning phase the surveillance phase is automatically entered. All subsequently captured analysis during the surveillance phase is automatically compared with the learned tolerances and from this comparison a change spectrum is formed, reflecting the rate of change from the learned, normal, behaviour, **Figure 1**. The change spectrum is summed up and presented as the so called trend-index. It expresses the sum of all changes over time and shows the damage process of the engine. This process is further explained in the following examples.

3 Structure

For the measurement at least the revolution of the test object and the vibration from a vibration sensor is needed. Additional analogue/digital or CAN based signals are useful and above all the throttle-valve position and/or torque as well as oil temperature has proven very useful. A suitable location for the vibration sensor can well be in a free threaded hole for some accessory in the lower part of the cylinder head housing.

4 Results from Test Stand

In all following examples the engines have not been prepared with any kind of components prone to failure, or any predamaged material. These tests were selected in order to better understand the connection between the change in vibration pattern and the different types of damage. This connection is in all cases fully represented through the trendindex (change over time) and the corresponding waterfall plot of the change spectrum.

4.1 Turbine Wheel Separation from the Shaft of a Turbo Charger

The turbo charger was the object for this load test. At the start of the main test, the new test object shows just a small run-in phenomenon (Analysis 0 to 300), thus the raising trendindex, **Figure 2**, as a result of this effect. After this time there are no larger changes to see until after analysis 1800 when a further change is seen, indicating the initial start of the damaging process of the turbo charger. This initial damage is also clearly seen in the change spectrum, Figure 2, through an increase in order 30. If you compare the revs speed of the crank shaft with the turbo charger speed, order 30 will be extracted. This is derived from the simple calculation; 6000 RPM = Order 1 and 180.000 RPM makes then order 30. (Revs speed from the turbo charger). Over the remaining test time, the energy in order 30 keeps increasing and at the same time the combustion order (order 2) is increasing, as well as several harmonic orders originating from the crank shaft order. This particular damage has developed slowly over a long period of time as also can be seen in the trendindex development and in the deviation spectrum.

4.2 Valve Spring Damage in a V-engine

In this example a valve spring breaks during the test. For a correct identification of the corresponding component order the calculation shown in Eq. (1) can be made.

$$\text{valve order} = \frac{\text{spring eigenfrequency [Hz]*60}}{\text{rotation speed[rpm]}} \qquad \text{Eq. (1)}$$

Through the trendindex development, **Figure 3**, the start as well as the development of the damaging process of the valve spring can be clearly followed.

The damaging process clearly starts at analysis 700 as seen in the trendindex plot. The already at this point outstanding order in the change spectrum corresponds well with the final result.

At a revs speed of 6250 RPM the corresponding order equals 3,56 and the harmonics are seen at orders like 7,12; 10,68; 14,25; 17,81. The test cell was shut down at the time of a complete break down of the valve spring.

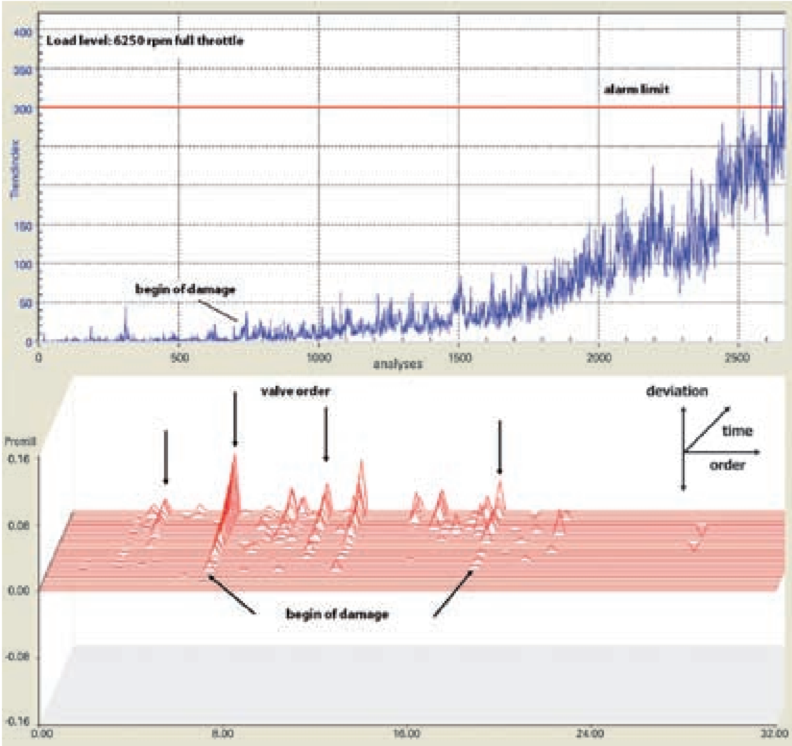

Figure 3: Trendindex and waterfall diagram from a valve spring damage

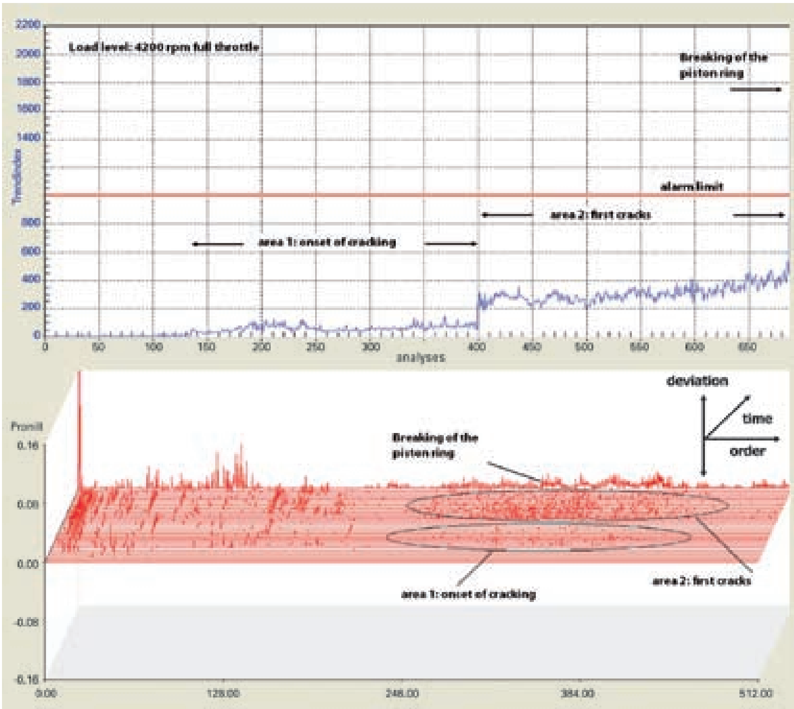

Figure 4: Trendindex and waterfall diagram from a piston ring damage

4.3 Piston Ring Damage

The trendindex development in **Figure 4** reveals two areas of interest. The first area is characterised by a slow increase

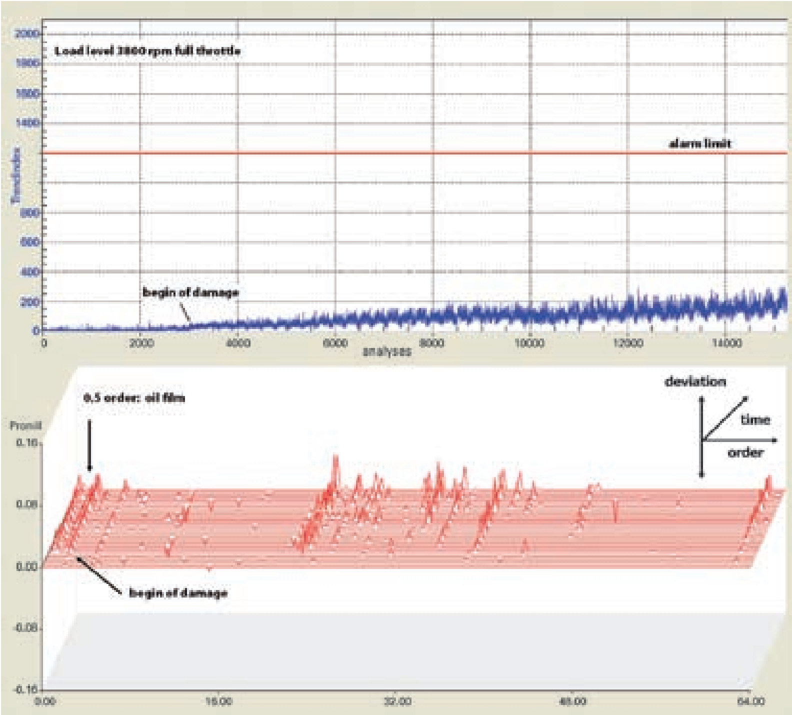

Figure 5: Trendindex and waterfall diagram from a pitting on two connecting rod bearing

(small changes). The second area starts with a trendindex jump and continues with a slow increase until the end. The last steep increase indicates the breaking of the piston ring. In the change spectrum, two concentrated areas are recognised. The first one contains the lower frequencies (left side) and its mechanical origins. The second one contains the higher frequency contributions (right side), from cracks leading to the piston ring damage. In the lower frequency area, orders up to 15 corresponding to frequencies of up to about 1 kHz, the orders are declining, indicating weaker combustions and lower combustion pressure. Acoustically the combustions are getting quieter. In the higher frequency part, orders 250 to over 420 corresponding to frequencies 17 kHz to 30 kHz, the changes are getting increasingly larger. From this process we can conclude that the damage was built up step by step, finally leading to a component failure. No mechanical engine parts can emit frequencies in this range as natural frequencies. These frequencies in the ultra high region can only originate from metallic contacts between different parts. This is also a very clear evidence of friction noise from the fact that the piston ring comes loose in the groove and starts oscillating around its own natural frequency

4.4 Pitting in Two Connecting Rod Bearings

In this test two different pitting processes on two different connecting rod bearings are visualised. The trendindex, **Figure 5**, shows a small increase over the test time. In the change spectrum especially order 0,5 stands out. The changes present themselves not just on the exact order but rather as a broader hill. This phenomenon is a very clear indicator of rotational irregularity, in this case originating from the variations in the lubrication process in the bearing. Always, when the lubrication grease in the bearing reaches the pitting area during each revolution, it looses its “stable” form and travels in the pitting grooves a slightly longer way before it after a short while returns to its “normal” distribution over the bearing surface. Later on the pitting is so severe that the grease can no longer distance the rotating part from the stationary. The lubrication surface breaks down and so the bearing looses its function and the two parts, rotating and stationary, comes into metallic contact. This is the beginning of a friction variation based damage process and the crank shaft order starts to become visible. Since the lubrication grease in the bearing travels basically with half the rotation speed of the crank-shaft the visual order will become 0,5.

5 Benefits and Financial Justification

The „delta-ANALYSER“ has been in usage since 2005 as a supportive technology in the surveillance of engine durability testing at Volkswagen. Since then a large number of units have been protected from secondary damage and more conclusive knowledge as to the correct origin of the damages has been reached. A deeper knowhow in the analysis of structure born vibrations and the corresponding limits for test shut down has been gained. The fact that this has not only lead to valuable time savings but also to significant cost reductions is an outstanding advantage. Also conclusions regarding component durability are made clearer and can be taken as guideline contributions for shortening the associated development time.

6 Looking Forward

Reilhofer KG is presently developing processes for finding the true origin of a structural damage. With a correct pinpointing of the damage place the failure classification becomes much easier. The conclusive knowledge from these tests, with the underlying damage processes and their corresponding orders are taken further into the production system. When the ready developed engines later on are cold- and warm tests in the production system, and defects must be recognised and classified, this knowledge can be gathered and implemented in the production defect pattern recognition system. ■

Lorenz-Knoll-Design

Internet & e-magazines

Benefit from the interactive possibilities of ATZonline. It covers all our publications and offers many useful extra features. Experience the new dimension of information. Get all the information you need digitally and in English as the newly launched e-magazines!

Publications

Read the latest articles on research and developement within the automotive industry on a technical and scientific-based level. Let these sources of information help you boost your carreer and stay ahead.

personal buildup for Force Motors Ltd.

Events

Meet the representatives of the industry at top-class, sectoral conferences sharing experiences and recruiting. ATZlive is your partner for professional continuing education!

A strong fleet of success: Information that keeps you on track!

Since 1898 ATZ is a publication for technically oriented management within the automotive industry – and therefore the eldest automotive publication of the world. An essential source of information for all engineers of automotive construction, worldwide. We have kept his tradition successfully until today. Along the printed publications we launched ATZonline and ATZlive, two additonal stands in the foundation of news coverage and in the exchange of experiences. You will find all information at **www.ATZonline.com.**

Springer Automotive Media subscription service | Abraham-Lincoln-Str. 46 | 65189 Wiesbaden | Telefon +49 611.7878 151 | Telefax +49 611.7878 423 | SpringerAutomotive@abo-service.info | www.ATZonline.com

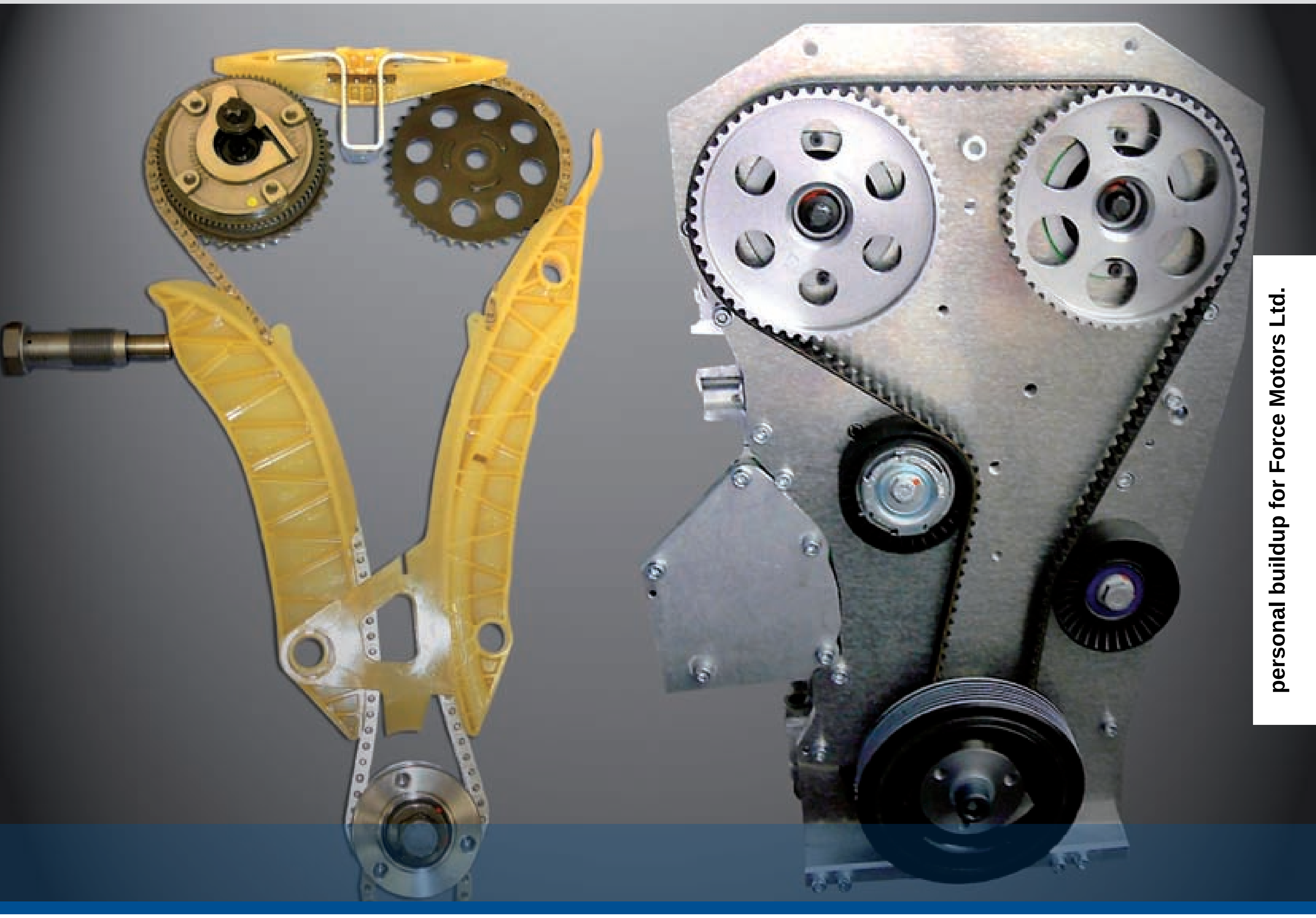

Belt Versus Chain

Study on the CO_2 Saving Potential of the Timing Drive

Regarding the ongoing efforts to reduce CO_2 emissions of internal combustion engines, the potential friction benefits of toothed-belt drives become more important. In the course of the present study – which has been carried out by FEV on behalf of the belt drive system suppliers Contitech, Dayco and Gates – differences between chain and toothed-belt drives, with respect to friction, as well as noise-relevant excitations were quantified based on test bench investigations, also, the impact on fuel consumption and NVH was evaluated.

1 Introduction

Today, the camshafts of internal combustion engines, produced for passenger car engines, are almost exclusively driven by toothed belt or chain. Even though European engines are most commonly fitted with belt drive systems, within the last decade, however, chain driven systems have risen in popularity in engine development processes, as chain meets the demand for a maintenance-free service life. In the meantime, manufacturers of toothed belts were able to develop timing drives for both gasoline and diesel engines which are maintenance-free during their entire service life [1].

Due to its favourable damping characteristics, the utilization of a toothed belt has a positive effect on the engine's acoustic behaviour, and, in comparison with the chain, it is able to absorb dynamic load peaks without being subject to irreversible, wear-induced elongation. Furthermore, resulting from the potentially lower friction of toothed-belt drives, there is the chance to reduce CO_2 emissions. The aim of the investigations described in the following was to quantify this CO_2 saving potential.

2 Test Engine Set-up

As a test engine for the measurements of friction behaviour and noise-relevant excitations, a current, on the market, European 1.6 l in-line four-cylinder gasoline engine was selected as the reference engine.

The timing drive of the reference engine is a one-stage chain drive with an 8 mm pitch single strand roller chain. The tensioning rail is positioned on the slack side of the system and there are two guide rails, one positioned between the two camshaft sprockets, the other between the exhaust camshaft and the crankshaft, these are made of plastic. The hydraulically actuated chain tensioner is located in the cylinder head within the cast-on chain case, **Cover Figure**.

Upon completion of base line reference measurements, the engine was converted to a belt timing drive. Converting the engine, the cast-on chain case was removed and in its place, a carrier plate was mounted, this served as a sealing element for the front of the engine and onto which the idler and tensioner pulleys were fixed, Cover Figure.

The employed toothed belt material is made up of heat resistant and non-aging „HNBR" high-performance elastomer (Hydrogenated Nitrile Butadiene Rubber) with fibre reinforcement and a high-strength glass cord tension member as well as a polyamide fabric surface for increasing the belt's wear resistance.

3 Chain/Belt Drive Dynamics and Friction Measurements

In order to measure the torsional vibration of the camshafts and the crankshaft, all of the timing chain sprockets (respectively belt pulleys) were fitted with high-resolution speed and angle of rotation sensors. Subsequently, the dynamic behaviour of the timing drive was documented in an engine speed run-up.

The friction investigations were conducted according to the „strip method", where the engine is driven by an electric motor. Successively, the engine components or modules under investigation are demounted or shut off one after the other. The friction losses induced by the various components or modules can then be deduced from the differences in friction observed between the measurements.

4 Vibration Measurements to Predict the Engine's Acoustic Behaviour

The various excitations induced by the belt and chain drives have an influence on the engine's acoustic behavior. As the prototype of the belt drive engine realized for the present project is not representative for an NVH optimized series production solution, a direct comparison of the noise radiation of the two engine variants would not lead to any conclusive results.

Therefore, in order to obtain insights on the acoustic effects of the employed timing drive variants, vibration measurements of the engine structure were performed, which allow an assessment

The Authors

Dipl.-Ing.
Christof Tiemann
is Senior Project Manager in the Division Design at FEV Motorentechnik GmbH in Aachen (Germany).

Dr.-Ing.
Christoph Steffens
is Department Manager Powertrain NVH at FEV Motorentechnik GmbH in Aachen (Germany).

Dipl.-Ing.
Stefan Wedowski
is Department Manager Gasoline Engines and Powertrain Application at FEV Motorentechnik GmbH in Aachen (Germany).

Dipl.-Ing. Ralf Walter
is Manager Advanced Synchronous Tensioner Development at Gates GmbH in Aachen (Germany).

Dipl.-Ing.
Hermann Schulte
is Manager Research & Development for Toothed-Belt Drives at ContiTech Power Transmission Group in Hanover (Germany).

Dr.-Ing Tommaso
Di Giacomo
is Director Research & Development at Dayco Europe in Chieti Scalo (Italy).

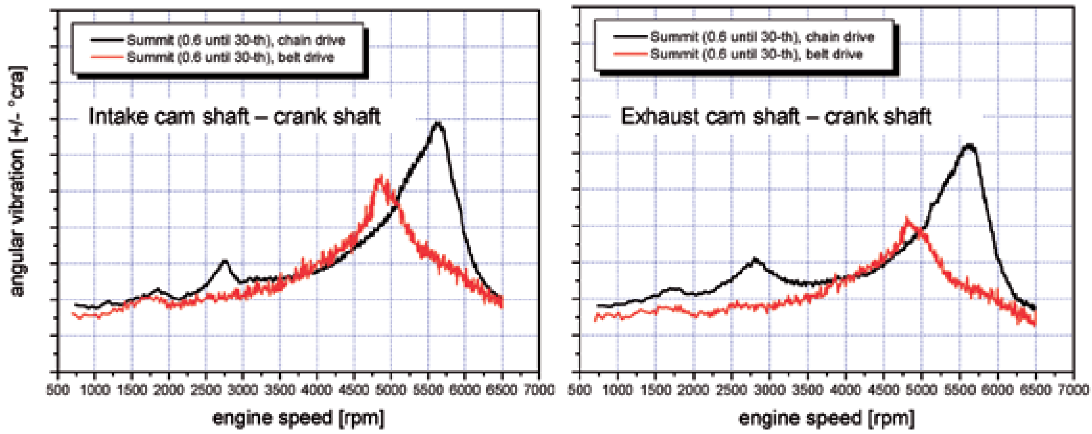

Figure 1: Angular vibration (differential angle) of intake and exhaust camshafts versus crankshaft

of the structure-borne noise excitation and its transfer within the structure. For the measurements, the two engine variants were equipped with acceleration sensors, which were positioned in relevant areas of the timing drive as well as on representative noise-radiating surfaces, allowing the measurement of excitations and their attenuation through the structure during engine speed run-ups under motored operating conditions.

5 Results of the Comparative Measurements

5.1 Chain and Belt Drive Dynamics

As part of the dynamics and friction measurements, different belt drive versions were investigated. These belt drives varied pulley diameter, belt geometry and system pre-load as well as idler and tensioner pulley positions.

Figure 1 shows the angular vibrations (differential angle between crank shaft and intake respectively exhaust camshaft) of the selected belt drive layout in comparison with those of the chain drive. The eigenfrequency of the belt drive is moved toward lower engine speeds, and the resonances induced by the chain drive at approximately 1750 rpm and 2750 rpm are barely visible for the belt drive. In large sections of the engine speed range, the vibration amplitudes of the belt drive are smaller, especially for the exhaust camshaft. For a series production solution, the speed range between 3500 rpm and 5000 rpm offers potential for optimization.

5.2 Chain and Belt Drive Friction

Analyzing the results of the friction measurements, all of the investigated belt layouts turned out to be either equal to or more favourable than the chain drive. Thus, for the belt system optimization, it was possible to focus on parameters essential to component durability.

Figure 2 shows the results of the friction analysis of the valve train. By utilizing a belt-driven valve train, it was possible to improve on the engine‘s friction behaviour in the entire speed range, at times quite distinctly. The friction benefits of the belt in the lower to medium engine speed range amount to approximately 0.04 bar.

The benefits of the belt drive are due to the friction characteristics of the guidance and tensioning elements of the timing drive which are basically more favourable: With a belt drive, it is possible to utilize low-friction rollers, whereas chain drive systems typically employ sliding contacts. Moreover, the friction conditions of the contact surfaces between the belt and the pulleys are more favourable than those between the chain and the sprockets. The scatter bands for chain and belt drives displayed in Figure 2 illustrate these basic benefits of the belt drive.

Furthermore, for the reference engine under investigation, the resonance at 5500 rpm already observed in the dynamics measurements adversely affects the chain drive‘s friction behaviour.

5.3 Vibration Measurement to Predict Acoustic Behaviour

An overview of the impact on the vibration behavior due to the replacement of the timing drive is provided by the overall level at the respective measuring locations. As an example, **Figure 3** shows the

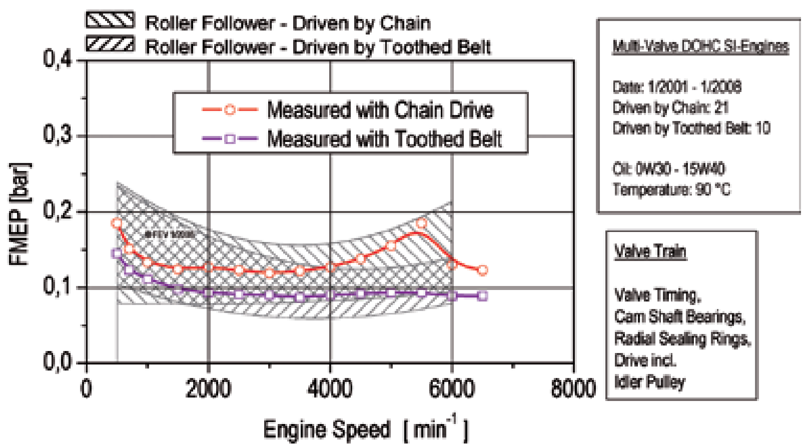

Figure 2: Valve train friction at 90 °C

results of the measurements of the timing drive-induced excitation at the first camshaft bearing, one point on the outer cylinder head surface close to the source location, and one point on the outer engine block structure in the area of cylinder 2. By means of these measuring points, the source of the noise-relevant excitation and its transfer paths can be examined and evaluated.

For the measuring point in the area of the location of the excitation source (in this case, the vibration of the first exhaust-side camshaft bearing), the difference in overall noise level for the two variants is pronounced.

Almost throughout the entire engine speed range the benefits (up to 5 dB) of the belt drive engine can be observed. Due to its higher (material) damping capability and its more elastic coupling, the vibration excitation is on a lower level combined with a more broadband character. Furthermore, it can be observed that the vibration behavior of the belt drive engine is affected by resonance effects to a lesser extent.

At the measuring locations more distant to the excitation source location, in many areas the detected acceleration levels were also distinctly lower for the belt drive concept. On the other side it must be noted that in the speed range above approximately 3500 rpm the level of the variants converge.

In order to arrive at a root cause analysis, the measuring data were analyzed with regard to the frequency content. To do so, the gear meshing order level of the variants were investigated. The analyses reveal that the relevant order level of the chain drive were closer to the overall level than those of the belt drive. For the chain drive it is even possible to identify certain engine speeds at which the overall level is largely determined by the gear meshing orders.

In summary, it can be concluded for the investigated engine that the belt drive variant tends to show a more favorable acoustic behavior with regard to mechanical noise. The actual acoustic benefit, however, cannot be reliably quantified by means of the present investigations. It becomes clear that the NVH development process for a chain drive engine requires more attention and care. In that context, the timing drive components have to be carefully designed with regard to noise excitation, and the design of the housing structures has to take into account the structures' noise and vibration transfer behavior.

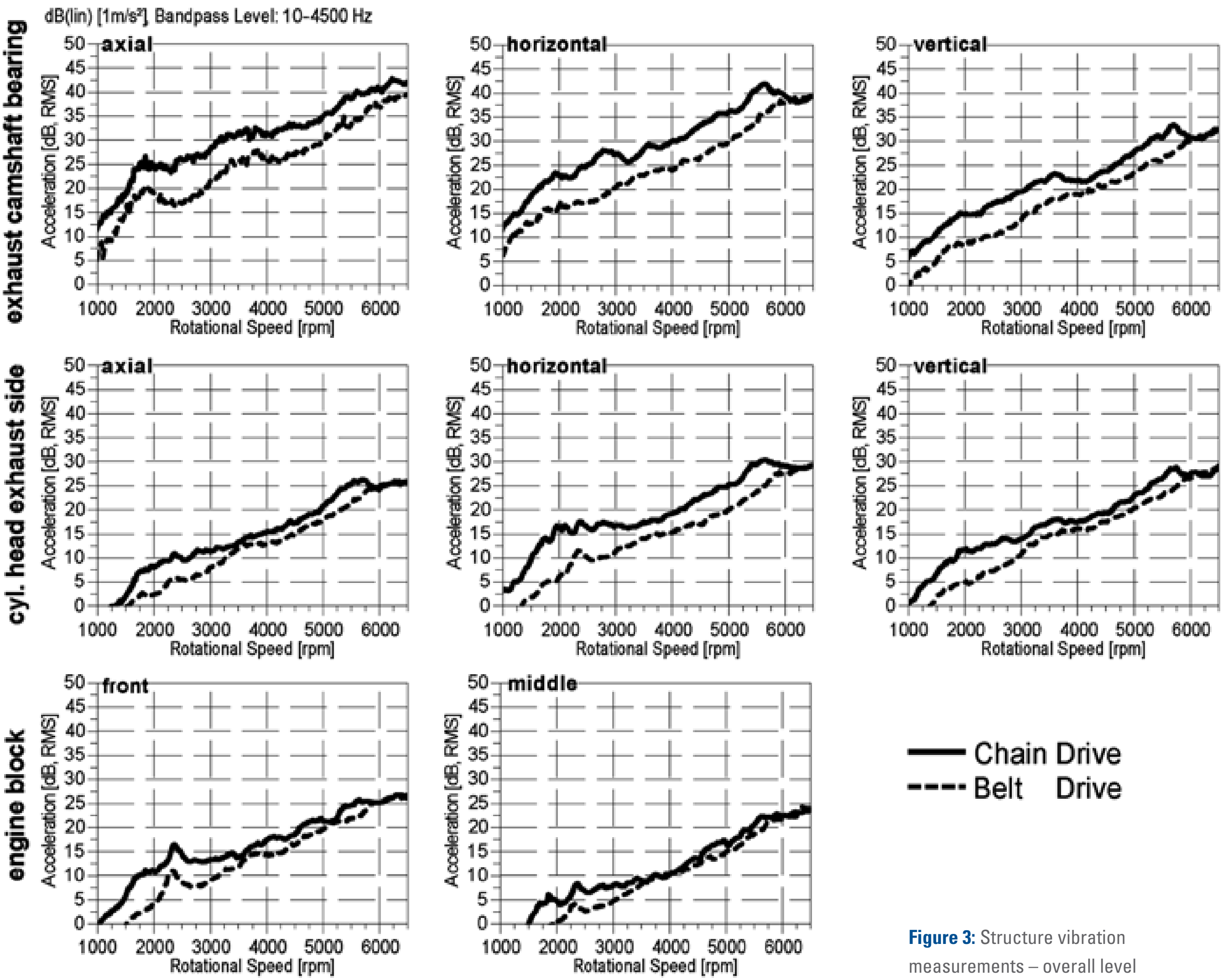

Figure 3: Structure vibration measurements – overall level

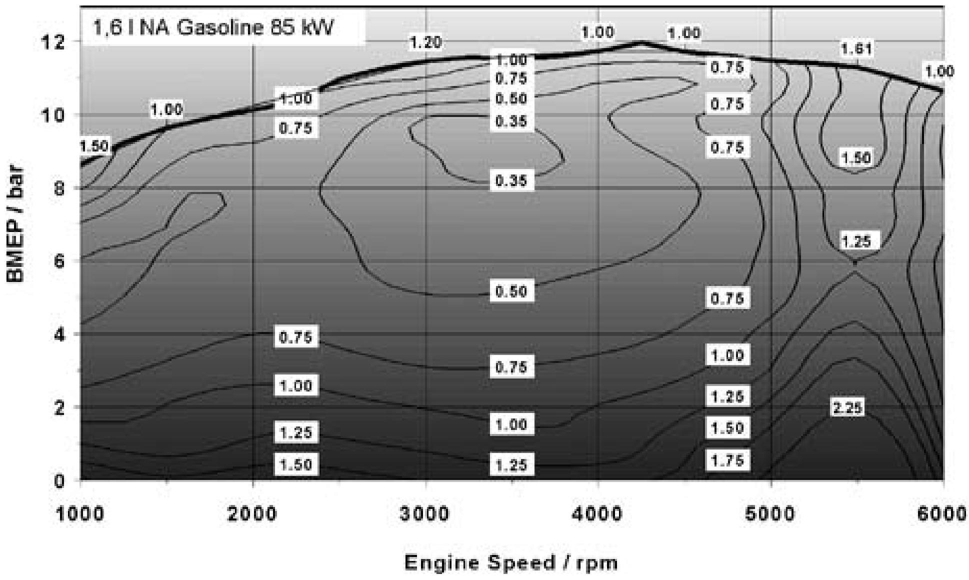

Figure 4: Relative fuel consumption benefit in percent of the belt drive compared to the chain drive in stationary operating points

6 Prediction of Differences in Fuel Consumption

Figure 4 shows at first, the map of the consumption benefits resulting from the friction reduction at steady state operating points, based on the fuel consumption map of a naturally aspirated 1.6 l gasoline engine producing 85 kW.

Due to the fact that friction behaviour – by contrast with combustion and gas exchange behaviour – is largely independent from engine load, the relative friction contribution increases with reduced engine loads. Thus, the positive effect of reduced friction losses at constant engine speeds is especially marked under part load conditions.

The fuel consumption map also takes into account the load point shift with the reduction of friction losses. At low loads, the positive effect of the friction reduction is counteracted by an increase in fuel consumption through the displacement of the operating point towards lower efficiencies. In the area of very high loads, this effect is reversed, as the load point is displaced in the direction of more favourable efficiencies. Due to lower enrichment requirements, this effect is especially pronounced for the full load curve.

At 5500 rpm, as a result of the resonance effect induced by the chain drive, a comparatively high fuel consumption benefit can be attested for the belt drive system.

Drawing on the attested consumption improvement in the engine map, Figure 5 shows the consumption reduction potential under constant-speed driving conditions at various driving speeds.

Along with increasing engine speeds and loads at higher vehicle speeds, the fuel consumption improvement potential diminishes according to the mechanisms discussed in the context of the engine map. At maximum speed, however, the consumption benefit is again more pronounced, which is due to the resonance effect as well as the favourable load point shift.

The above diagrams illustrate that the fuel consumption benefit depends on the dwell times in the various areas of the engine map. Thus, the CO_2 reduction potential is separate from the driving profile, also, a function of the specific engine-vehicle combination.

With regard to the aforesaid, therefore, exemplary NEDC calculations were carried out for different vehicles, Figure 6. In general, the consumption benefits increase with decreasing engine weight, as the proportion of low-load operation increases. For vehicles equipped with the

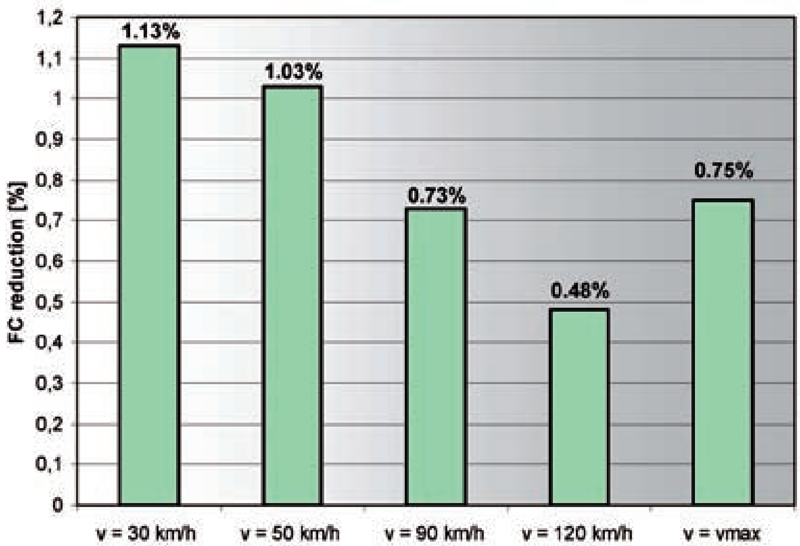

Figure 5: Fuel consumption benefits of the belt drive at constant vehicle speed (1.6 l NA gasoline engine, vehicle weight 1150 kg, six-gear manual transmission)

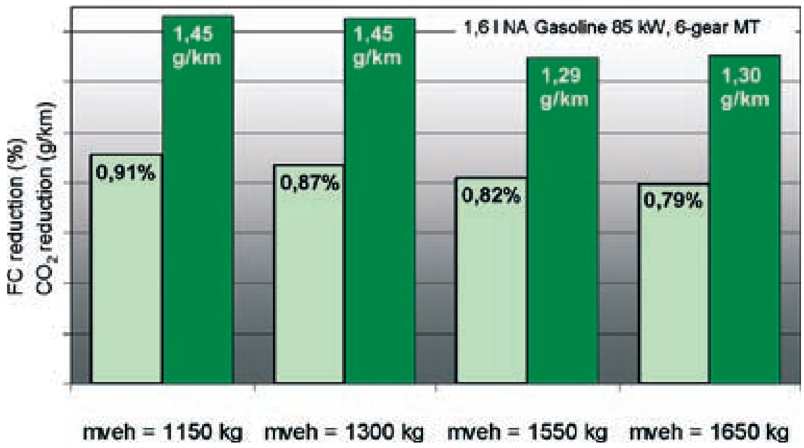

Figure 6: CO_2- and fuel consumption benefit of belt drive in NEDC for different vehicle weight

1.6 l 85 kW naturally aspirated gasoline engine, consumption benefits of between 0.79 and 0.91 % respectively a reduction in CO_2 emission from 1.29 to 1.45 g/km were achieved.

7 Summary and Conclusion

The overall engine friction of the investigated 1.6 l gasoline engine can be reduced in the medium engine speed range by approximately 0.04 bar by replacing the chain drive with a belt drive. The reduction in friction losses observed in the present investigation confirms other studies [2, 3] as well as the predictions from benchmark investigations; thus, it can be generalized for similar engines. The dynamic behaviour of the prototype belt drive is comparable to the reference chain drive; for a series production solution, further optimization potential can be opened up.

The fuel consumption projections indicate consumption benefits of over 1 % for typical steady-state part load operating points. In the NEDC, the CO_2 reduction potential amounts to between 1.29 and 1.45 g/km according to the vehicle/engine combination.

The structural vibration measurement results indicate an improvement potential of the engine‘s acoustic behaviour.

The here presented investigations are showing trends – the belt drive has potential for friction reduction. But as is known, only the detail design is decisive for the real impact on friction and acoustics. Furthermore, for a concept decision belt versus chain drive: for every single engine development process, such a decision must be made under consideration of various factors such as engine/vehicle package, (existing) production lines, costs, synergies with existing engine families or brand philosophy.

References

[1] Schulte, H.: Zahnriemen, Entwicklungsmeilensteine und Innovationen. In: Motortechnische Zeitschrift MTZ (66) 2005 Nr. 12

[2] Körfer, W.; Lacy, F.: Zahnriementriebe und ihre Vorteile hinsichtlich Reibverlusten und Akustik. In: Motortechnische Zeitschrift MTZ (67) 2006 Nr. 7/8

[3] Kyoul, OH.; Plaumann, M.; Romanick, J.; Farmer, I.; Aimone, M.; Barnaby, D.: Performance Comparison between Chain and Belt Cam-Drive Systems. SAE Paper 2001-01-0365, SAE 2001 World Congress Detroit, Michigan, March 5-8, 2001

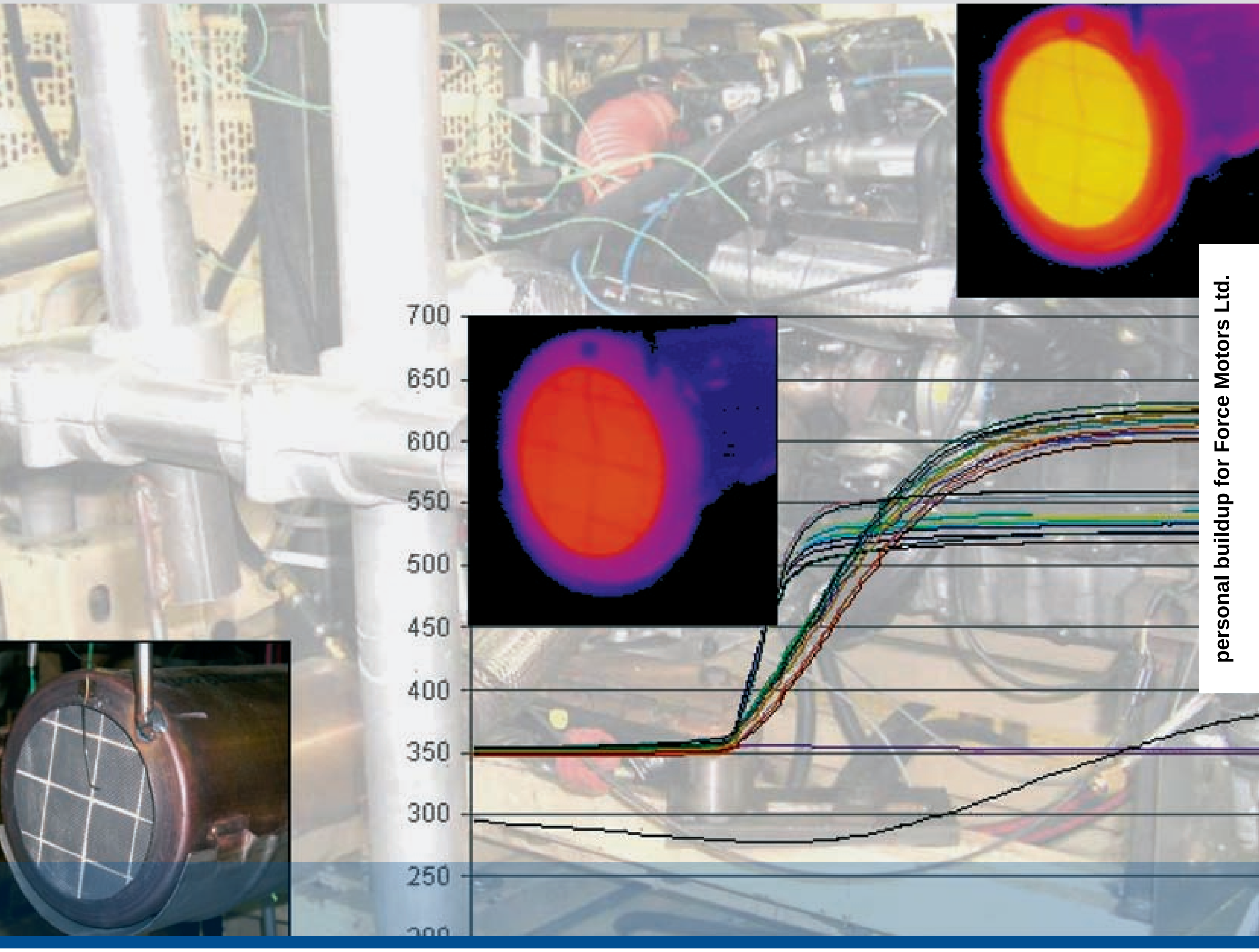

Diesel Vaporizer for Particulate Filter Regeneration

Regenerating a diesel particulate filter requires heat. Therefore, direct diesel dosing upstream the diesel oxidation catalyst is currently being researched. In comparison with engine modifications through post injection, this process avoids oil dilution and it reduces heat loss. This paper describes the joint development project initiated by Beru and Tenneco about direct diesel dosing via vaporizer.

1 Introduction

Both existing and future emission regulations make the use of diesel particulate filters (DPF) in motor vehicles mandatory. The current wall-flow filters must be regenerated at regular intervals because of the constantly increasing soot load. For this purpose the temperature of the exhaust gas is raised to the soot combustion temperature of 600 °C, which burns off the soot accumulated in the filter. In order to avoid partial regeneration, risking damage to the filter, the temperature must be increased independently from the driving condition and over the entire duration of regeneration.

The current state-of-the-art technology is filter regeneration by means of modifications made inside the engine, e.g. to increase the exhaust gas temperature by changing the main injection process. Since this way of increasing the temperature is limited by the admissible turbine entry temperature, the exhaust gas is additionally enriched with unburned diesel by post injection. Downstream the diesel is then converted in the diesel oxidation catalyst (DOC), which leads to a further temperature increase.

As an alternative to post injection it is possible to pass the diesel into the exhaust pipe system directly before the DOC. This results in a number of advantages – it is possible, for example, to entirely avoid the problem of oil dilution. Furthermore, it is not necessary to heat up the entire exhaust gas installation in front of the particulate filter, meaning that heat loss during regeneration is reduced and the thermal inertia of the system minimised. Feeding the diesel directly in addition allows full use of exhaust gas recirculation and moreover offers potential with respect to the regeneration of retrofit filters.

In technical terms, this can be achieved by either an injector or a vaporizer. A direct comparison reveals advantages when using a vaporizer. For example, it can operate without additional cooling, which makes integrating it into the exhaust gas system much easier. At the same time, the evaporating diesel droplets dissipate heat from the exhaust gas, which is why up to 4 % more diesel fuel has to be fed in if an injector is used. Heat losses and the cooling-down of exhaust gases play an important role in particular for engine operating points with low exhaust gas temperatures or a packaging position that is far away from the engine.

In order to allow carmakers to benefit from these advantages, Tenneco and Beru are jointly developing direct diesel feed based on the vaporizer. The two companies can draw here on vast experience in the field of exhaust gas aftertreatment and their comprehensive knowledge of diesel cold start technology. The current state of development is presented and discussed in the following.

2 Diesel Vaporizer

In the vaporizer, liquid diesel flows around an electrically heated glow plug that heats up the diesel and then evaporates it. Because of the increase in volume caused by the phase change, the diesel vapour flows via an outlet into the exhaust gas stream. A standard metering pump controls the fuel amount. Depending on customer requirements, power connection can be made with either single or twin-core cables.

To optimise the surface area for heat transfer as well as to adapt the power performance to the diesel mass flow, use is made of components known as thermal plugs that are fitted with several thermal elements. Beru is able to precisely position the thermal elements inside the vaporizer, as the X-ray photograph in **Figure 1** shows. Furthermore, thermal plugs provide the option to investigate the coke formation in detail. The graph shows three local temperatures for the heating-up phase, the diesel evaporation and the post-conditioning that were measured over time.

3 Test Procedure

A 2.0 l four-cylinder test engine with turbo charger served as the basis for the test series. The standard exhaust gas system

The Authors

Dr.-Ing.
Christian Friedrich
is Supervisor Advanced Engineering Hot End at Tenneco-Gillet in Edenkoben (Germany).

Dipl.-Ing. (FH)
Tobias Inclán
is Development Engineer Advanced Engineering Hot End at Tenneco-Gillet in Edenkoben (Germany).

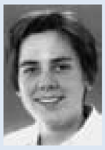

Dr.-Ing.
Birgit Wilmes
is CFD Simulation Engineer Hot End at Tenneco-Gillet in Edenkoben (Germany).

Dr. rer. nat.
Volker Brichzin
is Manager Development Cold Start at Beru in Ludwigsburg (Germany).

Dipl.-Ing. (FH)
Martin Eller
is Project Engineer Media Heating at Beru in Ludwigsburg (Germany).

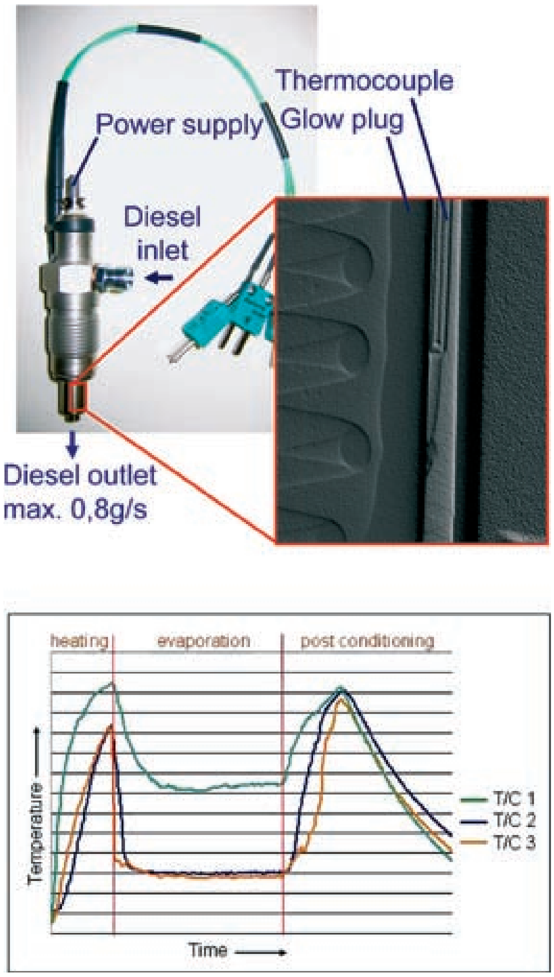

Figure 1: Thermal plug with enlarged X-ray image and temperature curves over the duration of the test

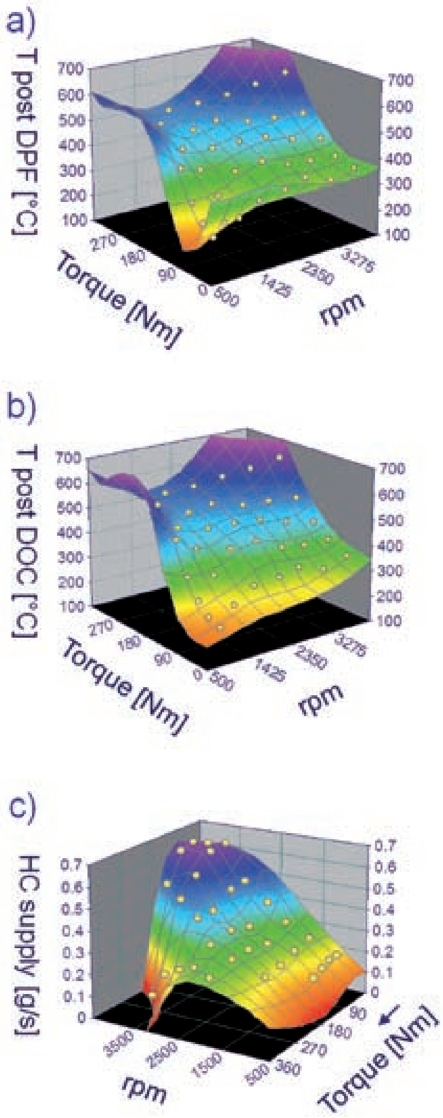

Figure 2: Measurements in serial standard exhaust gas system of the 2.0 l test engine

of the engine conducts the gas through the manifold, the turbo charger and the close-coupled DOC and then cleans it in the DPF that is installed in the underbody. The exhaust gas mass flow and the exhaust gas temperature were measured at several points of the system depending on number of revolutions and torque.

The gas temperatures measured after the DPF in **Figure 2** (a) clearly show that it is necessary to increase the temperature for filter regeneration. The temperature is only sufficiently high in the area around the full load point. As expected, the gas temperatures after the DOC depicted in Figure 2 (b) show a picture similar to the DPF temperature. In addition, we can clearly see that the light-off temperature of the DOC of 200 °C is not reached when the number of revolutions and the torque is low. Since catalytic conversion is not complete below this temperature, hydrocarbons may escape through the exhaust gas system into the environment. For this reason diesel may not be fed in through a vaporizer in this area of the engine map. Nor are engine modifications alone able to ensure a stable regeneration process [1]. However, combining the diesel vaporizer and engine modifications opens up new ways to solve this problem. It is possible to calculate for each operating point the amount of diesel that is necessary to achieve the required temperature increase via the exhaust gas temperature and mass flow. This is shown in Figure 2 (c) and also depends on torque and the number of revolutions.

Another important factor for safe and complete regeneration in addition to increasing the exhaust gas temperature is ensuring that temperature distribution over the cross-section of the filter substrate is as homogeneous as possible. However, only looking at the temperature distribution of the DPF is not always sufficient for development purposes. For example, the DPF in **Figure 3** shows a homogeneous temperature distribution at the same operating point, while the DOC, which is separated from the DPF by a decoupling element, shows a clear temperature peak upstream. Inadmissible temperature gradients increase the ageing of the DOC and may sometimes cause substrate damage that becomes apparent when melting begins to take place in isolated areas.

In comparison with post injection, the diesel and the exhaust gas must mix sufficiently on a shorter stretch when using a vaporizer. For this reason the design of the vaporizer outlet and the optimisation

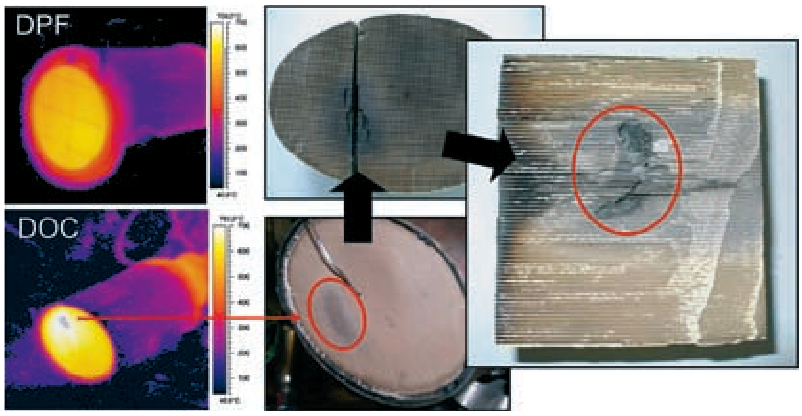

Figure 3: Example of an inadmissible temperature distribution on the DOC

Table: Influential parameters investigated

Boundary conditions	Exhaust mass flow	200-460 kg / h
	Exhaust temperature	200-550 °C
Vaporizer	Outlet	7 geometries
	Installation angle	45-315°
	Penetration depth	0-32 mm
	Orientation	90-270°
Application	Mixing length	0-600 mm
	Inlet cone DOC	2 cones
	Mixer type	2 mixers
	Mixer position	4 positions
	Mixer orientation	2 positions

of the application are of utmost importance. This has a decisive impact on the homogeneity of temperature distribution in the DOC and DPF, in addition to influencing the exhaust gas mass flow and the exhaust gas temperature, conditions that depend on the engine. A summary of all parameters that were assessed up to this point can be found in the **Table**.

In order to make sure that measurements were taken under clearly defined conditions, all test were made in a flow laboratory. Compressors and electric heating elements there allow fast and repeatable measurements under realistic conditions. **Figure 4** shows the exhaust gas system that was used, which is based on the serial standard system of the test engine. However, the serial standard DOC was replaced by a smaller close-coupled DOC and a DOC installed in the underbody. Furthermore, no use is made of a DPF. The modular structure chosen offers the advantage of enabling investigation of all parameters with varying configurations.

Possible measurement methods are thermography or temperature readings using thermal elements. A disadvantage of measuring with thermal elements is that preparation before measurement and analysing the data are more complicated. Furthermore, it is not possible to determine the precise position of a temperature peak. The advantages are dynamic measurements and higher precision. For example, the analysis of local temperature measurements on the substrate surface shows an uncertainty of ± 5 K for the thermal elements as well as ± 15 K for the inserted camera. Since the errors at the individual temperature points cancel each other out, measurement errors for the average temperature $T_{average}$ as well as for the temperature difference ΔT between minimum and maximum temperature on the DOC surface are reduced in both cases. This difference serves as a gauge for the homogeneity of temperature distribution and thus for the mix of exhaust gas and diesel vapour.

4 Results

In the following, three of the large number of parameters tested are presented in detail. Based on thermographic images, the article discuss the use of a mixer, variations in the mixing stretch and the impact of the vaporizer's outlet geometry.

Figure 4: Modular exhaust gas system for the parameter study

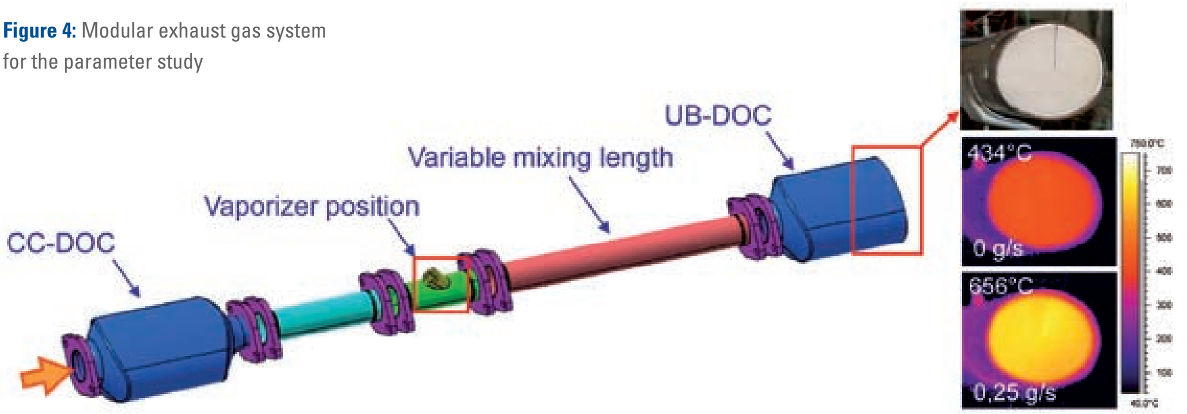

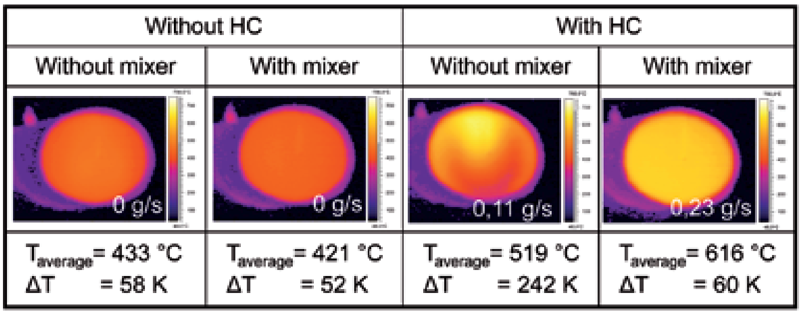

Figure 5: Impact of a mixer with/without diesel insertion

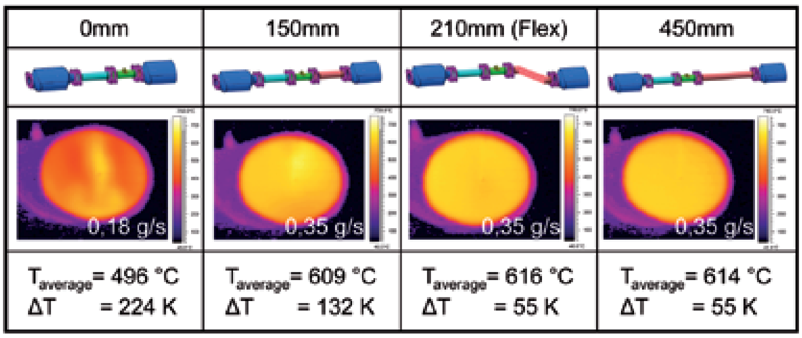

Figure 6: Impact of various mixing lengths with diesel insertion

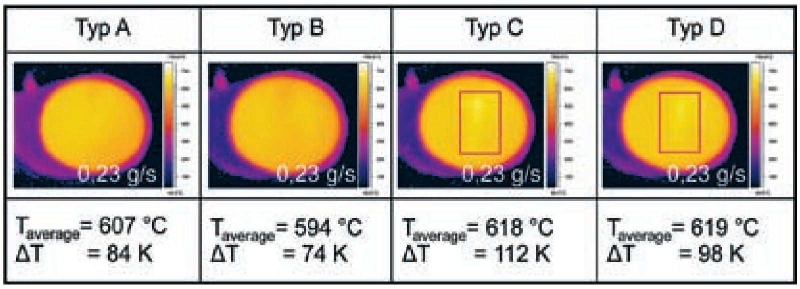

Figure 7: Impact of various vaporizer outlet geometries

Figure 5 shows the images of the DOC substrate surface with an air mass flow of 185 kg/h and a gas temperature before the DOC of 450 °C. Without adding diesel, the measurements with and without mixer vary only slightly. The deviations found for $T_{average}$ and ΔT are within the range of the measurement uncertainty already determined. When diesel is fed in, this behaviour changes substantially. For example, the image without mixer shows high temperature gradients on the DOC surface even with a diesel amount of only 0.11 g/s. This inhomogeneous distribution is caused by an insufficient mix between exhaust gas and diesel vapour. Using a mixer leads to a significant improvement. A diesel amount of for example 0.23 g/s achieves a higher average temperature while the temperature difference is equivalent to the level measured without adding diesel.

Another mixer that is not depicted here show a further improvement in direct comparison, in particular at operating points with larger amounts of diesel. However, this mixer also shows a two times higher pressure loss with a mass flow of 500 kg/h and an exhaust gas temperature of 500 °C. Thus, when selecting a mixer it is important to find the best possible compromise between thorough mixing and pressure loss. Here, use can be made of Tenneco's vast experience in developing mixers for the SCR technology.

Figure 6 illustrates the need to have a sufficiently long mixing stretch. It shows thermographic images of mixing stretches of varying lengths using the example of the operating point with mixer that was already discussed above. Since feeding directly before the DOC does not allow the substances to mix through sufficiently, it is not possible to add the required amount of diesel here. When the mixing stretch is increased to 150 mm or 210 mm, the ΔT clearly decreases under the given conditions while the average temperature remains almost unchanged. However, increasing the length further does not result in any additional improvement. This behaviour was confirmed by the straight mixing stretches of 300 and 600 mm that are not shown here. If a flex-element is used instead of a straight mixing stretch, its wavy interior structure additionally improves the mixing process.

In order to highlight the impact of the vaporizer outlet geometry, **Figure 7** compares four different geometries using the example of a mixing stretch of 150 mm at 185 kg/h and 450 °C. The geometries C and D result in a visible hot strip in the middle of the surface where the escaping diesel is concentrated. The geometries A and B, on the other hand, avoid this effect and thus reveal lower temperature differences on the surface.

The measuring results presented here clearly show that a diesel vaporizer enables an even distribution of temperature on the DOC surface, thus allowing for the regeneration of the DPF. The results of the parameter study should now be verified using an exhaust gas system similar to the standard series system that was developed for the test engine. This system consists of a close-coupled DOC followed by a flex-element, a straight mixing stretch as well as a DOC and a DPF located in the underbody. The vaporizer is integrated according to the parameter study. For example, the inlet cone of the underbody DOC has a more elongated design, and a mixer with optimised orientation is welded in. In direct comparison with a serial system, these changes result in an improved flow distribution so that a lower temperature difference on the DOC and the DPF can be expected.

In order to illustrate the potential for optimisation, **Figure 8** compares three different exhaust gas systems for the operat-

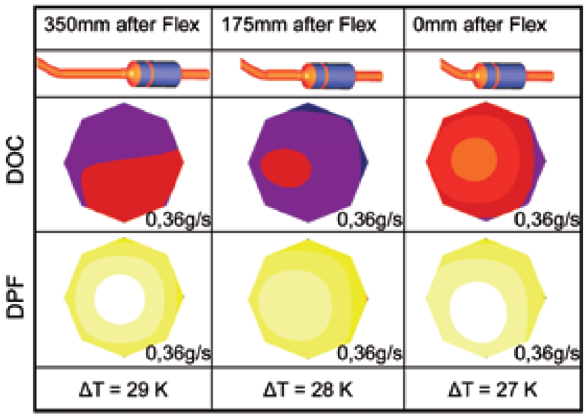

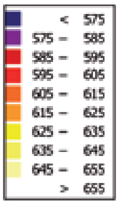

Figure 8: Variations of the mixing length in optimised exhaust gas system

ing point 185 kg/h and 350 °C. 0 mm and 350 mm represent the limits for positioning a converter for the DOC and the DPF in the underbody because of packaging space. The temperatures shown for the DOC and the DPF are based on interpolation between twelve fixed thermal elements.

Regardless of the length chosen, the results show that a part of the added diesel only converts on the coating of the particulate filter. Thus, the DPF always shows the higher temperature. The reason for this is the use of a smaller DOC. Furthermore, the expected temperature difference of 30 K is achieved through the DPF in all mixing stretches. This result can be confirmed for all operating points.

5 Computational Fluid Dynamics

Numeric simulation of the fluid flow plays an important role in the development of exhaust systems. Since any catalyst is subjected to the process of ageing, due to the uneven use of the converter's volume, CFD calculation provides valuable information about catalyst performance [2].

Based on the three-dimensional CAD model of the exhaust gas system, a structured mesh consisting of hexahedra is generated with the software „ICEM CFD" from the Ansys Company. However in the area of the mixer a volume mesh of tetrahedra with prism layers close to the wall is generated. This hybrid mesh represents a good balance between the efforts to link the mesh sizes and the required accuracy of computation.

The mathematical basis for numerical flow simulation is formed by Reynolds averaged Navier-Stokes equations (RANS), which describe the base fluid flow.

IMPRINT

MTZ WORLDWIDE

www.MTZ-online.com

05|2009 · May 2009 · Volume 70
Springer Automotive Media | GWV Fachverlage GmbH
P.O. Box 15 46 · 65173 Wiesbaden · Germany
Abraham-Lincoln-Straße 46 · 65189 Wiesbaden · Germany

Managing Directors Dr. Ralf Birkelbach, Albrecht Schirmacher
Advertising Director Thomas Werner
Production Director Ingo Eichel
Sales Director Gabriel Göttlinger

EDITORS-IN-CHARGE

Dr.-Ing. E. h. Richard van Basshuysen
Wolfgang Siebenpfeiffer

EDITORIAL STAFF

Editor-in-Chief
Johannes Winterhagen (win)
Phone +49 611 7878-342 · Fax +49 611 7878-462
E-Mail: johannes.winterhagen@springer.com

Vice-Editor-in-Chief
Dipl.-Ing. Michael Reichenbach (rei)
Phone +49 611 7878-341 · Fax +49 611 7878-462
E-Mail: michael.reichenbach@springer.com

Chief-on-Duty
Kirsten Beckmann M. A. (kb)
Phone +49 611 7878-343 · Fax +49 611 7878-462
E-Mail: kirsten.beckmann@springer.com

Sections

Electrics, Electronics
Markus Schöttle (scho)
Phone +49 611 7878-257 · Fax +49 611 7878-462
E-Mail: markus.schoettle@springer.com

Engine
Dipl.-Ing. (FH) Richard Backhaus (rb)
Phone +49 611 5045-982 · Fax +49 611 5045-983
E-Mail: richard.backhaus@rb-communications.de

Heavy Duty Techniques
Ruben Danisch (rd)
Phone +49 611 7878-393 · Fax +49 611 7878-462
E-Mail: ruben.danisch@springer.com

Online
Dipl.-Ing. (FH) Caterina Schröder (cs)
Phone +49 611 78 78-190 · Fax +49 611 7878-462
E-Mail: caterina.schroeder@springer.com

Production, Materials
Stefan Schlott (hlo)
Phone +49 8191 70845 · Fax +49 8191 66002
E-Mail: Redaktion_Schlott@gmx.net

Service, Event Calendar
Martina Schraad
Phone +49 212 64 235 16
E-Mail: martina.schraad@springer.com

Transmission, Research
Dipl.-Ing. Michael Reichenbach (rei)
Phone +49 611 7878-341 · Fax +49 611 7878-462
E-Mail: michael.reichenbach@springer.com

English Language Consultant
Paul Willin (pw)

Permanent Contributors
Christian Bartsch (cb), Prof. Dr.-Ing. Peter Boy (bo), Prof. Dr.-Ing. Stefan Breuer (sb), Jörg Christoffel (jc), Jürgen Grandel (gl), Ulrich Knorra (kno), Prof. Dr.-Ing. Fred Schäfer (fs), Roland Schedel (rs), Bettina Seehawer (bs)

Address
P.O. Box 15 46, 65173 Wiesbaden, Germany
E-Mail: redaktion@ATZonline.de

MARKETING | OFFPRINTS

Product Management Automotive Media
Sabrina Brokopp
Phone +49 611 7878-192 · Fax +49 611 7878-407
E-Mail: sabrina.brokopp@springer.com

Offprints
Martin Leopold
Phone +49 2642 9075-96 · Fax +49 2642 9075-97
E-Mail: leopold@medien-kontor.de

ADVERTISING | GWV MEDIA

Ad Manager
Britta Dolch
Phone +49 611 7878-323 · Fax +49 611 7878-140
E-Mail: britta.dolch@gwv-media.de

Key Account Manager
Elisabeth Maßfeller
Phone +49 611 7878-399 · Fax +49 611 7878-140
E-Mail: elisabeth.massfeller@gwv-media.de

Ad Sales
Frank Nagel
Phone +49 611 7878-395 · Fax +49 611 7878-140
E-Mail: frank.nagel@gwv-media.de

Display Ad Manager
Susanne Bretschneider
Phone +49 611 7878-153 · Fax +49 611 7878-443
E-Mail: susanne.bretschneider@gwv-media.de

Ad Prices
Price List No. 52

SUBSCRIPTIONS

VVA-Zeitschriftenservice, Abt. D6 F6, MTZ
P. O. Box 77 77, 33310 Gütersloh, Germany
Renate Vies
Phone +49 5241 80-1692 · Fax +49 5241 80-9620
E-Mail: SpringerAutomotive@abo-service.info

SUBSCRIPTION CONDITIONS

The eMagazine appears 11 times a year at an annual subscription rate of 269 €. Special rate for students on proof of status in the form of current registration certificate 124 €. Special rate for VDI/ÖVK/VKS members on proof of status in the form of current member certificate 208 €. Special rate for studying VDI members on proof of status in the form of current registration and member certificate 89 €. The subscribtion can be cancelled in written form at any time with effect from the next available issue.

PRODUCTION | LAYOUT

Heiko Köllner
Phone +49 611 7878-177 · Fax +49 611 7878-464
E-Mail: heiko.koellner@gwv-fachverlage.de

HINTS FOR AUTHORS

All manuscripts should be sent directly to the editors. By submitting photographs and drawings the sender releases the publishers from claims by third parties. Only works not yet published in Germany or abroad can generally be accepted for publication. The manuscripts must not be offered for publication to other journals simultaneously. In accepting the manuscript the publisher acquires the right to produce royalty-free offprints. The journal and all articles and figures are protected by copyright. Any utilisation beyond the strict limits of the copyright law without permission of the publisher is illegal. This applies particularly to duplications, translations, microfilming and storage and processing in electronic systems.

Springer Automotive Media is part of the specialist publishing group Springer Science+Business Media.

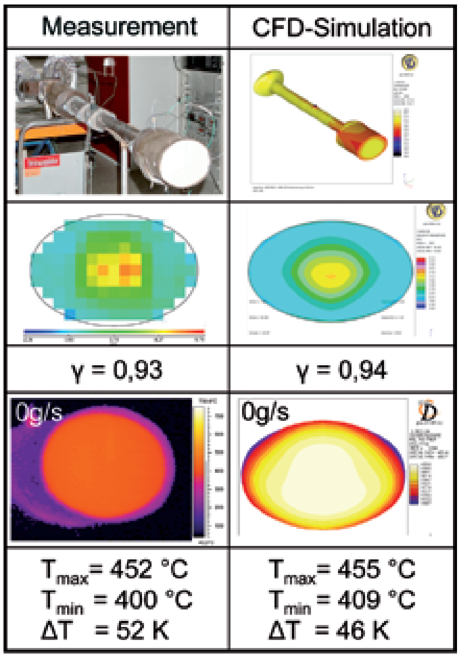

Figure 9: Comparison of measurement and CFD simulation without diesel insertion

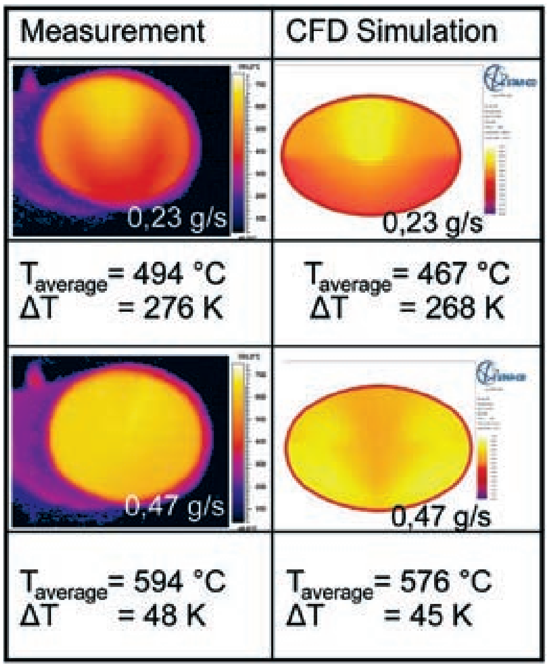

Figure 10: Comparison of measurement and CFD simulation with diesel insertion

The turbulent part of the flow is specified by k-e turbulence model. The resulting differential equation system is quantified using the Finite Volume Method on the stationary grid and then resolved iteratively. The CFD calculations are made using the software StarCD from the CD-adapco company.

Modelling the catalytic diesel combustion in the DOC represents a major challenge. On the one hand, diesel is a mixture of a large number of hydrocarbons, and on the other hand heterogeneous reactions are very complex to model. In addition to the reactions on the surface, it comprises many rather complex effects like transport through the boundary layer, diffusion through the pore structure of the wash coat to the wall of the catalytic converter, as well as the absorption and desorption of the partners in the reaction on the wall of the catalytic converter. Because of this complexity and the wide variety of influential parameters, it is currently not possible to model diesel combustion in detail. Instead, the diesel mixture is substituted by hexadecane $C_{16}H_{34}$. This substitute fuel provides a satisfactory picture of how heat is released in the catalytic converter, and it is able to indicate temperature peaks in the DOC and DPF. **Figure 9** shows a comparison of the flow distribution and the temperature distribution in the modular exhaust system without adding diesel. In terms of both quality and quantity, it shows a good match between calculation and measurement. These CFD calculations enable us to estimate the achievable temperature difference under the given conditions.

By using this robust model it is possible to calculate the temperature distribution with added diesel and to compare it with the actual measurements. Here, too, a good correlation is achieved, as demonstrated in **Figure 10**. The problem of concentration is easily recognisable in the upper example, both in the measurement and in the simulation. By contrast, the lower example shows a homogeneous temperature distribution.

6 Summary and Outlook

The joint development project initiated by Beru and Tenneco aims at allowing carmakers to benefit from the conceptual advantages of direct diesel feed by means of an vaporizer. Collaborating on this project enables the two developers to take advantage of their comprehensive experience with respect to diesel cold start technology and exhaust gas aftertreatment so that a cost-efficient and effective product can quickly be put into serial production.

The parameter study and subsequent measurements made using a model similar to the serial system show that the best results for diesel particulate filter regeneration, with a sufficient increase in temperature while maintaining homogeneous temperature distribution, are offered by a vaporizer. To develop such a system a large number of factors must be optimised and various conditions must be examined more closely. Measurements with thermal plugs led to more efficient heat transfer surfaces and a power supply adapted to the diesel mass flow. The parameter study that was carried out in the flow laboratory compared the different factors that influence the integration of the vaporizer, and reduced their number for future applications. The achievable temperature distribution was estimated with CFD calculations and new configurations were computed.

Future work will focus on investigating service life and coking rate, particulate filter regeneration including the determination of secondary emissions that might develop, as well as optimising the pressure loss and mixing performance of the mixer.

References

[1] Bosch (Hrsg.): Dieselmotormanagement. Wiesbaden: Vieweg
[2] Terres, F.; Michelin, J.; Weltens, H..: Partikelfilter für Diesel-Pkw – Beladungs- und Regenerationsverhalten. In MTZ 63 (2002) Nr. 7/8

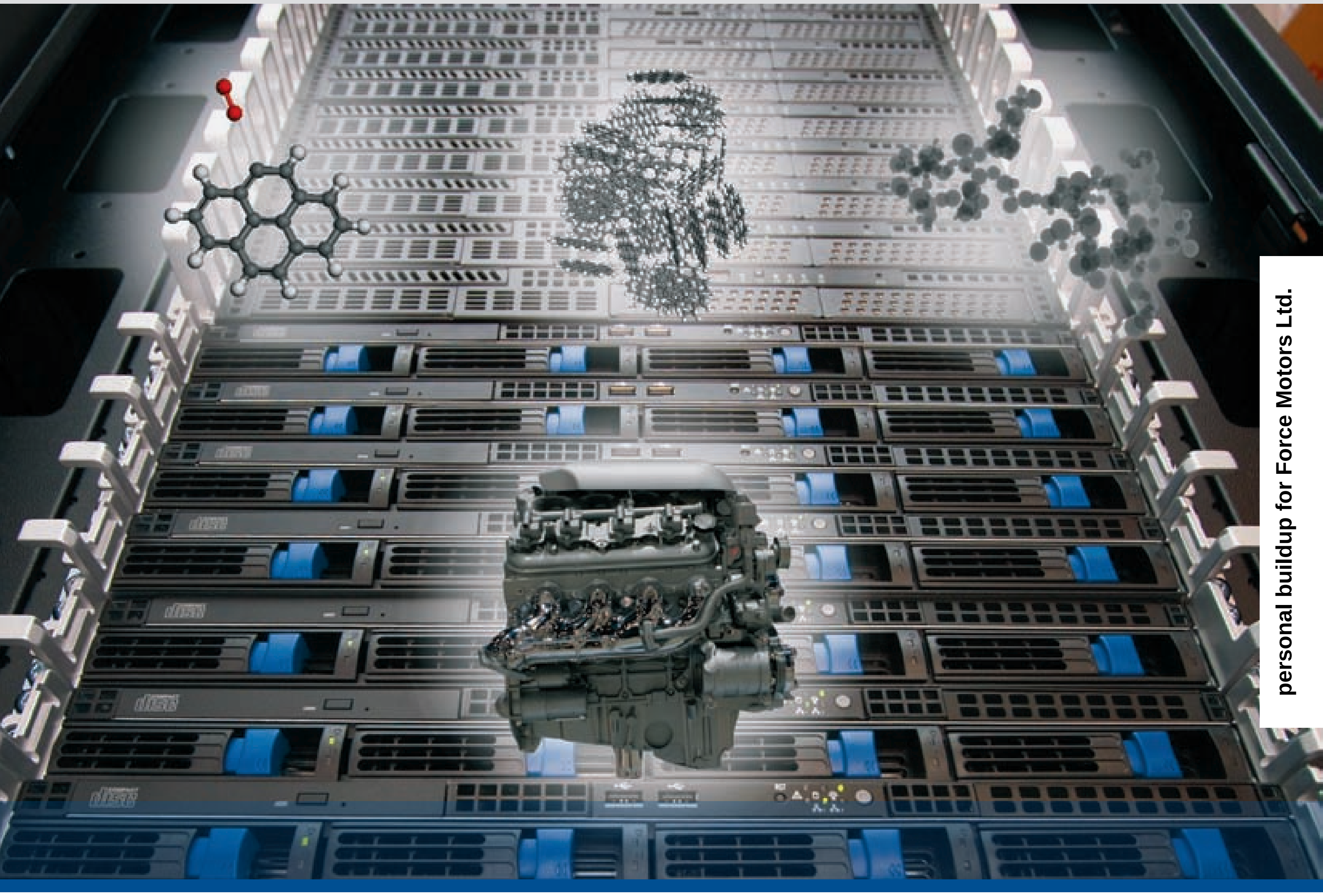

personal buildup for Force Motors Ltd.

Towards a Detailed Soot Model for Internal Combustion Engines

At the University of Cambridge, the formation of soot was studied in an n-heptane fuelled Homogeneous Charge Compression Ignition (HCCI) engine, operated at a rich equivalence ratio of 1.93, by means of in-cylinder snatch sampling as well as by applying a new engine model which features a highly detailed description of soot. This new computationally efficient model is capable of providing not only averaged quantities as functions of crank angle like soot mass, number density, volume fraction, aggregate diameter, and the number of primary particles per aggregate for example, but also aggregate and primary particle size distribution functions and additionally can give detailed information on aggregate morphology and chemical composition.

1 Introduction

The formation of soot and other particulate matter in internal combustion engines is a common problem [1, 2]. While soot formation is usually associated with conventional diesel, i.e. Compression Ignition Direct Injection (CIDI) engines, other engine types are increasingly coming under scrutiny as well [2 to 4].

Given the importance of direct injection technology for mixture preparation and combustion control in modern engines, and the fact that stratified operation bears the possibility of locally fuel-rich mixtures, the formation of soot is an important factor in the design of cleaner engines, irrespective of whether after-treatment systems are employed or not. Such development is assisted by detailed understanding of the processes involved, to which modelling and simulation can contribute significantly.

The literature on soot modelling in engines has been largely restricted to diesel engines and to strongly simplified soot models [5, 6] using descriptions based on only a small number of quantities. Although this is beneficial for computational expense, one drawback is for example that the important influence of aggregate morphology, which is usually complex, on surface area and collision diameter can only be captured through the use of empirical constants and assumptions. Furthermore, while the surface chemistry in the soot models has increased significantly in detail, a major remaining shortcoming is the fact that the chemical composition of the soot particles, which strongly affects their reactivity, is not accounted for. In light of this, it has been emphasized that there is a need for more detailed but still computationally affordable engine soot models.

In this work, a computationally cheap engine simulation code is presented, containing a highly detailed soot model which describes not only soot mass, number density, volume fraction, and surface area but also the morphology and chemical composition of soot aggregates. The model is applied to simulate an n-heptane fuelled Homogeneous Charge Compression Ignition (HCCI) engine operated at an equivalence ratio of 1.93. A key advantage of such a setup, aimed at a fundamental study, is that the complications relating to mixture preparation, in particular the notoriously difficult sprays, do not need to be considered. We chose this simple case mainly for validation purposes – the model can indeed be applied in more complex situations.

Table: Engine specification and operating condition

Bore	86 mm
Stroke	86 mm
Displaced volume	499 cm^3
Compression ratio (CR)	12
EGR mass fraction	22 %
Speed	600 RPM
Inlet temperature	412 K
Fuel/air equivalence ratio Φ	1.93

2 Model Description

2.1 Engine Model

The engine model is a so-called Stochastic Reactor Model (SRM) [7], which uses detailed chemistry and possesses sub-models for turbulent mixing and convective heat transfer, thereby accounting for in-cylinder inhomogeneities, i.e. stratification in composition as well as temperature. The SRM has been successfully employed in a number of earlier studies not involving soot formation such as port fuel injected HCCI combustion with a variety of fuels [8], direct (dual) injection HCCI [9], multi-cycle transient simulation and control [10], and cycle-to-cycle variations in a spark ignition (SI) engine [11].

The main strength of the SRM is its ability of qualitatively predicting emission trends of CO, CO_2, NO_x, and unburnt hydrocarbons at reasonable computational cost of one to two hours per engine cycle on a conventional desktop PC. This enables convenient multi-cycle, sensitivity, and parameter studies.

The Authors

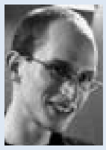

Sebastian Mosbach, PhD is a Postdoctoral Research Associate in the Computational Modelling Group at the Department of Chemical Engineering and Biotechnology at the University of Cambridge in Cambridge (United Kingdom).

Dr. rer. nat. Dipl. Math.-techn. Markus Kraft is the head of the Computational Modelling Group and University Reader of Chemical Engineering at the Department of Chemical Engineering and Biotechnology at the University of Cambridge in Cambridge (United Kingdom).

Hongzhi R. Zhang, PhD is a Research Associate at the Institute for Clean and Secure Energy at the University of Utah in Utah (USA).

Shuichi Kubo, PhD is Manager of the DPF Department Division at Ibiden Co. Ltd. (Japan).

Kyoung-Oh Kim, PhD is Project Manager at Higashifuji Technical Center of Toyota Motor Corporation (Japan).

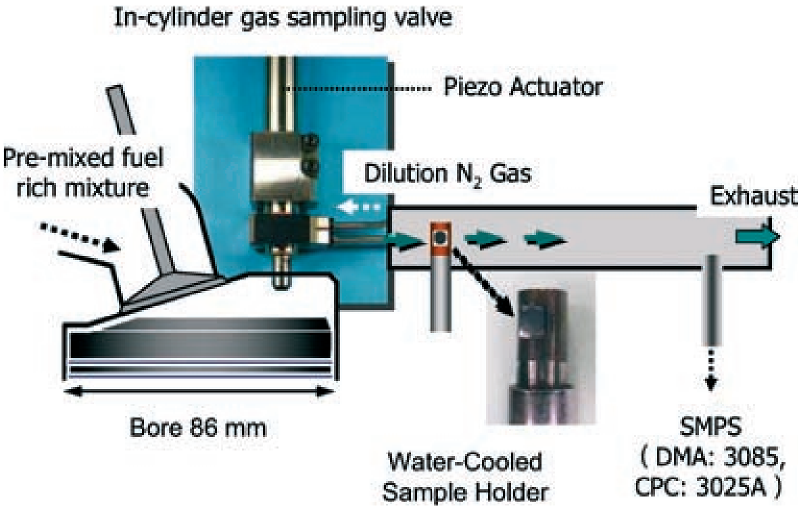

Figure 1: Experimental setup of in-cylinder snatch sampling measurements

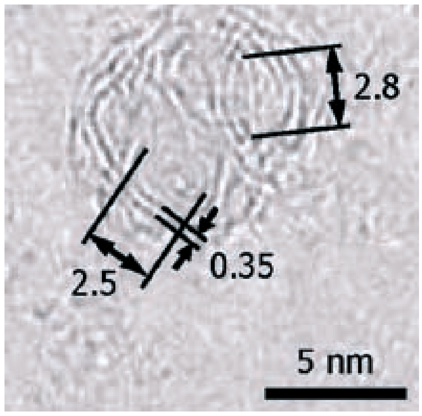

Figure 2: Experimental HR-TEM image of an aggregate sampled at about 16 CAD ATDC; indicated are length scales of structures within a primary particle

2.2 Soot Model

The soot model is able to accommodate highly detailed particle descriptions covering aggregate structure and chemical composition. As far as the morphology of soot aggregates is concerned, it tracks for each aggregate the surface area, the number of primary particles, and for each primary particle its diameter (assuming sphericity). The chemical composition of soot is modelled by storing for each aggregate the number of carbon atoms, the number of hydrogen atoms, the number of PAH molecules, and the number of occurrences of five different types of functional sites on PAH.

The modelled processes which soot aggregates undergo include the following: Inception, i.e. dimerization of gas-phase molecules to form a particle, condensation, i.e. addition of a molecule taken from the gas-phase to an existing particle, and surface growth are the three possible pathways in our model from the gas-phase to the particulate phase, i.e. when molecules are held together in a particle through physical forces rather than chemical bonds. In the particulate phase, coagulation and surface chemistry, including growth and oxidation reactions on the surface of particles are taken into account [12 to 14].

In order to describe the gas-phase combustion chemistry, we employ a detailed kinetic mechanism for Primary Reference Fuels (PRFs, n-heptane/iso-octane mixtures) used previously [7 to 10], which is targeted at the prediction of quantities such as pressure, CO, NO_x, and unburnt hydrocarbon emissions. However, the main aim of this study is soot formation, so we included small Polycyclic Aromatic Hydrocarbons (PAH) and other highly unsaturated hydrocarbons. The extended chemical kinetic mechanism contains 208 species and 1002 reactions. The mechanism has been validated against a variety of experimental data sets for fuel-rich laminar flames obtained from literature.

3 Experimental Setup and Measurements

Experiments were carried out on an SI engine converted for single-cylinder HCCI operation. The engine was run port-injected, fuelled with pure n-heptane, at an equivalence ratio of Φ=1.93. The main reason for running the engine fully premixed is that complications involved in mixture preparation, such as the difficulties arising from the direct injection process which are notoriously hard to model like droplet evaporation and mixing, can largely be avoided. Using n-heptane as a fuel has the advantage that it is relatively simple and well-defined compared to conventional gasoline or diesel, thereby circumventing substantial modelling challenges posed by the large number of aromatic and oxygenated compounds contained in those fuels.

The engine was run throttled and with a fraction of trapped residual gases (internal EGR rate) of 22 %, **Table**.

Particle-laden in-cylinder gases were extracted through snatch sampling over a number of cycles in steady-state operation. The obtained aggregates were analyzed through a Scanning Mobility Particle Sizer (SMPS) and a High-Resolution Transmission Electron Microscope (HR-TEM), as depicted in **Figure 1**.

4 Simulations, Results and Discussion

It turns out that aggregates recirculated in exhaust gases play an important role, which is why all simulations are conducted over ten consecutive cycles, starting with trapped residuals with typical gas-phase composition, but not containing any soot. When carrying out such studies, it becomes clear that low computational cost is highly desirable. Even under heavily sooting conditions with large numbers of primary particles per aggregate, one engine cycle consumes usually less than four hours of CPU-time.

Figure 2, **Figure 3** and **Figure 4** show an experimental as well as a simulated aggregate both sampled at about 16 CAD ATDC. In Figure 2, an experimental HR-TEM image of a primary particle is shown together with some indicated internal length scales. A simulated aggregate is shown in a TEM-style projection in Figure 3. The largest simulated primary particles are about the same size as the ones in Figure 2, which are also among the largest experimentally. The size distribution of pri-

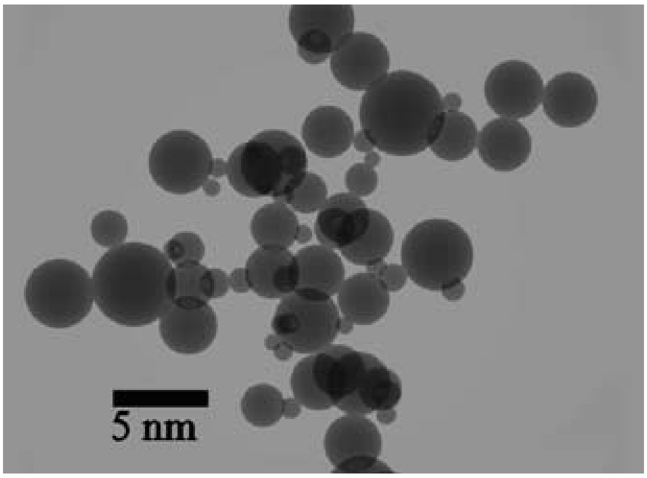

Figure 3: TEM-style image of simulated aggregate (sampled at 15.6 CAD ATDC, 65 primaries, collision diameter 16.5 nm, C/H ratio 1.61)

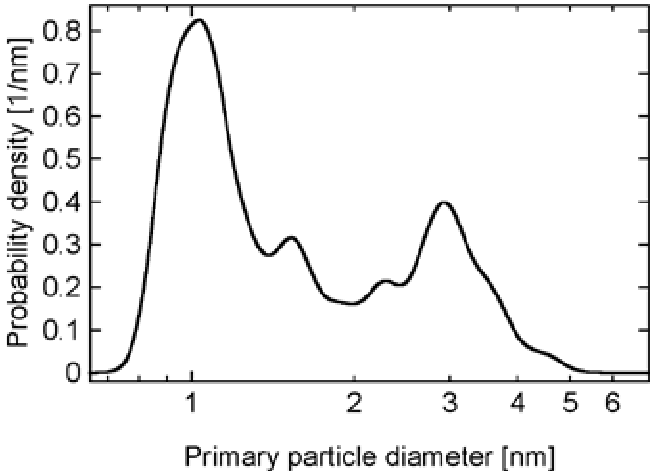

Figure 4: Primary particle size distribution of simulated aggregate in Figure 3

mary particles of the simulated aggregate is plotted in Figure 4. **Figure 5** shows experimental as well as simulated in-cylinder aggregate size distributions at various crank angles, ranging from just after the start of ignition to about the time when peak pressure is reached. Both the shape of the distributions and the trends of their time evolution agree well qualitatively. In particular, the aggregates recirculated in trapped residual gases is recognized as a prominent feature.

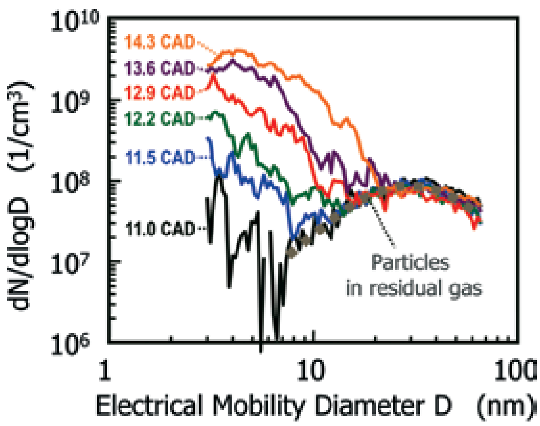

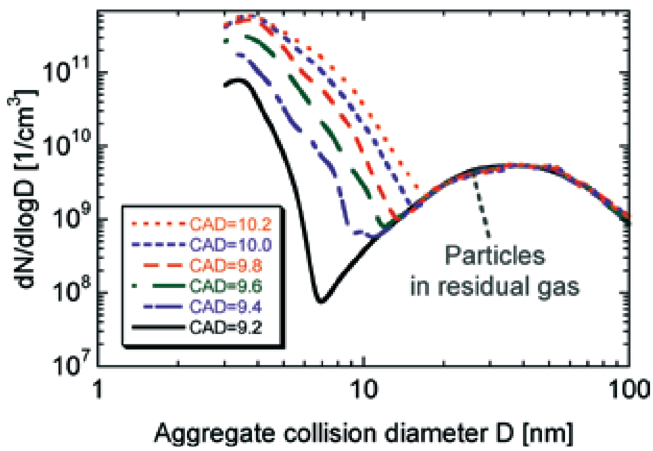

Figure 5: Experimental (top) and simulated (bottom) in-cylinder aggregate size distribution functions at various crank angles

In **Figure 6**, aggregate size distributions at 10 CAD ATDC are plotted for ten consecutive cycles, where the first starts without any soot present in the residual gases. We observe that the distribution has stabilized by the tenth cycle, and we readily identify the aggregates larger than about 20 nm as being recirculated for possibly several times before being emitted from the engine.

5 Conclusions

At the University of Cambridge, an engine simulation code has been developed which includes a detailed model for soot formation, describing soot aggregate morphology and chemical composition. The new model, being computationally relatively cheap, enables the study of size distribution, morphology, and composition of soot aggregates formed over the course of several engine cycles.

The integrated code to simulate an n-heptane fuelled HCCI engine operated at an equivalence ratio of 1.93 is used. The simulated aggregate size distributions as well as their time evolution qualitatively agree with those obtained experimentally. It is also seen both in the experiment and in the simulation that, in the considered case of about 20 % EGR, soot emissions in terms of mass stem mostly from recirculated aggregates, whereas in terms of number mostly from newly formed ones.

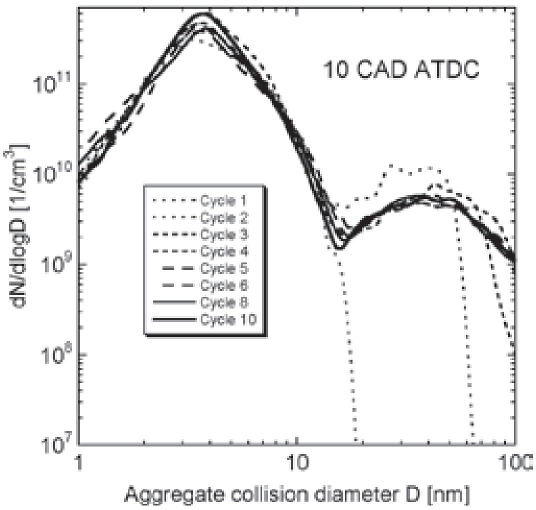

Figure 6: Size distribution at 10 CAD ATDC for ten consecutive cycles; The recirculated aggregates can be clearly identified as the ones larger than about 20 nm

The present study focused on fully premixed compression ignition operation. However, the integrated model is currently applied to SI engines and first steps have been taken towards operating modes which utilize direct injection such as partially stratified HCCI as well as conventional Compression Ignition Direct Injection (CIDI) engines.

References

[1] Kittelson, D. B.: Engines and nanoparticles: a review. In: Journal of Aerosol Science, 29 (5-6): 575-588, 1998
[2] Eastwood, P.: Particulate Emissions from Vehicles. Wiley-PEPublishing Series. John Wiley & Sons, 2008
[3] Price, P.; Stone,R.; Misztal, J.; Xu, H.; Wyszynski, M.; Wilson, T.; Qiao, J.: Particulate emissions from a gasoline homogeneous charge compression ignition engine. SAE Paper 2007-01-0209, 2007
[4] Price, P.; Twiney, B.; Stone, R.; Kar, K.; Walmsley, H.L.: Particulate and hydrocarbon emissions from a spray guided direct injection spark ignition engine with oxygenate fuel blends. SAE Paper 2007-01-0472, 2007
[5] Hong, S.; Wooldridge, M. S.; Im, H. G.; Assanis, D. N.; Pitsch, H.: Development and application of a comprehensive soot model for 3D CFD reacting flow studies in a Diesel engine. Combustion and Flame, 143:11-26, 2005
[6] Hiroyasu, H.; Kadota, T.: Models for combustion and formation of nitric oxide and soot in direct injection Diesel engines. SAE Paper 760129, 1976
[7] Kraft, M.; Maigaard, P; Mauss, F.; Christensen, M.; Johansson, B.: Investigation of combustion emissions in an HCCI engine – measurements and a new computational model. Proceedings of the Combustion Institute, 28:1195-1201, 2002
[8] Mosbach, S.; Kraft, M.; Bhave, A.; Mauss, F.; Mack, J H.; Dibble, R. W.: Simulating a homogenous charge compression ignition engine fuelled with a DEE/EtOH blend. SAE Paper 2006-01-1362, 2006
[9] Mosbach, S.; Su, H.; Kraft, M.; Bhave, A.; Mauss, F.; Wang, Z.; Wang, J.-X.: Dual injection HCCI engine simulation using a stochastic reactor model. International Journal of Engine Research, 8(1): 41-50, 2007
[10] Mosbach, S.; Aldawood, A. M.; Kraft, M.: Real-time evaluation of a detailed chemistry HCCI engine model using a tabulation technique. Combustion Science and Technology, 180(7): 1263-1277, 2008
[11] Etheridge, J. E.; Mosbach, S.; Kraft, M.; Wu, H.; Collings, N.: Investigating cycle to cycle variations in an SI engine through experiments and a new computational model. submitted for publication, 2009
[12] Celnik, M. S.; Raj, A.; West, R. H.; Patterson, R. I. A.; Kraft, M.: An aromatic site description of soot particles. Combustion and Flame, 155(1-2): 161-180, 2008
[13] Raj, A.; Celnik, M. S.; Shirley, R. A.; Sander, M.; Patterson, R. I. A.; West, R. H.; Kraft, M: A statistical approach to develop a detailed soot growth model using PAH characteristics. accepted by Combustion and Flame, 2008
[14] Celnik, M. S.; Sander, M.; Raj, A.; West, R. H.; Kraft, M.: Modelling soot formation in a premixed flame using an aromatic-site soot model and an improved oxidation rate. Proceedings of the Combustion Institute, 32(1):639-646, 2009

The authors express their gratitude towards Mr Abhijeet Raj and Dr Matthew S. Celnik for their important contributions to the development and application of the soot model.

WWW.VIEWEGTEUBNER.DE

Gasoline Engines are the answer to the challenges of future

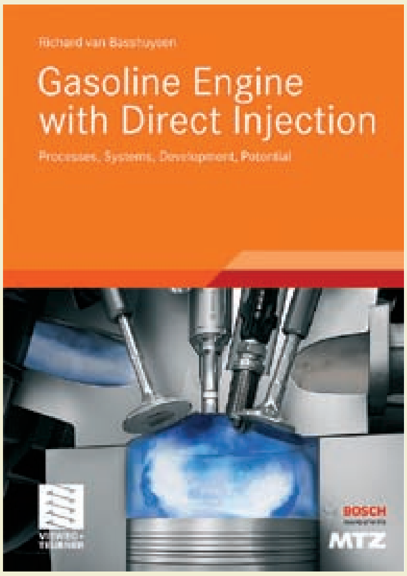

Richard van Basshuysen

Gasoline Engine with Direct Injection

Processes, Systems, Development, Potential

2009. xviii, 437 pp. With 399 Fig. Hardc. EUR 49,00

ISBN 978-3-8348-0670-3

Direct injection spark-ignition engines are becoming increasingly important, and their potential is still to be fully exploited. Increased power and torque coupled with further reductions in fuel consumption and emissions will be the clear trend for future developments. From today‘s perspective, the key technologies driving this development will be new fuel injection and combustion processes. The book presents the latest developments, illustrates and evaluates engine concepts such as downsizing and describes the requirements that have to be met by materials and operating fluids. The outlook at the end of the book discusses whether future spark-ignition engines will achieve the same level as diesel engines.

authors | editors

Dr.-Ing. E. h. Richard van Basshuysen was Head of Development for premium class vehicles and for engine and transmission development at Audi. Today, he is editor of the magazines ATZ and MTZ. The editor was supported by a distinguished team of authors consisting of 22 experts and scientists from industry and universities.

Please send me

Fax +49(0)611.7878-420

____ Copies
Gasoline Engine with Direct Injection
ISBN 978-3-8348-0670-3
EUR 49,00
(+ shipping and handling)

Company | Last name | First name | 321 09 001

Department

Street name | Postcode/Zip | City, Country

Date | Signature

Please supply at retail price via bookshop or directly from Vieweg+Teubner Verlag. Subject to change without notice. 1|2009.
Managing Directors: Dr. Ralf Birkelbach, Albrecht F. Schirmacher. AG Wiesbaden HRB 9754

TECHNIK BEWEGT.

VIEWEG+TEUBNER

Testing of Engine Air Intake Filter Elements under Realistic Conditions

With the soot test bench and new fixing technique, Mann+Hummel has created development tools to examine the deposition characteristics of dust particles. Through these tools, it is now possible to test far more quickly and accurately the suitability of new filter systems and forward-looking filter elements, e.g. with innovative pleat structures, under realistic conditions.

1 Introduction

The principle task of engine air intake filter elements in automotive applications is to retain solid airborne contamination (soot) which are carried to the engine with the combustion air and which lead to increased wear [1, 2]. The engine management system can also be affected by inadequate separation of the particles from the ambient air if particles are deposited on the air flow meter. This contamination may lead to deterioration of signal accuracy resulting in loss of power and increased fuel consumption.

To separate the particles from the intake air Mann+Hummel generally uses filter elements comprising a pleated filter medium and a sealing geometry. The filtration performance of the filter elements essentially depends on the filter media used, which define the required functional parameters such as efficiency, service life and dust holding capacity. Classic filter media used for engine air filtration consist of cellulose fibres protected through special impregnation over their lifetime against environmental impact such as humidity, oil or fuel vapour. Fully synthetic filter media with gradient structure, multilayered design or refined with nanofibres are also applied [3].

The advances in modern engines have also provided great impetus in recent years to further develop filtration in modern vehicles. Through reduced installation space for the air filter system in the engine compartment, continuously improved filter media have been developed. Basic prerequisites for this development are standardised testing procedures in the laboratory to enable different media to be compared and evaluated, as well as thorough knowledge about particles existing in the ambient air and their impact on filtration.

2 Testing of Engine Air Intake Filters

In order to evaluate the performance of air filter elements, efficiency and dust capacity are tested according to ISO 5011 in an air conditioned laboratory with standardized test dusts consisting of quartz particles (ISO 12 103) with particle sizes between 0.3 and 300 μm.

Dust comparable in size and composition to the test dust also occurs in ambient air, originating mainly from agricultural areas, construction sites, industry or desert regions. Regarding to the particle size these test dusts also cover pollens and fly ash particles from industrial or domestic combustion sites, **Figure 1**.

As well as these comparatively coarse dust particles, intake air filters are exposed to a large number of very fine particles less than 1 μm in size. These fine particles are created primarily from combustion processes in diesel engines, domestic heaters or industry and mainly consist of soot [4]. Existing filter media

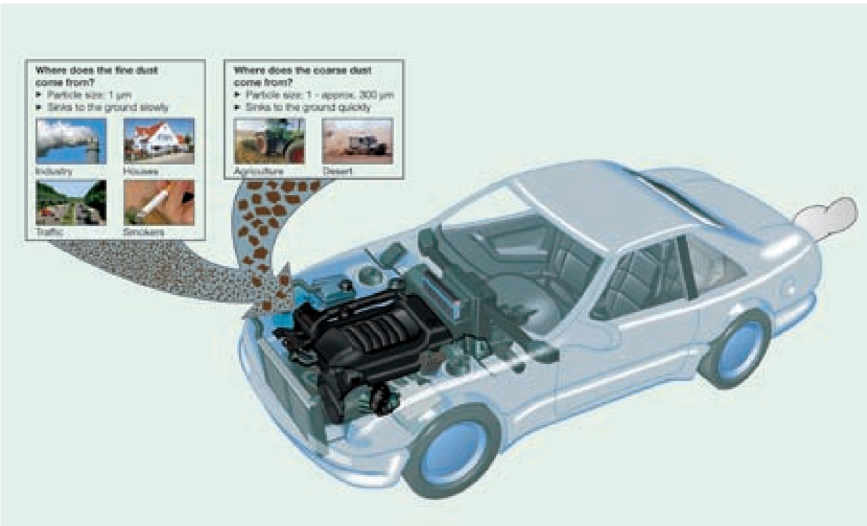

Figure 1: Pressure loss through fine and coarse dust particles

The Authors

Dr.-Ing. Sabine Fleck
works for Development of Air Filter Elements and Air Filter Media and is Project Manager Air Filter Elements at Mann+Hummel GmbH in Ludwigsburg (Germany).

Michael Heim
works for Development of Air Filter Elements and Air Filter Media at Mann+Hummel GmbH in Ludwigsburg (Germany).

Andreas Beck
is the Head of the Air Filter Test Laboratory at Mann+Hummel GmbH in Ludwigsburg (Germany).

Dr. Nikolaus Moser
is Manager Development Air Filter Elements at Mann+Hummel GmbH in Ludwigsburg (Germany).

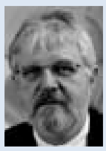

Dr.-Ing. Michael Durst
works for Development Filter Elements at Mann+Hummel GmbH in Ludwigsburg (Germany).

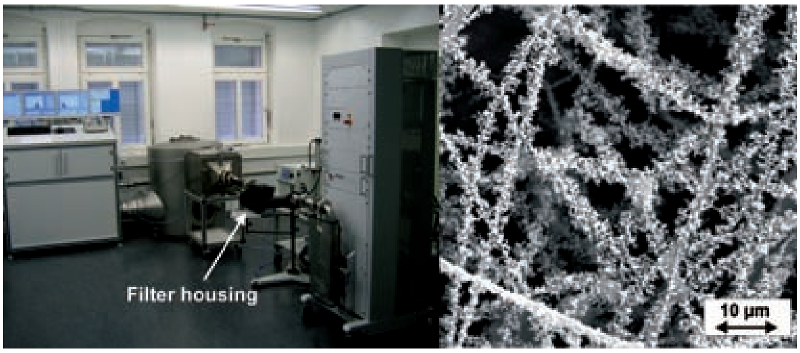

Figure 2: Soot test bench by Mann+Hummel (left); REM photograph of particulates from the test bench adhering on nanofibre (right)

made from cellulose only separate these ultrafine particles to a limited extent.

In addition, fine particles retained in the filter media contribute disproportionately to the increase in pressure loss [3]. Due to their size, the primary transport mechanism for ultrafine particles to the fibres of the media is diffusion and not inertia as it is the case for significantly larger particles, leading to basically different structures of the separated particles in the filter media. The complex structure of the soot particles also plays an important role. Each soot particle consists of a large quantity of significantly smaller primary particles ranging from 10 to 20 nm in size, and through its dendritic structure, displays different separation behaviour [5]. As diffusion is the main transport mechanism, the soot particles block the pores over time, which reduces the free cross section and thus leads to an increase in the pressure loss of the filter element.

Mann+Hummel has developed a soot test bench for automotive filters, **Figure 2**, to study the filtration behaviour of filter elements loaded with fine soot particles under repeatable laboratory conditions. A basic requirement during this development was the generation of particles similar in size (approximately 100 nm [6]) and structure to the soot particles present in ambient air, that are emitted mainly from diesel vehicles. A computer-controlled soot generator produces soot particles with an average diameter of 80 to 110 nm through combustion of propane. The concentration and the particle size distribution of the soot aerosol is continuously monitored by a high resolution particle size spectrometer (Scanning Mobility Particle Sizer – SMPS). A comparison of the particle size distribution of the soot test bench and a typical diesel exhaust aerosol is shown in **Figure 3** [7]. Both distributions show an excellent correlation in terms of the particle size and differ only in the particle concentration.

In the test, the generated soot aerosol is sucked through the filter element. The amount of the generated soot and the filtration efficiency are determined gravimetrically in accordance with ISO standard 5011. The filter element is loaded with soot particles until a defined pressure increase is attained. Due to the high particle concentration that the soot generator is able to produce, a whole filter element can be tested in the original filter housing within a few hours. The SMPS measuring system can also be used to determine the fractional efficiency which indicates how effectively particles of a certain size are retained by the filter element. All the results gained with the new test bench are also used to support development of a new ISO standard for testing filter elements.

In the laboratory tests, virtually the entire range of particles occurring in ambient air can be generated under reproducible conditions. The soot particle test bench and dust feeding test with standardised test dusts according to ISO 5011 create the widest range of particles sucked in by an air filter during its service life, **Figure 4**.

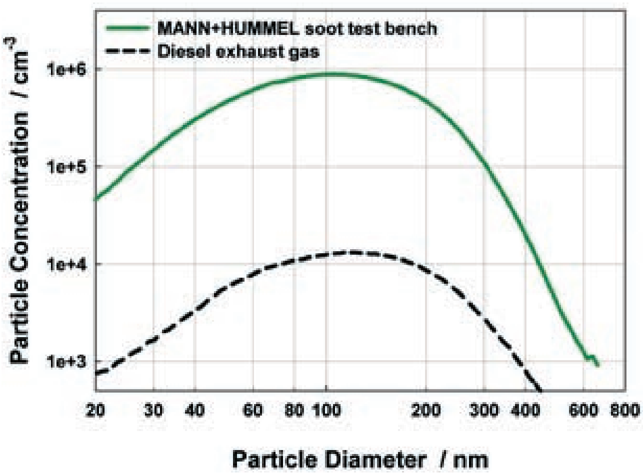

Figure 3: Comparison of the particle size distributions of a typical diesel exhaust gas aerosol and the test soot aerosol generated by the Mann+ Hummel soot test bench

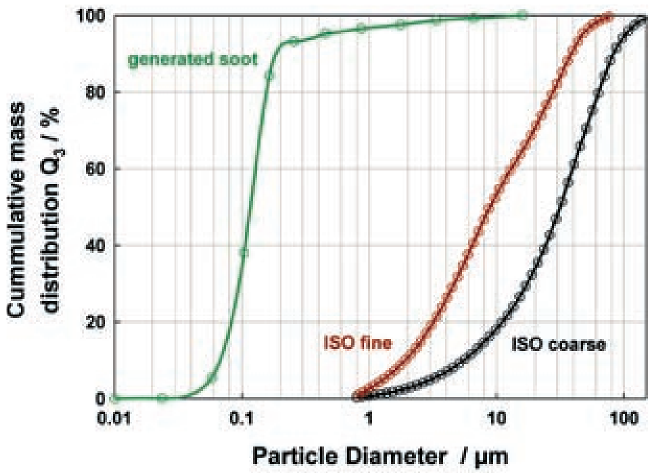

Figure 4: Comparison of the mass weighted particle size distributions of generated soot (measured by a Berner impactor) and the test dusts according to ISO 5011 (measured by a Malvern Mastersizer 2000)

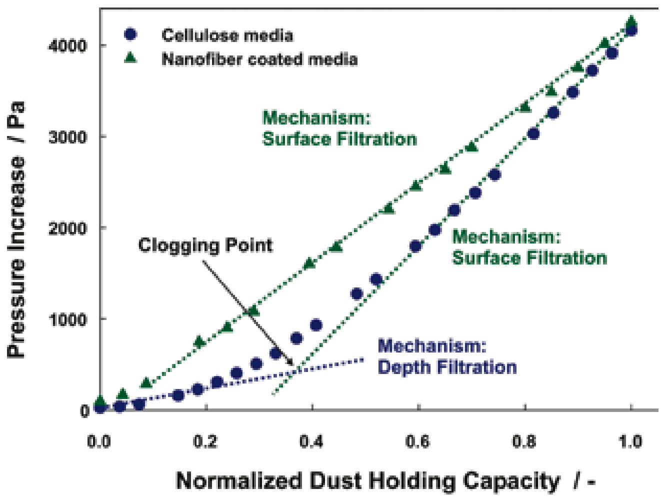

Figure 5: Pressure increase of a cellulose media (depth filter) and a nanofibre coated media (surface filter) when loaded with test dust ISO fine

As well as tests in the laboratory, road tests on various vehicle fleets are carried out for the development of new filter media, taking into account additional parameters such as humidity, temperature fluctuations and other environmental effects. These on-road tests are however very time consuming and a direct comparison of elements containing different media is hardly possible, as the vehicles are not driving under exactly the same conditions. To compare air filter elements loaded with environmental dust (and including the influence of humidity and temperature fluctuations),Mann+Hummel has been successfully using a stationary outdoor test bench close to a busy main road for several years. Several filter elements in the original filter housing are tested simultaneously by sucking ambient air through the filters, while measuring the pressure increase of the filter element, the relative humidity and the temperature of the ambient air. Even while operating night and day the test-duration vary between three and 30 weeks depending on the filter media and the field of application, with the longest test-durations are assigned to the field of heavy duty applications. Experience gained to date from measurements in the outdoor test bench confirm the strong influence of finest dust particles (e.g. soot) and the relative humidity on the filtration performance of a filter element. A first comparison of measurements between the soot test bench and the outdoor test bench based on non-woven filter media shows a good correlation [7] and demonstrate the potential of the new soot test bench for the development of filter media.

3 Examination of Air Filter Media

In addition to testing complete filter elements, the performance of filter media can be determined by testing round flat samples. Under air-conditioned laboratory conditions and with defined flow rates, standardised test dust (ISO 12103-1) is loaded onto the samples on the test bench. To evaluate the performance of filter media, the dust holding capacity, the gravimetric filtration efficiency and the fractional efficiency are determined. The latter can be measured online with an optical particle counter integrated into the test bench [8]. Based on all these information the performance of a filter media can be evaluated.

The initial fractional efficiency of a typical cellulose filter medium after a dust feeding of approximately 0.3 mg/cm^2 range between 70 % for particles with a diameter of 0.30 μm and 100 % for particles with diameters around 10 μm. With increased dust feeding the fractional efficiency of the filter media improves. In the initial filtration phase the dust particles are deposited in the inner structure of the filter media, increasing the surface available for particle capture and therefore improving the filtration efficiency. As additional dust is loaded, there is clogging of the filter media close to the surface. In this way, a filter cake of dust particles is formed which is relevant for subsequent filtration [9]. The transition from the depth filtration phase signified by the deposition of dust in the filter media to the mechanism of surface filtration is marked by the so called clogging point, which can be derived by the functional change of the pressure increase during the dust loading. With surface modified filter media coated with a thin layer of nanofibres between 80 and 1000 nm in diameter, the formation of a filter cake on the surface starts at a very early stage, with virtually no dust deposition phase observed in the filter media, **Figure 5**.

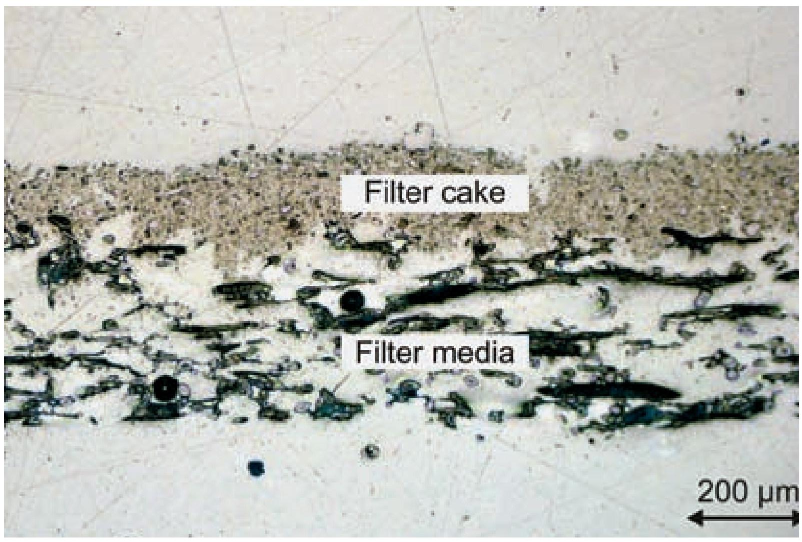

Figure 6: Microscopic picture of cellulose filter media with fixed filter cake

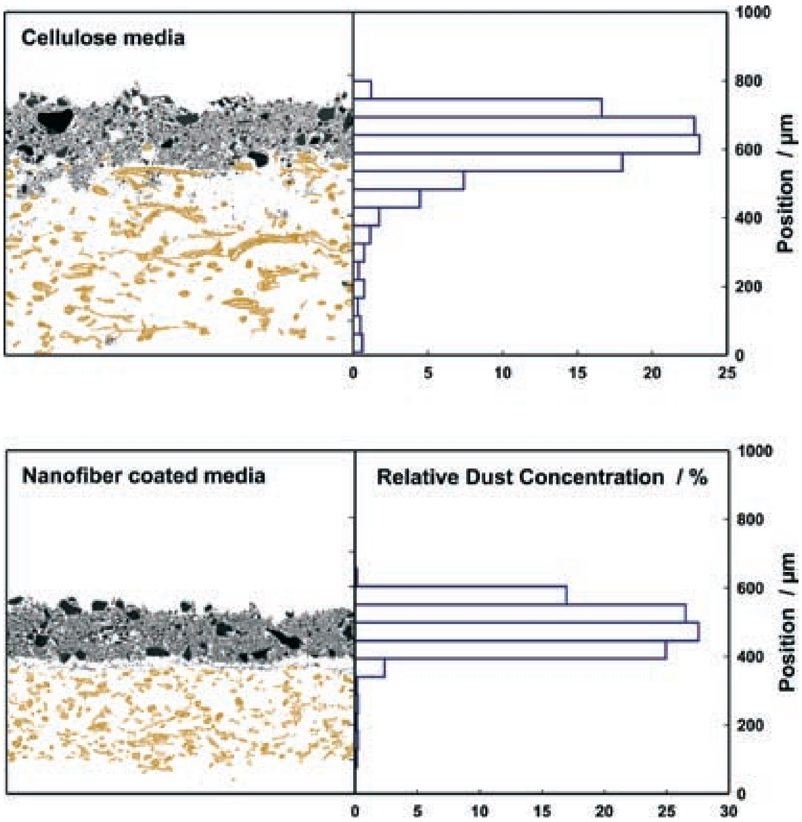

Figure 7: Comparison of dust deposition on standard cellulose media and nanofibre coated cellulose media loaded with test dust

The characteristic values of the filter cake such as the thickness and packing density were not until now easily accessible due to the fragile structure of the cake itself. Hence a special technique was adopted to study the properties of the filter cake. The dust particles in the filter cake and the media are first fixed then embedded together with the filter media using an epoxy resin [10]. After grinding and surface polishing of the hardened sample, the filter media including the filter cake can be optically analysed and measured, **Figure 6**.

The new technique also enables the quantitative measurement of the spatial distribution of dust particles in the filter cake and filter media through EDX analysis (energy dispersive X-ray spectroscopy).

Figure 7 shows a direct comparison between cellulose and nanofibre filter media with identical pressure increase in each case. With the cellulose media, it is clear that the test dust is deposited within the fibre structure whereas for the media coated with nanofibres, almost all the dust particles are located within the filter cake. However, as the clogging point has already been exceeded, the surface filtration phase is reached even for cellulose media, so that a large proportion of the filtered dust is in the filter cake.

As mentioned at the beginning, the way particles are deposited within the structure of filter media is strongly dependent on the nature and above all the particle size distribution of the filtered dust. Particularly when dealing with the previously described soot particles, surface filtration with nanofibre media has proved beneficial for heavy duty applications, as both a high soot capacity and increased filtration efficiency can be achieved through modification of the surface [4, 7].

Due to the chemical composition of the soot particles, EDX analysis cannot be carried out. Mann+Hummel is thus currently investigating other methods such as e.g. X-ray tomography, to study the characteristics of soot deposition.

4 Summary

The performance of new, innovative filter media when handling extremely fine and coarse dust can be replicated realistically thanks to the very good testing facilities in the air filter lab. With the soot test bench and new fixing technique, development tools have been created to examine the deposition characteristics of dust particles. Through these tools, it is now possible to test far more quickly and accurately the suitability of new filter systems and forward-looking filter elements, e.g. with innovative pleat structures, under realistic conditions. Mann+Hummel can thus provide even more efficient and advanced solutions for engine intake air filtration.

References

[1] Affenzeller, J.; Gläser, H.: Springer Wien, New York, 1996
[2] Durst, M. et al.: Filtration. In: Kraftfahrzeug-Motoren, Auslegung und Konstruktion. 4. Auflage, Vogel 2006
[3] Sanders, R.; Bühler, A.; Durst, M.; Moser, N.; Pelz, A.: Effiziente Motorluftfiltration durch den Einsatz von Nanofasern. In MTZ 68 (2007) Nr. 2
[4] Bundesumweltamt: Hintergrundpapier zum Thema Staub/Feinstaub (PM). Berlin, März 2005
[5] Balazy, A.; Podgórsky A.: J. Colloid and Interface Science 311, 2007, S. 323-337
[6] Kittelson, D.B. et al.: J. Aerosol Science 37, 2006, S. 913-930
[7] Fleck, S. et al.: 8th Stuttgart International Symposium Automotive and Engine Technology. March 2008
[8] Moelter, L.; Kessler, P.: Gefahrstoffe – Reinhaltung der Luft 10, 2004
[9] Löffler, F.: Staubabscheiden. Thieme: Stuttgart, 1988
[10] Schmidt, E.; Löffler, F.: Powder Technology 60, 1990, S. 173-177

Automotive

Choose certai
Add value.

personal buildup for Force Motors Ltd.

tank.tech 2009

Congress with accompanying technical exhibition

November 10 – 11, 2009

The Monarch Hotel, Bad Gögging near Munich, Germany

Information online: www.ATZlive.com

In cooperation with

ATZ

TÜV SÜD Automotive GmbH

TÜV®

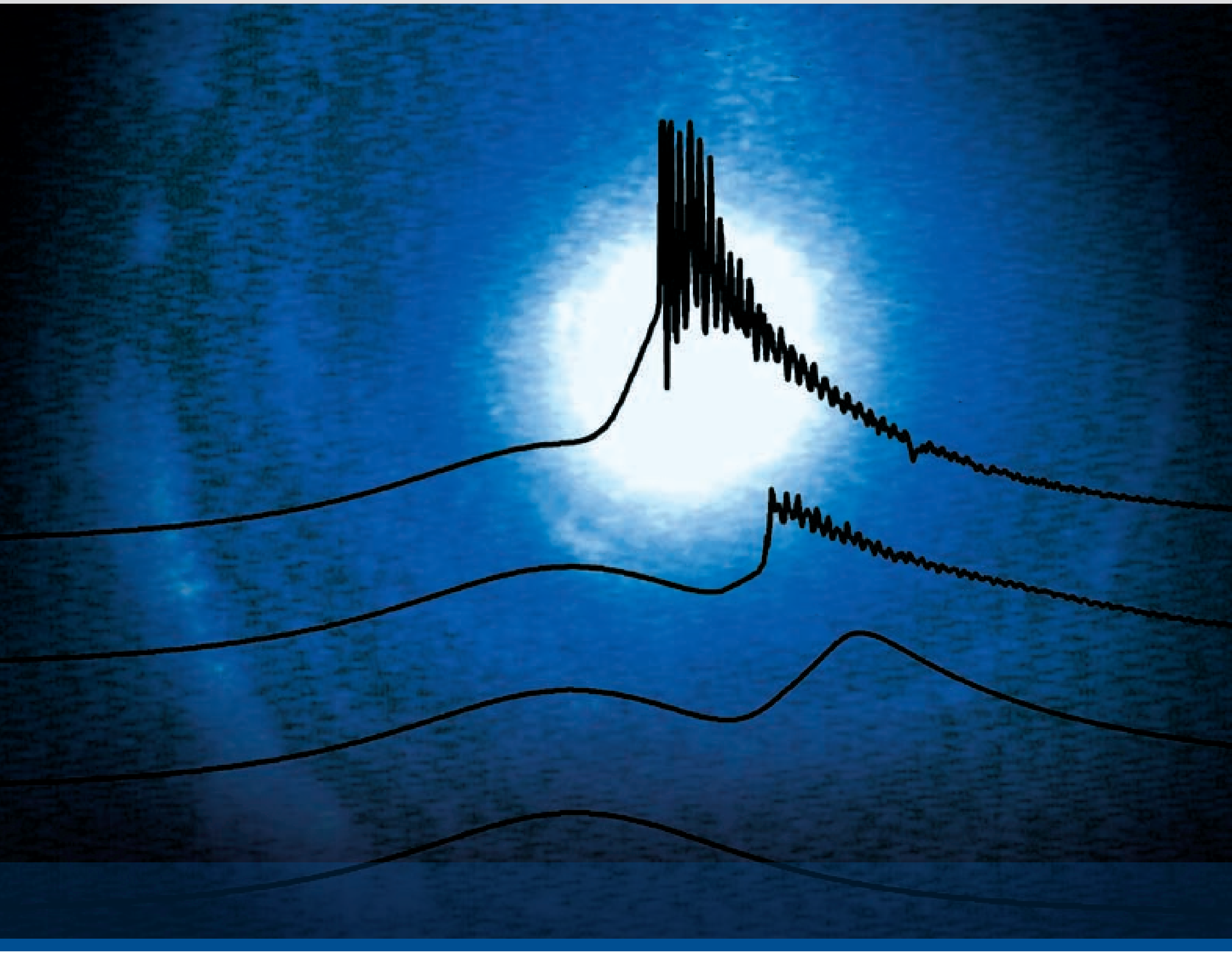

Limits on Downsizing in Spark Ignition Engines due to Pre-ignition

The combination of gasoline direct injection and supercharging technologies allows the substitution of naturally aspirated engines through downsized supercharged engines with comparable performance. However, increasing the mean effective pressure is limited by the occurrence of unwanted pre-ignition phenomena. The following article provides an insight into the pre-ignition phenomenon and its relevant triggering mechanisms. The presented results stem from a research project by Volkswagen AG Group Research, in cooperation with the Institute for Internal Combustion Engines and Automotive Engineering at Vienna University of Technology.

1 Introduction

The pursuit to meet the increasing energy demand, the objective to maintain individual mobility as well as future statutory provisions regarding CO_2 emissions have seen the automotive industry called on to take suitable measures. Fuel consumption has been continuously reduced through the introduction of new engine technologies. When it comes to reduce fuel consumption in gasoline engines, Volkswagen AG relies on a combination of downsizing, supercharging and direct injection. Its latest engine generation shows high mean effective pressure values and is characterised by high efficiency and driving enjoyment. In order to raise even further potential on the basis of the downsizing strategy, future engines will achieve even higher mean effective pressure values. However, this increase is associated with unwanted combustion phenomena, which represent the focus of this paper.

2 The Pre-ignition Phenomenon

The pre-ignition phenomenon is more likely to occur at low engine speeds and high charging pressures close to full load. Pre-ignition is initiated when auto-ignition conditions are reached in the fuel/air mixture before the spark ignition time. Therefore, unlike the case of knocking phenomena, delaying the spark ignition time cannot prevent pre-ignitions.

The flame propagation during pre-ignition takes place suddenly and leads to rapid pressure increases and considerable pressure fluctuations in the combustion chamber. **Figure 1** shows cylinder pressure traces for a regular combustion, a knocking combustion and a combustion exhibiting pre-ignition. High cylinder pressures (> 200 bar) during a pre-ignition generally result in engine damage and must be avoided at all costs during regular engine operation.

Investigations on the engine test rig have made it possible to ascertain the following influencing parameters and mechanisms for triggering pre-ignition:

- oil droplets and deposits
- „hot spots“ (hot components in the combustion chamber)
- reaction kinetics.

2.1 Oil Droplets and Deposits

One factor that influences the tendency towards pre-ignition concerns oil droplets present in the combustion chamber, as those transported into it inadvertently by the crankcase ventilation. These can be ignited during the compression stroke and therefore function as the origin of a pre-ignition. Furthermore, oil droplets can also be present in deposits in the combustion chamber. The latter can

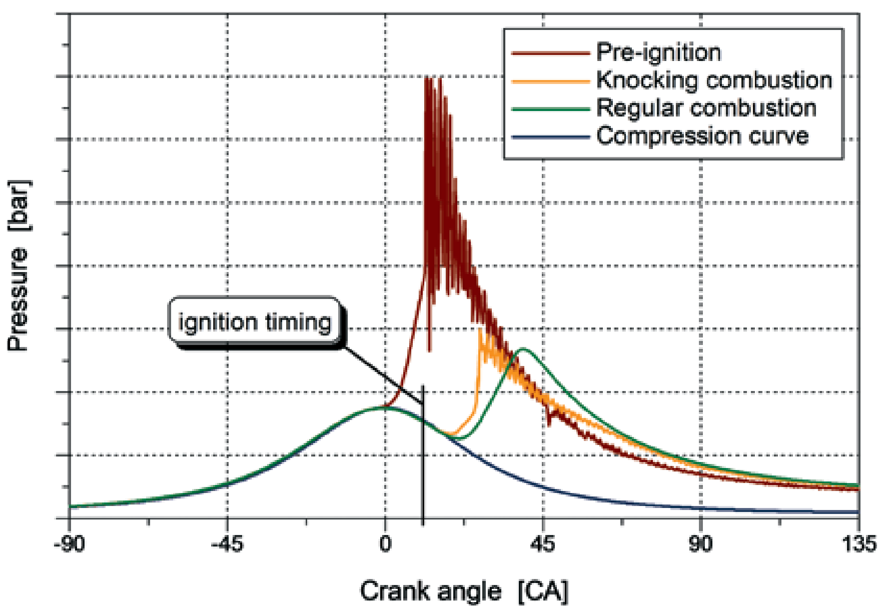

Figure 1: Cylinder pressure traces

The Authors

Dipl.-Ing. Jürgen Willand is Head of the Gasoline Engines Division at Volkswagen AG Group Research in Wolfsburg (Germany).

Dr.-Ing. Marc Daniel is Researcher in the Field of Thermodynamics at the Gasoline Engines Division of Volkswagen AG Group Research in Wolfsburg (Germany).

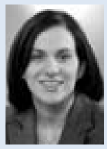

Dr. Emanuela Montefrancesco is Researcher in the Field of CFD / Reaction Kinetics at the Gasoline Engines Division of Volkswagen AG Group Research in Wolfsburg (Germany).

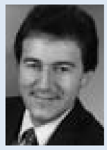

Prof. Dr. Bernhard Geringer is Head of the Institute for Internal Combustion Engines at the Vienna University of Technology (Austria).

Dr. Peter Hofmann is Lecturer at the Institute for Internal Combustion Engines at the Vienna University of Technology (Austria).

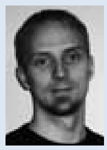

Dipl.-Ing. Markus Kieberger is Research Assistant at the Institute for Internal Combustion Engines at the Vienna University of Technology (Austria).

Table: Technical data of the test engine

Type	Four-cylinder in-line engine
Displacement	1390 cm^3
Stroke / Bore	75.6 / 76.5 mm
Valves per cylinder	4
Compression	10:1
Max. power	125 kW at 6000 rpm
Max. torque	240 Nm at 1750 to 4500 rpm

function as ignition sources in two ways. Firstly, particles can break away from the cylinder head or piston and remain suspended in the combustion chamber. These follow the gas temperature during combustion and, due to the lack of heat conduction and their high heat capacity, maintain a relatively high temperature level during the subsequent gas exchange stroke. In this way, these deposits can function as sources of pre-ignitions in the combustion chamber at an early stage. In the second case, the deposits lose contact with the combustion chamber wall only partially and can therefore function spontaneously as a „hot spot“. These separation mechanisms can be identified since always occurring at a fixed location and for not showing a thermal heating-up phase that lasts through many cycles [1].

2.2 Hot Spots

Operating the engine at full load leads to high heat transfer flows to the combustion chamber components. These can reach critical temperature values and cause the gas temperature to rise beyond the auto-ignition value. Among such components figure the spark plug, the exhaust valves, the piston and the squish edges in the cylinder head. By using optical measurement techniques, it is possible to identify „hot spots“. Their negative effects can only be limited by modifying components design.

2.3 Reaction Kinetics

Recirculated or retained exhaust gases in the combustion chamber have negative consequences on subsequent combustion. On one side, they influence the charge pressure and temperature; furthermore they contain reactive elements that can have a significant influence on the reaction kinetics [2]. These influences result from the complex reaction behaviour of long-chain hydrocarbons which are highly dependent on temperature, pressure, air/fuel ratio [3], EGR composition and EGR quantity [4]. Reaction kinetic calculations allow representing critical conditions depending on the above described parameters.

3 Engine Test Rig Results

In order to induce pre-ignitions deliberately in a production engine, it is necessary to increase significantly the level of charge if compared to the standard application. At the same time, the test engine must be equipped with various safety systems to make the operation at pre-ignition limit possible. In order to detect possible influencing factors, many engine parameters can be varied. In this context, changing the gas exchange was proved to be the most effective method.

3.1 Test Specimen

The test specimen used is a Volkswagen 1.4 l TSI spark ignition engine with direct gasoline injection and a homogenous combustion process, with the technical data specified in the **Table**. The engine is equipped with a mechanically driven compressor and a turbocharger. It has four cylinders, two overhead camshafts (with phase adjuster on the intake side) and four valves per cylinder.

To reach the critical operating range of pre-ignition, it is necessary to raise the charge level of the test engine to values significantly above the production level. As a result, an externally driven charger is connected to the intake of the test specimen. The intake manifold pressure or charge level can therefore be set independently of the engine speed. The intake air temperature is set to 30 °C for all investigated operating points using an additional intercooler. Each cylinder is equipped with pressure transducers, while cylinder 4 is also provided with optical access.

In order to investigate the pre-ignition phenomenon, the test specimen is operated at a speed of 1750 rpm at full load with equivalence ratio 1.0, and the charge pressure is increased by means of the externally driven compressor until pre-ignition occurs. The ignition time is manually set to the knock limit. In order to avoid sporadic pre-ignitions due to oil

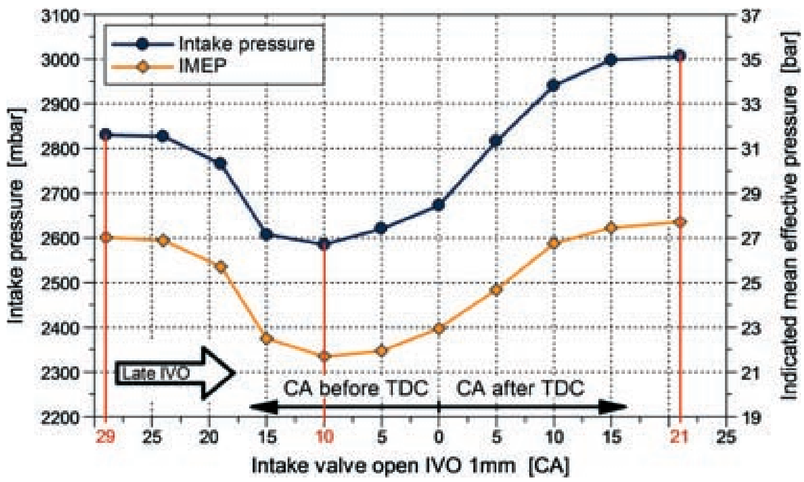

Figure 2: Inlet manifold pressure and indicated mean effective pressure at the pre-ignition limit plotted against inlet valve timing

droplets, the test specimen is equipped with modified crankcase ventilation.

Optical measurement results clearly indicate the effect of „hot spots“ on the tendency to pre-ignition. Improving components design further shifts the pre-ignition limit by therefore allowing an increasing in the target mean effective pressure. However, the influence of engine operating parameters such as the valve timing remains apparent. This shows how hot spots in the combustion chamber do influence the pre-ignition tendency, but still their elimination does not assure the disappearance of pre-ignitions. In fact, triggering factor of pre-ignition phenomena is mainly represented by the reaction-kinetic limits being exceeded. Therefore further investigations on pre-ignition occurrence can be carried out on the initial unmodified geometry layout.

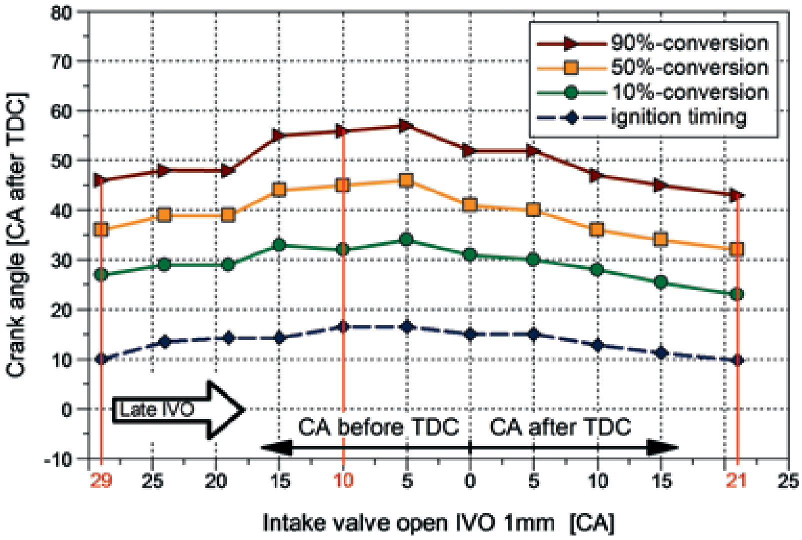

Figure 3: Combustion parameters at the pre-ignition limit as function of inlet valve timing

3.2 Influence of the Charge Motion

The test engine is equipped with an intake camshaft phase adjuster in order to investigate the influence of the valve overlap and consequently the influence of internally recirculated exhaust gas rate on the pre-ignition limit. It is observed that changing the valve overlap leads to a significant change in the pre-ignition tendency of the test specimen. **Figure 2** shows the maximum intake manifold pressure as well as the maximum indicated mean effective pressure which can be reached at the pre-ignition limit as function of different inlet valve timing. In other words, the intake manifold pressure values corresponds to those operating points in which the test engine can still be operated without pre-ignition phenomena.

The indicated mean effective pressure curve shows a minimum value for an inlet valve timing of IVT=10° CA before gas exchange TDC. Earlier or later IVT shift the pre-ignition limit further on, which is reflected by a higher obtainable indicated mean effective pressure. In fact, both earlier and later IVT lead to equally high indicated mean effective pressure values. However, the required intake manifold pressures for the two configurations are very different, the value for later inlet valve timing being significantly higher due to a loss of effective compression ratio.

The increase in the indicated mean effective pressure when the valve timing is moved away from the position IVT=10° CA before TDC of gas exchange can be explained by two effects. Firstly, the higher intake manifold pressure leads to a higher in-cylinder mass. Secondly, the 50 % energy conversion time can be shifted in the earlier direction in spite of an increased in-cylinder mass, **Figure 3**. This means adjusting the valve timing results in a reduction of the pre-ignition tendency. The increase in indicated mean effective pressure involves interplay of higher in-cylinder mass and more efficient combustion timing.

These results clearly indicate the existence of limits beyond which sporadic pre-ignitions occur. The explanation for the significant change in the tendency towards pre-ignition when changing the valve timing is the modified gas exchange. When the exhaust valve opens, a pressure wave is generated in the exhaust system. When a shared exhaust manifold is used for a four cylinder engine, this pressure wave affects 180° CA later the intake stroke of the cylinder which follows up in the firing order. **Figure 4** shows the pressure profiles of cylinder 4 at the pre-ignition limit for the worst case IVT=10° CA before TDC of gas exchange. The scavenging pressure drop (difference between the induction manifold pres-

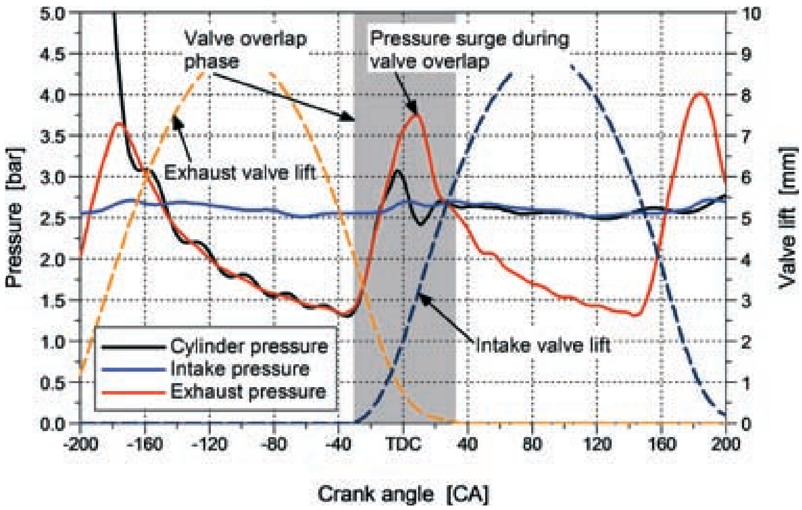

Figure 4: Pressure conditions for inlet valve timing IVT=10° CA before TDC of gas exchange at the pre-ignition limit

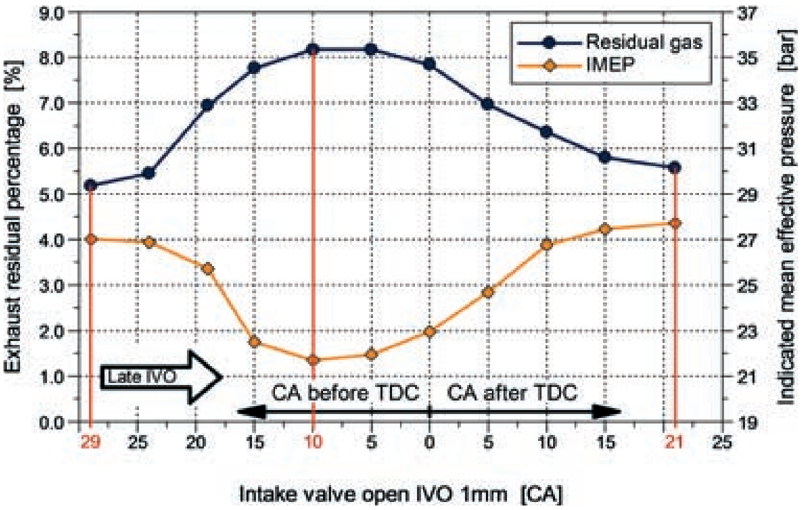

Figure 5: Calculated residual gas rate and indicated mean effective pressure over the inlet valve timing

sure and the exhaust pressure) which normally drives fresh air into the cylinder results into a negative scavenging effect. In this way the exhaust gas flows back into the combustion chamber despite a high intake manifold pressure. Once the exhaust valve closes the exhaust gas remains trapped in the combustion chamber. In this context, the inlet valve timing plays a decisive role. If the intake valves open before the pressure wave arrives, the fresh charge flows into the exhaust system during the valve overlap. In this way, the intrusion of exhaust gas from the exhaust manifold can be avoided. If the inlet valves open much later, they occlude the passage to the pressure wave. Flow-back from the exhaust manifold into the intake system through the cylinder is also in this case effectively avoided.

1D simulation calculations were carried out in order to evaluate the effect of the modified gas exchange depending on the inlet valve timing. **Figure 5** shows the calculated exhaust gas rate over the inlet valve timing at the pre-ignition limit. The residual gas rate curve reaches its maximum at a valve timing of IVT=10° CA before TDC of gas exchange with a value of 8.2 %. Then it decreases when the valve timing is shifted towards earlier or later positions. Furthermore, Figure 5 also shows the indicated mean effective pressure. Comparing the residual gas rate and the indicated mean effective pressure they show an inversed profile. A higher residual gas rate due to internal exhaust gas recirculation shifts the pre-ignition limit towards lower values and therefore has a negative effect on the target indicated mean effective pressure.

4 Reaction Kinetics Simulations

In this paragraph, reaction kinetics simulations of a Multi-Reactor System [4] are described, which are carried out with the software „DARS" [5]. For assigned pressure, EGR rates and compositions a system of many homogeneous reactors is simulated in order to determine their ignition delay time. Additionally, an indirect coupling to 3D-CFD simulation with detailed chemistry allows taking into account temperature and air/fuel ratio fluctuations.

Figure 5 has shown how depending on different intake valve timing, i.e. different internal EGR rates, it is possible to achieve different indicated mean effective pressure targets.

Results of reaction kinetics simulation are shown in **Figure 6** for valve timing of IVT=29° CA before TDC of gas exchange, with an internal EGR rate of 5 % and indicated mean effective pressure of 27 bar and in **Figure 7** for valve timing of IVT=10° CA before TDC of gas exchange, with an internal EGR rate value of 8.2 % and indicated mean effective pressure of 22 bar.

Figure 6 and Figure 7 clarify the relationship between pre-ignition phenomena and reaction kinetics. The 3D CFD calculation cells (clouds of black dots) inside the combustion chamber do approach the area characterised by short ignition delays, but do not overcome the critical ignition delay value indicated by „t_1".

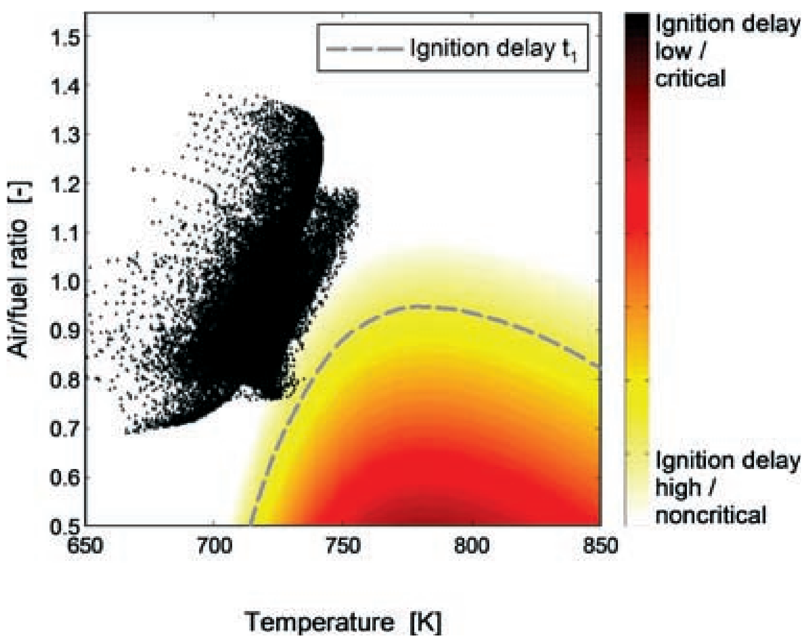

Figure 6: Ignition delay of all 3D-CFD combustion chamber cells at TDC accounting for cell temperature and air/fuel ratio values, inlet valve timing of IVT=29° CA before TDC of gas exchange, full load at the pre-ignition limit, imep=27 bar

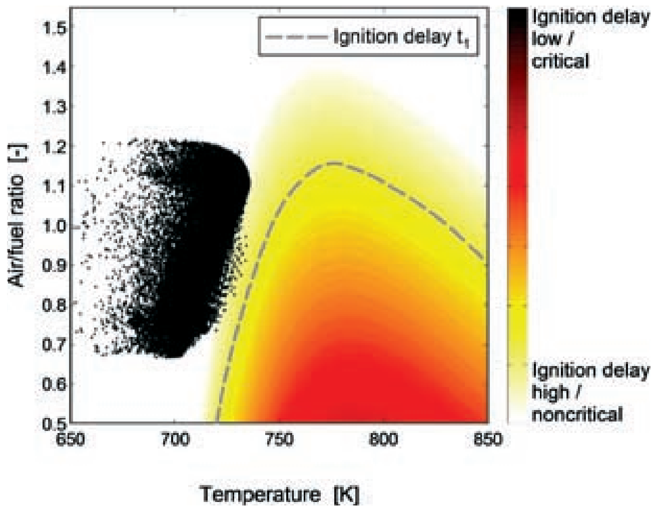

Figure 7: Ignition delay of all 3D-CFD combustion chamber cells at TDC accounting for cell temperature and air/fuel ratio values, inlet valve timing of IVT=10° CA before TDC of gas exchange, full load at the pre-ignition limit, imep=22 bar

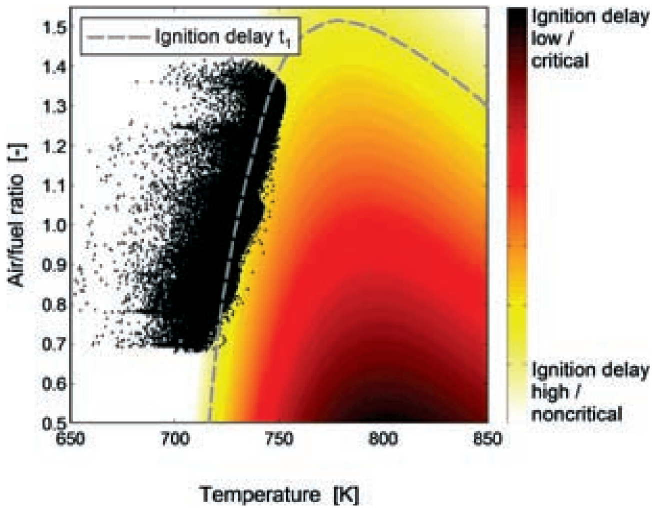

Figure 8: Ignition delay of all 3D-CFD combustion chamber cells at TDC accounting for cell temperature and air/fuel ratio values, inlet valve timing of IVT=10° CA before TDC of gas exchange, crossing the full load pre-ignition limit, imep=27 bar

This represents a configuration at pre-ignition limit as observed on the test bed.

Figure 8 shows the results for the case in which the load is not set at the pre-ignition limit at imep=22 bar but at imep=27 bar for the valve timing IVT=10° CA before TDC of gas exchange. This case describes an evident crossing of the critical ignition delay value „t_1“.

The simulation results confirm that a reduction of the engine load cannot be avoided for the valve timing IVT=10° CA before TDC of gas exchange. The cause is represented by the higher internal EGR percentage for this particular configuration. Lowering the internal EGR percentage in the combustion chamber is consequently an essential requisite to avoid pre-ignition phenomena.

5 Summary

Supercharged gasoline engines see, beside the well known effect of knocking, also pre-ignition phenomena as limiting condition.

Pre-ignition phenomena result from the auto-ignition limit set by reaction kinetics for a given fuel/air mixture in the combustion chamber. A necessary requirement to avoid pre-ignitions is represented by a homogeneous air/fuel mixture, as well as an efficient design of cylinder head coolant and air cooling system.

However, engine measurements and reaction kinetic simulation results have shown further influencing parameters able to decrease pre-ignition tendencies and revealed triggering mechanisms of this phenomenon. It is possible to classify those into three categories.

Oil droplets and deposits cause stochastically occurring pre-ignitions which cannot therefore be predicted.

To a second category of the triggering mechanisms belong „hot spots“, which cause intolerable component temperature levels. Design measures for preventing „hot spots“ allow reducing the pre-ignition tendency.

The third category features reaction kinetic and particularly the thermodynamic status of the air/fuel charge and its composition as decisive influencing factors. As confirmed by reaction kinetics simulations, temperature, pressure and residual gas rate are in this case crucial parameters. A pre-ignition limit is set depending on these parameters, beyond which pre-ignition is unavoidable. It is possible to influence significantly the pre-ignition tendency of a mixture by optimising intake valve timings. Suitable valve timings affect the gas dynamics and the in-cylinder flow so that internal exhaust gases and their negative effects can be minimised and consequently a higher mean effective pressure can be achieved.

References

[1] Prochazka, G.; Hofmann, P.; Geringer, B.; Willand, J.; Jelitto, C.; Schäfer, O.: Selbstzündungsphänomene an einem hochaufgeladenen Ottomotor und Abhilfemöglichkeiten. Internationales Wiener Motorensymposium 2005

[2] Beck, L. M.; Hoffmeyer, H.; Mauss, F.; Montefrancesco, E.; Willand, J.; Ziebart, F.: CARE – Catalytic Reformated Exhaust gases in turbocharged DISI-Engines. Detroit: SAE Technical Paper 2009 (to be published)

[3] Ahmed, S. S.: A detailed modeling study for primary reference fuels and fuel mixtures and their use in engineering applications. PhD Thesis Lund University. Sweden: 2006

[4] Beck, L. M.: Reaktionskinetische Analyse des Einflusses von chemisch modifizierter Abgasrückführung auf das Selbstzündungsverhalten von Ottokraftstoffen. Diplomarbeit Brandenburgische Technische Universität Cottbus, 2008

[5] DigAnaRS LLC, DARS – Software for Digital Analysis of Reactive Systems. New York: 2008

[6] Krebs, R.; Szengel, R.; Middendorf, H.; Fleiß, M.; Laumann, A.; Voeltz, S.: Neuer Ottomotor mit Direkteinspritzung und Doppelaufladung von Volkswagen Teil 1: Konstruktive Gestaltung. In: MTZ 66 (2005) Nr. 11